CAPITAL UNIVERSITY OF SCIENCE AND TECHNOLOGY, ISLAMABAD

Determination of Potential Antioxidants of *Artemisia annua* by Computational Approaches

by

Zarina Khurshid

A thesis submitted in partial fulfillment for the degree of Master of Science

in the

Faculty of Health and Life Sciences
Department of Bioinformatics and Biosciences

2021

I dedicate this thesis to my loving mother ***"sabira bibi"*** *who prays day & night for my success.*

CERTIFICATE OF APPROVAL

Determination of Potential Antioxidants of *Artemisia annua* by Computational Approaches

by

Zarina Khurshid

(MBS191005)

THESIS EXAMINING COMMITTEE

S. No.	Examiner	Name	Organization
(a)	External Examiner	Dr. Maria Shabbir	NUST, Islamabad
(b)	Internal Examiner	Dr. Syeda Marriam Bakhtiar	CUST, Islamabad
(c)	Supervisor	Dr. Erum Dilshad	CUST, Islamabad

Dr. Erum Dilshad
Thesis Supervisor
March, 2021

Dr. Sahar Fazal
Head
Dept. of Biosciences & Bioinformatics
March, 2021

Dr. Muhammad Abdul Qadir
Dean
Faculty of Health & Life Sciences
March, 2021

Author's Declaration

I, **Zarina Khurshid** hereby state that my MS thesis titled "**Determination of Potential Antioxidants of *Artemisia annua* by Computational Approaches**" is my own work and has not been submitted previously by me for taking any degree from Capital University of Science and Technology, Islamabad or anywhere else in the country/abroad.

At any time if my statement is found to be incorrect even after my graduation, the University has the right to withdraw my MS Degree.

(Zarina Khurshid)

Registration No: MBS191005

Plagiarism Undertaking

I solemnly declare that research work presented in this thesis titled "**Determination of Potential Antioxidants of *Artemisia annua* by Computational Approaches**" is solely my research work with no significant contribution from any other person. Small contribution/help wherever taken has been dully acknowledged and that complete thesis has been written by me.

I understand the zero tolerance policy of the HEC and Capital University of Science and Technology towards plagiarism. Therefore, I as an author of the above titled thesis declare that no portion of my thesis has been plagiarized and any material used as reference is properly referred/cited.

I undertake that if I am found guilty of any formal plagiarism in the above titled thesis even after award of MS Degree, the University reserves the right to withdraw/revoke my MS degree and that HEC and the University have the right to publish my name on the HEC/University website on which names of students are placed who submitted plagiarized work.

(Zarina Khurshid)

Registration No: MBS191005

Acknowledgement

All the praises are to be for Almighty **ALLAH TALLAH** and then for his **prophet MUHAMMAD (SAW)**. I would like to express my wholehearted thanks to my family for the generous support throughout of pursuing the MS degree. I am heartily grateful to my supervisor **Dr. Erum Dilshad** (Assistant professor, Department of Bioinformatics & Biosciences, CUST) for her kind support, guidelines and arrangement of tutorial classes. I especially say thanks to Dr. Naeem Mahmood Ashraf (Lecturer Biochemistry & Biotechnology, University of Gujrat) for his assistance on computational approaches, provided by online tutorial classes. I cannot forget to say thanks to Muhammad Maaz and Uzma Saeed who helps me a lot in the installation of softwares.

Thanks to all.

(Zarina Khurshid)

Abstract

Antioxidants act as radicle scavenger, hydrogen donor, electron donor, peroxide decomposer, singlet oxygen quencher, enzyme inhibitor, synergist, metal chelating agent & antioxidant enzyme's stimulator. Each has its own role and they are not interchangeable. This is the reason that Global antioxidants Market was valued at $2,923 million in 2015 & expected to reach $4,531 million by 2022. Globally people become more concern to use natural products over synthetic ones. That's why this research is planned to discover potential antioxidants from *Artemisia annua*. Thirty-seven bio compounds representatives of all classes namely as alpha terpinene, apigenin, arteannuin B, arteether, artemether, artemetin, artemisia ketone, artemisinic acid, artemisinin, artesunate, beta caryophyllene, beta selinene, camphor, casticin, chrysosplenol D, coumarin, cynaroside, deoxyartemisinin, epifriedelanol, friedelin, germacrene D, isorhamnetin, kaempferol, limonene, luteolin, mearnsetin, myrtenol, quercetagetin, quercetin, quinic acid, retusin, rutin, scoparone, scopoletin, scopoline, stigmasterol, & transpinocarveol were selected. Virtual screening of these ligands was carried out against drug targets that are catalase, superoxide dismutase 2, & glutathione peroxidase 1 by CB-dock. Quercetin, luteolin, apigenin, kaempferol, & mearnsetin showed themselves as hit compounds. Further refining by screening filters represents quercetin as a lead compound. Nebivolol is used as the standard for comparison. Quercetin is also far more active than the standard drug. All the interaction visualization analysis studies are performed by PyMol molecular visualization tool and Ligplot^{+}. Finally, as a result of this study, I have discovered quercetin as a most potential antioxidant which might be a drug candidate to treat oxidative stress and related chronic diseases in future. However further research is necessary to investigate their potential medicinal use.

Keywords: Antioxidants, *A.annua*, virtual screening, CB-dock, Catalase, Superoxide dismutase 2, Glutathione peroxidase 1, Lead compound, Quercetin, & Nebivolol.

Contents

List of Figures

List of Tables

Abbreviations

A. annua	*Artemisia annua*
ADME	Absorption, Distribution, Metabolism & Excretion
ADMET	Absorption, Distribution, Metabolism, Excretion & Toxicity
AIDS	Acquired Immunodeficiency Syndrome
AP-1	Activator Protein 1
ART	Artesunate
As	Arsenic
CADD	Computer aided drug design
CAT	Catalase
CVDs	Cardiovascular diseases
CKD	Chronic kidney disease
Cu	Copper
Co	Cobalt
Cr	Chromium
Cd	Cadmium
COPD	Chronic obstructive pulmonary disease
DNA	Deoxy ribonucleic acid
ETC	Electron transport chain
EGCG	Epigallocatechin gallate
FDA	Food and drug administration
Fe	Iron
GPX1	Glutathione peroxidase 1
GTE	Green tea extract
Hg	Mercury

HUVEC	Human umbilical vein endothelial cells
LOOH	Lipoprotein Lipid Hydroperoxides
MDR	Multi drug resistance
MD	Macular degeneration
NSCLC	Non small cell lung cancer
NDs	Neurodegenerative diseases
NF-KB	Nuclear Factor Kappa of B Cells
NOSS	Specific Nitric Oxide Synthatase
Pb	Lead
ROS	Reactive oxygen species
RNS	Reactive nitrogen species
RNA	Ribonucleic acid
SOD2	Superoxide dismutase 2
TME	Tumor microenvironment
VS	Virtual screening
VEGF	Vascular Endothelial Growth Factor
WHO	World health organization

Chapter 1

Introduction

1.1 Background

Human beings depend on plants for survival from the first day. No one can imagine life on earth without plants. Medicinal plants or herbal medicine is one of the major sources of medicine all over the World. Ayurvedic, Unani, and Chinese traditional medicine are some examples of the oldest herbal medicine systems. South Asia, Africa, America, China, Australia, and Japan are some countries that use herbal medicine since ancient times. Among the top twenty pharmaceutical dealers of the world, seven deals with plant compounds and their derivatives and earn 20 billion dollars annually. According to an estimate, there are 400000 plant metabolites all over the world, out of which only 10000 are chemically isolated [1].

In Pakistan, only 600 angiosperm plants are reported out of 6000 for their medicinal usage [2]. Knowledge of traditional medicines in every country shifted from generation to generation have strong bases like religious, common practices, magical, and socio-cultural. People use medicinal plants or their parts in a combination of 2 to 10 plants or in decoction without knowing their chemical constituents.

Scientifically proven herbal medicines use only purified and standardized efficient phytochemicals in a systematic way for the prevention and treatment of diseases [3]. A decrease in efficacy and an increase in the side effects of synthetic drugs

brings again natural medicines at top usage [4]. *Artemisia annua* commonly known as scented wormwood is a shrub indigenous to parts of Asia. Wild species are found in Europe, the United States, and Argentina. Now *A.annua* cultivated through the world for artemisinin [5]. *Artemisia annua* belongs to the family Asteraceae and genus Artemisia which has more than 400 species. This is the only species with an annual cycle so-called as *annua*. In China, *A.annua* had been used as a remedy of hemorrhoids, as a food additive, and antimalaria and antifever. Now world health organization recommends artemisinin combination therapies for malaria.

Artemisia annua has many different classes of compounds such as sesquiterpenes, monoterpenes, triterpenoids, coumarins, flavonoids, steroids, aliphatic and sweet hydrocarbons [6]. Flavonoids present in *Artemisia annua* are highly antioxidant and being assessed for cancer and, parasitic diseases. Leaves are saturated with essential oils that show antimicrobial and antifungal activity. Furthermore, the plant also shows cytotoxic, antioxidant, and antipyretic properties. Pharmaceutical and food industries now focus on aromatic plants against lipid oxidation, as a drug, as food preservative and additive to ensures the safety and enhance the quality of food and health. Natural preservatives, drugs, and additives now preferred over synthetic ones due to safety aspects and beneficial for health. *Artemisia annua* is also highlighted as a single commercial source of artemisinin [7].

Atomic or free radicles are those molecules that have single electrons in their outer orbits. Cigarette smoke and pollutants constantly produced free radicals in our environment. Cellular metabolisms like respiration and enzyme reactions also produce free radicals. Radon and cosmic radiations are also sources of free radicals. Excessive free radicals can cause damage to biomolecules like DNA, proteins, lipids, glial cells, and neurons. Oxidative stress results in cancer, diabetics, myocardial infarction, atherosclerosis, rheumatoid arthritis, cardiovascular diseases, reoxygenation injury, stroke, persistent swelling, septic shock, aging, hypertension, vasospasm, and other regressive diseases in humans. Antioxidants are those compounds that remove, inhibit, and scavenge reactive oxygen species. Catalase, glutathione peroxidase, and superoxide dismutase are natural antioxidant enzymes while non-enzymatic antioxidants are mostly polyphenols, carotenoids, lipoic acid,

and ascorbic acid which are derived from dietary sources. These non-enzymatic compounds provide defense against oxidative stress [8]. Virtual screening (VS) is low cost, effective and direct drug discovery approach as compared to experimental approaches such as nuclear magnetic resonance spectroscopy and crystallography.

VS can be done by ligand-based and structure-based methods to find out lead compounds and molecular docking is one important tool of structure-based methods. Molecular docking predicts the interactions between small molecules called as ligands and target proteins, also known as receptors. Docking without knowing the location of binding sites called as blind docking [9]. Prediction of effective binding sites and affinity of 3Dproteins and ligands are the main function of computer-aided drug discovery. CB dock is an automatic blind docking, user-friendly web server [10]. 60 different docking tools and programs are developed in the last 20 years. Among them some are Autodock, Flexx, Surflex, GOLD, Glide, c docker, ICM, MC Dock, and Auto Dock Vina [11].

1.2 Problem Statement

The trend to use conventional medicines increases day by day in developed and undeveloped countries all over the world. In low-income countries, people prefer them over modern medicine due to low cost and lesser side effects. Major issues with these traditional medicines are limited bioavailability, quantity to be used, part or parts of plant or plants to be used, forms like extract or decoction which one with more efficacy, scientific validity, and less shelf life, etc. Furthermore, indigenous knowledge is degraded rapidly so its need for an hour to preserve and prove this knowledge scientifically for present and future generations.

WHO emphasis to prove scientifically traditional phytochemicals in order to get lead and hit compounds which would result in drugs with more efficacy and no or fewer side effects. To achieve that purpose present research is planned to determine potential antioxidants present in *Artemisia annua* which will be beneficial for everyone as these slow down processes of aging and reduce hypertension and blood

sugar levels. Besides the pharmaceutical industry, these potential antioxidants also prove themselves as efficient food additives and preservatives for the food industry.

1.3 Aims

Superoxide dismutase 2 (SOD2), catalase (CAT) and glutathione peroxidase 1 (GPX1) work as first-line defense systems within the human body which are degraded by free radicals. Antioxidative compounds agonists and increase the activity of antioxidant enzymes and suppress or prevent the formation of free radicals or reactive species in cells. So in order to control the formation of free radicals and suppress their degrative effects, antioxidant compounds are a competent choice.

1.4 Objectives

This study requires the following objectives:

- To identify artemisinin, its derivatives, and bio compounds from *Artemisia Annua* as novel agonists of antioxidant enzymes.
- To study the interaction between SOD2, GPX1, and CAT as target protein and compounds from *Artemisia annua* as ligands.
- To analyze the binding conformation between antioxidant enzymes and highly antioxidative compounds as standard antioxidant agents.
- To determine lead compounds with antioxidant properties.

1.5 Scope

CADD makes drug designing possible in a short time with efficacy. Today world turns again towards natural sources to determine lead compounds for more effective, non-resistant, with lesser or no side effects drugs. It's proper time to secure

our future by scientifically preserving our indigenous knowledge before its extinction. This research is an attempt to determine novel antioxidative compounds which would be stronger drug targets of the near future for these diseases like degradable, heart, diabetes Mellitus, cancer, microbial, fast aging, hypertension, and neural diseases. This work would be beneficial for everybody as it will be helpful in slowing the process of aging. Furthermore, these highly antioxidant compounds would be used as food additives and preservatives. So the results of this research work will be valuable for the pharmaceutical and food industries.

Chapter 2

Literature Review

2.1 Free Radicles and Oxidative Stress

Molecules with unpaired electrons in their outer orbitals are called free radicles and they can oxidize (removal of electrons) and reduce (addition of electrons) other atoms within the body. Mitochondria produce reactive oxygen species (ROS) by electron transport chain (ETC) as byproducts in the process of aerobic respiration. Most of these ROS reached to the third pump of ETC and only 1 to 3percent reacts with oxygen and forms superoxide radicles [12]. ROS and nitrogenous reactive species, either they play a beneficial role or harmful [13]. Beneficial effects of ROS occurs at low or moderate concentration like help in signaling systems, defense against infectious agents like bacteria and induction of mitogenic response whereas harmful effects of these radicles result in potential biological damage also known as oxidative stress and nitrosative stress [14].

These stresses occur in the body when there is the overproduction of ROS/NRS and deficiency of all types of antioxidants. In other words, a pro-oxidant and antioxidant reactions imbalance in the living system results in the form of stress. A equilibrium between harmful and beneficial effects of free radicles is sustained by a process called as redox regulations that maintain redox homeostasis by regulating redox status in the body [15]. ROS in the body degrade macromolecules like nucleic

acids, proteins, lipids and initiate many diseases like heart diseases, diabetes, atherosclerosis, cancer, and liver diseases [16].

2.2 Types and Sources of Free Radicles

Two main types of free radicles are ROS and NRS. These free radicles are produced by endogenous and exogenous sources. Endogenous sources include inflammation, heavy exercise, Infectious diseases, activation of immune cells, mental stress, cancer, ischemia, and aging. Exogenous sources include polluted water, air pollutants, smoking, alcohol consumption, heavy metals, some drugs (like tacrolimus and cyclosporine), radiations, benzene, and bad cooking process. All these sources decomposed into free radicles within the body [17].

2.2.1 ROS

ROS represents radicles derived from oxygen and it is the most important class of radicles of the human body. Dioxygen or molecular oxygen is itself a radicle and the addition of one electron makes it a superoxide anion radicle ($O_2^{\cdot -}$) [18]. This anion acts as primary ROS and further reacts to form secondary ROS [19]. Superoxide are mostly produced within mitochondria of a cell (Fig.2.1) [20]. 1 to 3 percent electrons leaks from complex I and III of ETC and forms superoxide's which cross the inner mitochondrial membrane and enters into matrix [21].

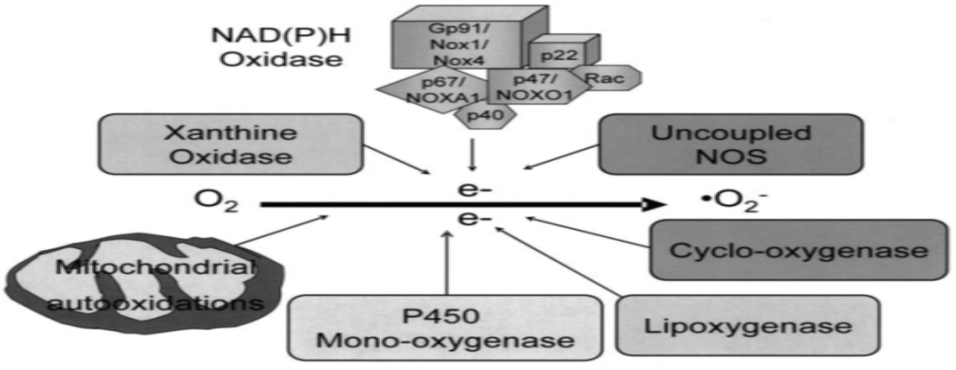

FIGURE 2.1: Endogenous Sources of Superoxide Anion ($O_2^{\cdot -}$) [22].

Hydroxyl radicle ($^{\cdot}OH$) is a highly reactive radicle but fortunately has a short half-life of approximately 10^{-9}s [23]. Under stress, condition superoxides release free iron from iron-containing molecules which are proved by dehydratase lyase family (4Fe-4S) cluster containing enzymes [24]. This released Fe^{+2} through Fenton reaction and produces hydroxyl radicles.

$$Fe^{+2} + H_2O_2 \rightarrow Fe^{+3} + OH^{\cdot} + OH \text{ [25]. Fenton Reaction.}$$

When Fenton reaction combines with Haber-Weiss reaction gives Fe^{+2} and oxygen as products.

$$O_2 + H_2O_2 \rightarrow O_2 + OH + OH^{\cdot} \text{ Haber-Weiss Reaction.}$$

$$Fe^{+3} + O_2 \rightarrow Fe^{+2} + O_2 \text{ [26].}$$

Peroxyl radicle ($ROO^{\cdot}$) is also derived from oxygen and has the simplest form called hydroperoxyl or per hydroxyl radicle ($HOO^{\cdot}$) which initiates peroxidation of lipids by fatty acid hydroperoxide (LOOH) dependant and independent pathways [27]. Peroxisomes are also known to produce H_2O_2 [28]. When a phagocytic cell-like neutrofill recognizes a outsider then undergoes a series of reactions called as respiratory burst. Result comes in the form of superoxides production and bacterial destruction [29].

TABLE 2.1: Major Endogenous ROS [30].

S No	**ROS**	**Formula**
1	Superoxide Anion	O_2^-
2	Hydrogen Peroxide	H_2O_2
3	Hydroxyl Radical	$OH^{\cdot}$
4	Hypochlorous Acid	HOCl
5	Peroxyl Radicals	$ROO^{\cdot}$
6	Hydroperoxyl Radical	$HOO^{\cdot}$

The three most significant ROS are superoxide anion ($O_2^{\cdot -}$), Hydroxyl radicle ($OH^{\cdot}$), and hydrogen peroxide H_2O_2 (Table 2.1). ROS is divided into two forms that is radicals with unpaired electrons called as free radicles and non-radicles which are produced by the sharing of unpaired electrons of free radicles [30].

2.2.2 Reactive Nitrogen Species (RNS)

Overproduction of RNS results in nitrosative stress and under such stress, the biological system becomes failed to eliminate or neutralize RNS. Nitrosylation reactions occur who change the structures and functions of proteins [31, 32]. Specific Nitric oxide synthases (NOSS) produce reactive Nitric oxide radical ($NO^{\cdot}$) in biological tissues [33]. It is an important signaling molecule in many physiological pathways like regulation of blood pressure, neurotransmission, relaxation of smooth muscle, defense mechanism and immune supervision [34]. Nitric oxide is soluble in aqueous and lipid media so it easily diffuses through the plasma membrane and cytoplasm. This radical is more stable in a hypoxic environment where its half-life increases from normal few seconds to more than 15 seconds [35]. The immune system produce nitric oxide and superoxide radicals during oxidative burst under inflammatory conditions.These radicals react to form peroxynitrite anion ($ONOO^-$) which is a potential oxidizing agent and can cause lipid oxidation and DNA fragmentation.

$$NO + O_2 \rightarrow ONOO^- \text{ [36].}$$

2.3 Oxidative Stress and Diseases

Aging is a gradual loss of organ function and tissue with time [37]. The oxidative stress theory of aging is based on the hypothesis of structural damage. This theory states that age-related functional losses are due to oxidative damage of lipids, proteins, and DNA by ROS and RNS [38]. The exact mechanism is still not clear[39]. Oxidative stress results in chronic and acute diseases like cardiovascular diseases

(CVDS) (Fig 2.2), macular degeneration (MD), chronic kidney disease (CKD), biliary diseases, neurodegenerative diseases (NDS) and cancer. Furthermore, major cardiovascular risk factors like diabetes, atherosclerosis, hypertension, and obesity along with inflammation increased cellular senescence or aging [40]. Lung diseases such as chronic obstructive pulmonary disease(COPD)and asthma determined by local and systemic chronic inflammation, are linked to oxidative stress [41]. Oxidants are known to increase inflammation by the activation of diverse kinases associating pathways and transcription factors like AP-1and NF-kappa B [42]. Rheumatoid arthritis is a chronic inflammatory disease of joints and nearby tissues having activated Tcell infiltration and macrophages [43].

Affected patients have elevated levels of isoprostane and prostaglandin which shows the role of free radicals at the site of inflammation in the initiation and progression of arthritis [44]. Kidney diseases like tubule-and glomerulo-interstitial nephritis, uremia, proteinuria, and renal failure are initiated due to oxidative stress [45]. Some drugs like bleomycin, gentamycin, tacrolimus, cyclosporine are known nephrotoxins because they increase free radicals levels and oxidative stress by lipid peroxidation [46].

Transition metals (Fe, Cu, Co, and Cr) and heavy metals like Cd, Hg, Pb, and As are strong oxidative stress inducers and responsible for some types of cancers and various forms of nephropathy [19]. Oxidative stress could be accountable for a delayed sexual maturation and puberty onset [47].

In a body, a number of free radical scavenging enzymes maintain a threshold level of oxidants but when the level of reactive species exceeds this threshold, excessive signaling occurs in the cell and the cell goes under oxidative stress. It means a balance between reactive species formation and detoxification favors an increase in free radical levels [48].

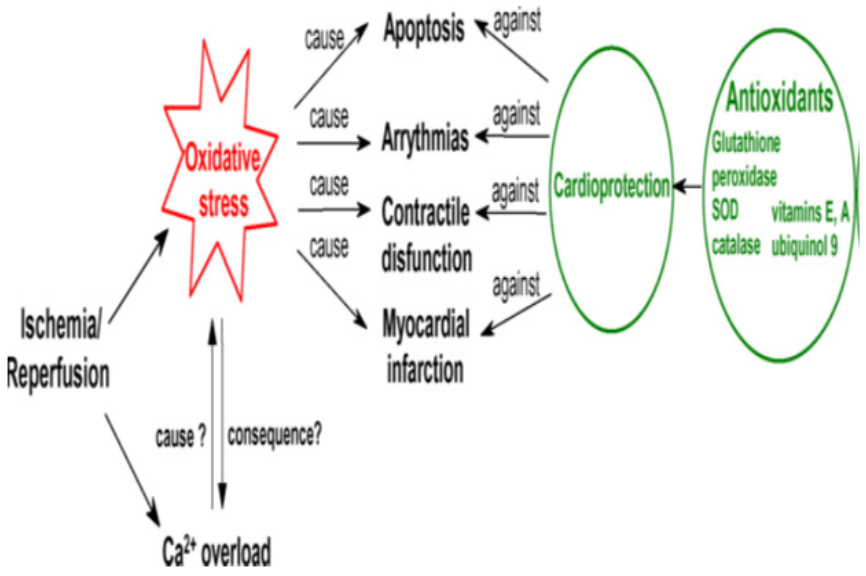

FIGURE 2.2: Effect of Oxidative Stress and Antioxidants in the Pathophysiology of Ischemia Heart Injury [17].

2.4 Antioxidants and their Defense Mechanisms

Against oxidative stress, the body has several defense mechanisms that involve a number of antioxidants and detoxifying enzymes. An antioxidant molecule has the ability to prevent or slow the oxidation of macromolecules. The function of antioxidants is to lower or stop chain reactions which are initiated by free radicals. Antioxidants mostly are reducing agents in nature [49]. The antioxidant defense followed the following mechanisms:

1. Oxidants scavenging.
2. The conversion of toxic free radicals into less toxic ones.
3. Blockage of free radicals production.
4. Blockage of production of toxic secondary metabolites and mediators of inflammation.
5. Repairment of injured molecules.
6. Initiation and enhancing the endogenous antioxidant defense system.

7. Blocking of the secondary oxidants chain reactions.

All these mechanisms work side by side for the protection of the body against oxidative stress. The antioxidant systems within the human body consist of non-enzymatic and enzymatic antioxidants [16].

2.5 Types of Antioxidants

2.5.1 Enzymatic Antioxidants (Target Proteins)

Three major classes of enzymatic antioxidants present in all body cells are Catalases (CAT), Superoxide dismutases (SOD) and Glutathione peroxidases (GPX). All three play significant roles in maintaining homeostasis within cells [50]. SOD scavenge superoxide radicals and shift into H_2O [51]. SOD removes O_2 by dismutation reaction. In the absence of SOD dismutation reaction becomes very slow [52]. GPX involved in reduction of hydrogen peroxide, organic hydroperoxides and lipid hydroperoxides [53] and helps in detoxification mechanism [54].

CAT also known as H_2O_2 oxidoreductase has four polypeptide chains, each chain made of more than 500 amino acids and has four porphyrin heme (iron) groups that allow it to react with H_2O_2. CAT has a much higher rate of absorption than other antioxidant enzymes. The rate of CAT rejuvenation activity depends on the concentration of H_2O_2 [55]. CAT is present in viral cells as well as all types of eukaryotic cells except red blood cells where different H_2O_2 oxidases are produced. A key role of CAT is to reduce H_2O_2 concentration [56].

2.5.2 Non-Enzymatic Antioxidants

Plants and animals have different non-enzymatic antioxidants such as vitamin C, vitamin E, and glutathione [43]. Vitamin C or ascorbic acid is found in both plants

and animals but humans should get it from food as it cannot be absorbed into the body. It can reduce and decrease ROS.

The beta carotene present in the liver, egg yolk, milk, butter, spinach, carrots, tomatoes and grains is a powerful antioxidant and protects against severe free radicals by removing singlet oxygen [57]. Vitamin E protects the cell membrane from oxidants by reacting with lipid radicals and eliminating the free radical intermediates [58].

2.5.3 Natural Antioxidants or Exogenous Non-Enzymatic Antioxidants

Natural agonists are agonists who are endogenous antioxidants and restore proper balance by reducing active species [59]. They inhibit the production of ROS and act as scavengers for free radicals (Fig 2.3) [60]. Flavonoids are natural antioxidants and play an important role in protection against oxidative stress [61].

They are found in cocoas, tea, fruits, vegetables, and red wine [62]. Phenolics are well known for free radical scavenging, metal ion chelatins, sinlet oxygen quenching, hydrogen donation and acting as substrate for superoxide and hydroxyl radicals [63]. Plant species like Olea europaea, Allium sativum, Coffea arabica, Mentha piperita, Petroselinum crispum, Curcuma longa, and Trigonella foenum graecum leaves showed antioxidant properties by having a pronounced hepatic protection against hepatotoxic agent [64]. Fenugreek, pomegranate, sesame, garlic, rosemary, parsley, peppermint, curcumin and propolis have shown protective effects against renal diseases and nephrotoxic agents by enhancement of antioxidant activity and inhibiting tissue lipid peroxidation [65]. The protective effect may be due to presence of flavonoids, alkaloids, terpenoids, steroidglycosides, glycosides, mono, di, and triterpenes, catechols, flavonolglycosides, benzoquinones, glycoalkaloids, polyphenols and sterols in these medicinal plants [66].

2.6 Antioxidative Phytomedicine and Bio Compounds

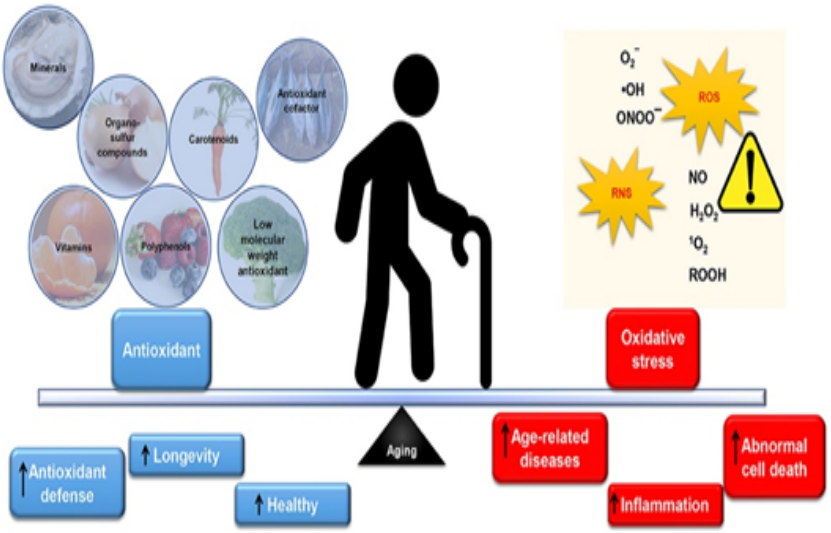

FIGURE 2.3: The Balance of Antioxidants and Oxidative Stress in Aging [67].

Antioxidant by removing free radical intermediates plays a significant role in the termination of oxidative chain reactions. Cancer a multifactorial disease when treated with a drug usually shows unsatisfactory or incomplete results due to side effects and drug resistance in cancer patients. Phytochemicals in combinational remedies by promoting ROS induction in cancer cells and anti-cancer drugs may reactivate the original signaling pathways and shows additive or synergistic effects in cancer treatments. Phytomedicine polypharmacology by providing multi-target drugs provides an opportunity for cancer management. The anticancer activities of herbal remedies or compounds taken from plants are found in the variability of oxidative stress. ROS can be produced endogenously from peroxisomes, mitochondria, and inflammatory cells and from UV light, cigarette smoke, industrial chemicals, ionizing radiation, and foods such as polycyclic-aromatic hydrocarbons, per oxidized lipids. , preservatives and drugs that contribute to the development of chronic diseases [68]. Phytocompound Curcumin separated from the root of

Curcuma longa (turmeric) has multiple functions like inhibiting rheumatism, hepatitis, colitis, arthritis, inflammation, and cancer [69].

Resveratrol which is present in Ampelidaceae, Solanaceae, Cannabacea, Vitaceae, Dipterocarpaceae, Fabaceae, Pinaceae, Polygonaceae, and Liliaceae [70] is found to be involved in various bioactivities like cardioprotection, antimicrobial, antioxidant, anti-obesity, anti-aging, anti-diabetes and anti-tumor [71, 72]. Paclitaxel is also known as Taxol isolated from Taxus brevifolia (Pacific yew) widely used as an anti-cancer drug in various cancer treatments [73].

Berberine (an isoquinoline alkaloid) isolated from Copis Chinensis (Huanglian) induced ROS production by xanthine oxidase and activates apoptosis in prostate cancer cells has significant anti-tumor activities [74]. Piperine present in spices like black pepper and long pepper shows anti-cancer activities in many cancers like lung, breast, prostate and colon by a ROS based mechanism. [75]. Noscapine (a benzylisoquinoline alkaloid of family Papaveraceae) is used as an antitussive drug. It can induce apoptosis in human breast cancer cells through NF-kB by increasing the Bax/Bcl-2 ratio [76].

Mistletoe extract obtained from Viscum album L., has been commonly used against cancer, inflammation, and AIDS in Europe. Its commercial products are available under trademark names of Iscador, Eurixor, Helixor, and Isorel [77].

Green tea is a communal drink in Asian countries which is made by the decoction of dry leaves of Camellia sinensis in hot water [78]. A prescription of 500mL of green tea was proved to be effective in colonocytes, hepatocytes, and lymphocytes protection against oxidative DNA damage [79]. Furthermore, green tea suppressed the appearance of the COX-2 (an inflammatory marker) in non-small cell lung cancer by upregulation of anti-inflammatory annexin -1 [80].

The antioxidant role of green tea extract (GTE) in human cancers was found to be correlated with noncoding intronic RNA expression. Lung cancer cells under GTE treatment showed a decrease in SOD enzymatic activity which suggests negative feedback to the antioxidant mechanism [81]. GTE not only suppresses ROS

produced by neutrophils by its antioxidant role but also works for suppression of tumor progression by eliminating oxidative stress from the tumor microenvironment (TME) [82]. Green tea has more bioactive polyphenol epigallocatechin gallate (EGCG) than black tea due to less fermentation during tea-leaf processing [83].

In a molecular docking experiment, EGCG showed a strong interaction with Arg-609 (a key residue) in the $STAT_3SH_2$ domain [84]. Effectiveness of green tea was reported in human colon, ovarian and other cancers additively or synergistically with chemotherapeutic drugs or non-steroidal anti-inflammatory drugs like sulindac and celecoxib in enhancing apoptosis [85]. Furthermore, EGCG showed clinical activity without side effects in women with symptomatic uterine fibroids [86].Broccoli isothiocyanate present in Brassica oleracea of family Brassicaceae showed anti-cancer activities in clinical trials [87].

Artemisinins are sesquiterpene trioxane lactones isolated from *Artemisia annua L.* are widely used as anti-malaria drugs and anti-cancer agents [88]. Artemisinins showed poor water solubility and a short half-life of almost 2.5 h in vivo. So in order to improve bioefficacy and bio tolerance of artemisinins, semisynthetic water-soluble compounds were developed like artesunate (ART), dihydroartemisinin, and fat-soluble derivatives like artemether and arteether [89].

Artemisinin inhibits tube formation of human-induced DNA damage, angiogenesis, immunostimulation, and reversal of multidrug resistance (MDR). Cellular heme (Fe^{2+} protoporphyrin IX) promoted the antimalarial mechanism of artemisinin. The cytotoxic activity of artemisinin in leukemia cells can be enhanced by intracellular endoperoxides by generation of ROS and initiation of mitochondrial membrane depolarization and arrest of sub-G0 / G1cell-cycle and activating caspases 3 and 7 [88]. Artemisinin inhibits the formation of tube of human umbilical vein endothelial cell (HUVEC) cells by inhibiting the growth of vascular endothelial factor (VEGF).

One hundred and twenty lung cancer patients (NSCLC) treated with vinorelbine (25 mg / m^2) or cisplatin (25 mg / m^2) in combination with artesunate (120 mg

/ day) may extend the progression period from 20 weeks to at 24 weeks, with an infection control rate ranging from 72.7 to 88.2% compared to monotherapy with any drug alone [90]. Antioxidants are potent ROS searchers and are probably involved in lowering high blood pressure [91].

Ascorbic acid (vitamin C) is a well-known water-soluble antioxidant can be used as therapy for hypertension [92]. Alpha tocopherol is an effective antioxidant in treatment of CVD and hypertension [93]. Other powerful antioxidants used as drugs are N- acetylcysteine (NAC), Nebivolol, Carvedilol, and Genistein are some examples [94].

2.7 *Artemisia annua L.*

Artemisia annua L. belongs to the family Asteraceae.

2.7.1 Taxonomic Classification

TABLE 2.2: The Following Table Shows Taxonomic Classification of *A.annua*

Serial No	**Domains**	**Eukarya**
1	Kingdom	Plantae
2	Division	Magnoliophyta
3	Class	Magnoliopsida
4	Order	Asteraceae
5	Genus	*Artemisia*
6	Species	*A.annua* [95].

2.7.2 Botanical Description

Asteraceae is the second large family of flowering plants. Artemisia is a significant genus of this family that contains almost 400 species which are either herbs or

shrubs. *A.annua* is a shrub of 50-150cm height with an annual cycle. *A.annua* is cultivated in the United States, Russia, East Africa, India, Brazil, and some other countries and it likes a temperate environment [96].

2.8 *Artemisia annua* in Pakistan

Artemisia annua L is commonly known as Afsantin or Afsantin jari in Pakistan and locally found in Gilgit, Baltistan, Kohat, and Skardu at an altitude from 1493 to 2286 m (Fig 2.4) . It is an annual herb of up to 190 cm in height with heavy branching and a strong aromatic smell.

Stems are hairy and leaves have punctate glands. Leaves are of two types, cauline and 3-pinnatipartite. In Pakistan, its flowering period is from August to September and have two types of florets;

1. Ray florets

Ray florets are 10-15 in number.

2. Disc florets

Disc florets are 15-25 in number with yellow or dark yellow color.

Ethnobotanical uses of this herb are;

1. Leaves are used for fever, cough, and the common cold.
2. The decoction of this plant is used for the treatment of Malaria.
3. Dried leaves are taken to treat diarrhea.
4. The whole plant is used as herbal medicines.
5. Local perfumes known as ettar are prepared from Afsantin's oil due to its pleasant fragrance [97].

FIGURE 2.4: *Artemisia annua L.* (A: Young plants, B: Flowers), Pakistan [97].

2.9 Molecular Docking

Molecular docking is a structure-based drug design method that predicts the binding affinity and mode between receptors and ligands and simulates the molecular interactions. Now, this technology is extensively used in the drug design research field. It is convenient for researchers to purchase, synthesize, and complete follow-up pharmacological tests by using the compounds database to screen potential pharmacophores.

Furthermore, molecular docking greatly improves efficiency and reduces the research cost. The basic theory of molecular docking is to simulate the optimal conformation according to the complementarity and pre-organization, which could predict and obtain the binding affinity and interactive mode between receptor and ligand [98]. The emergence of the reverse molecular docking technology significantly improves the drug target predictive capacity and understanding of the related molecular mechanism of the drug designing (Fig 2.6) [99]. The molecular docking software finds the optimal conformation and orientation according to complementarity and pre-organization with a specific algorithm, followed by applying a scoring function to predict the binding affinity and analyze the interactive mode (Fig 2.5) [100].

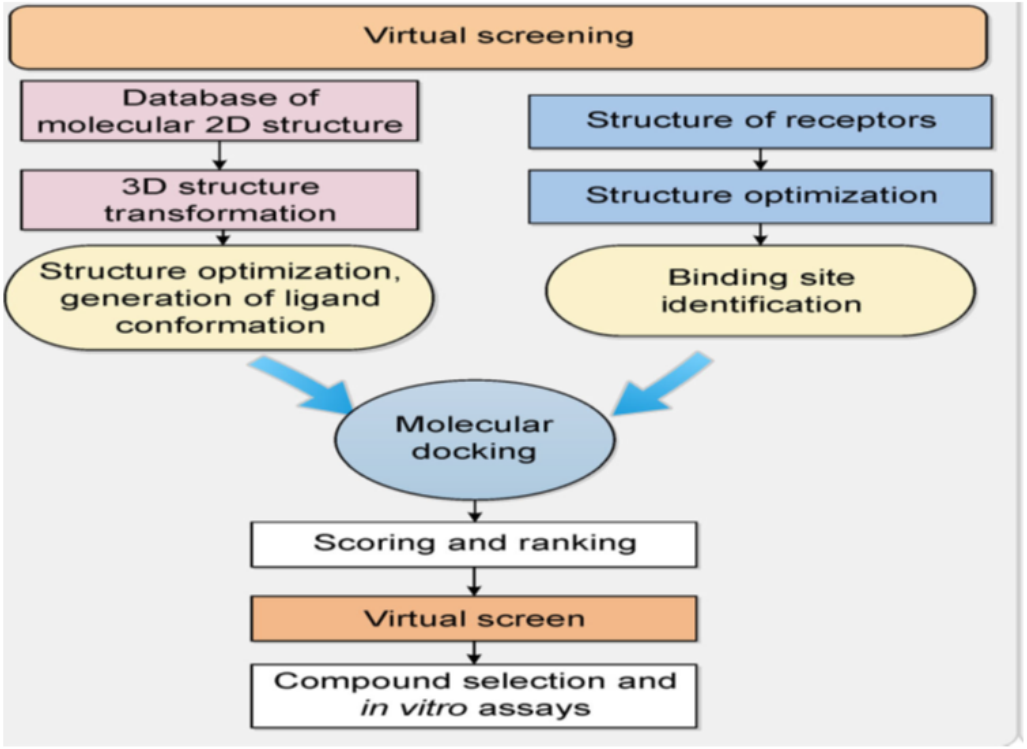

FIGURE 2.5: The Process of Molecular Docking [100].

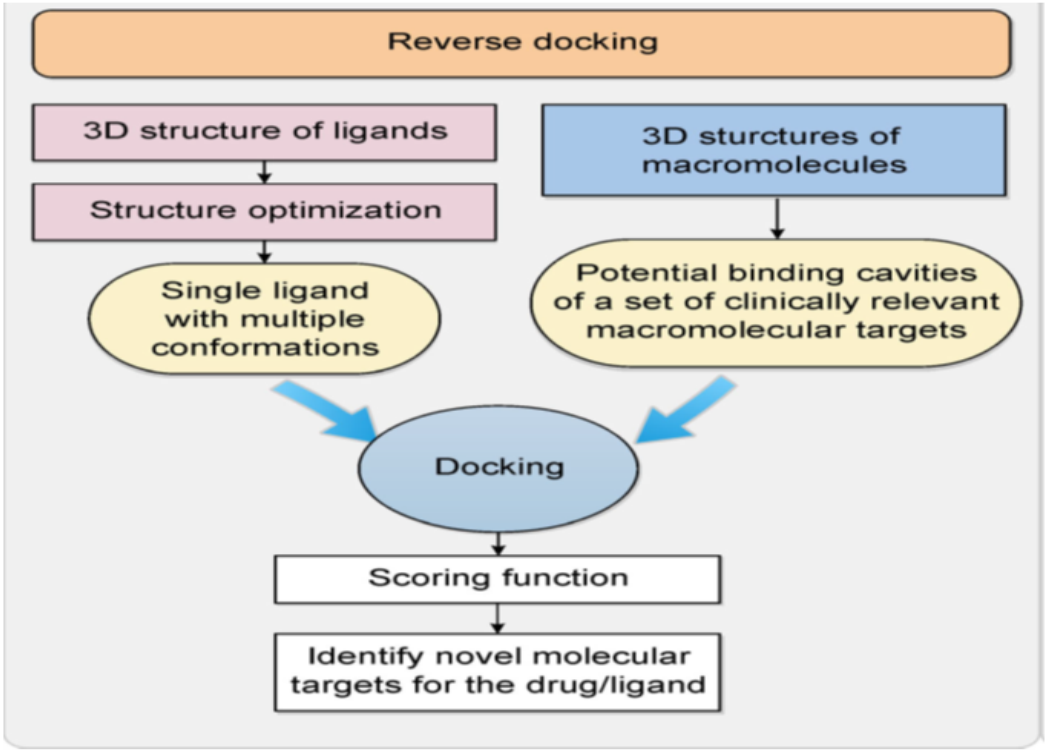

FIGURE 2.6: The Reverse Docking Technique [100].

Chapter 3

Methodology

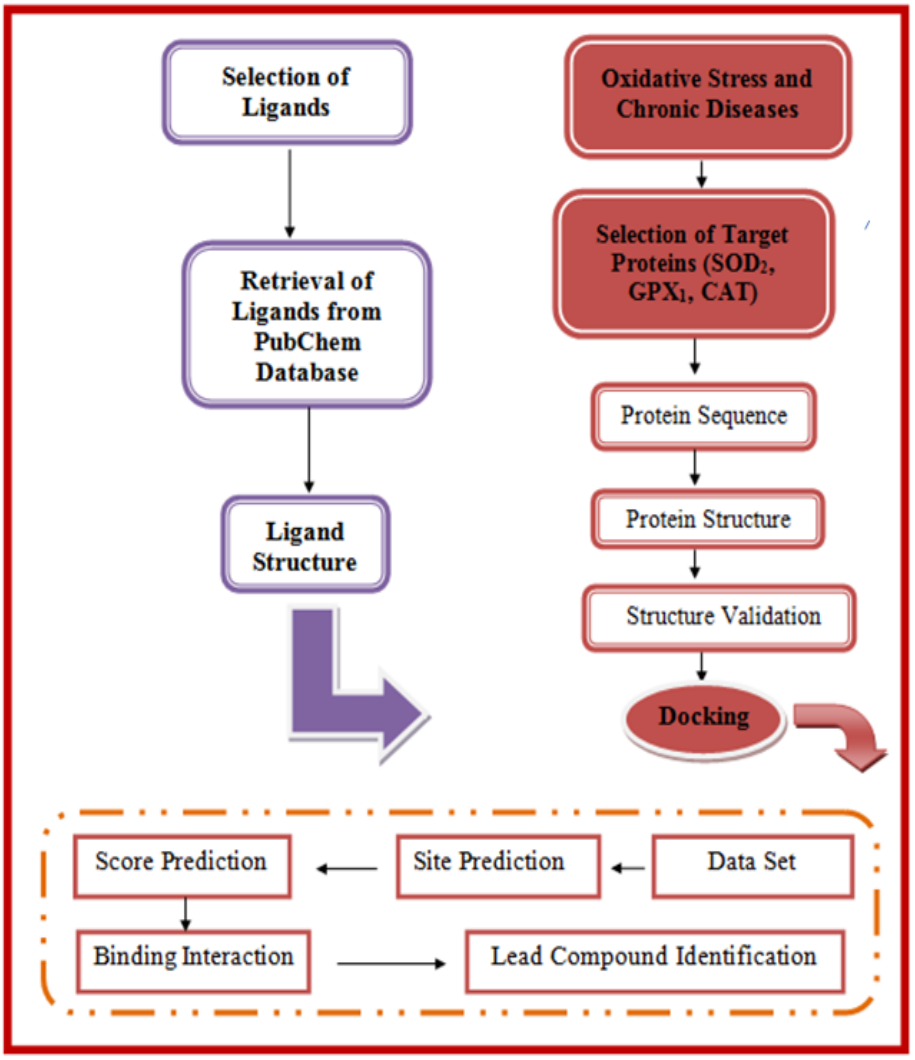

FIGURE 3.1: Flow Chart of Methodology (A).

3.1 Drug-Proposed Antioxidant Agent Comparison

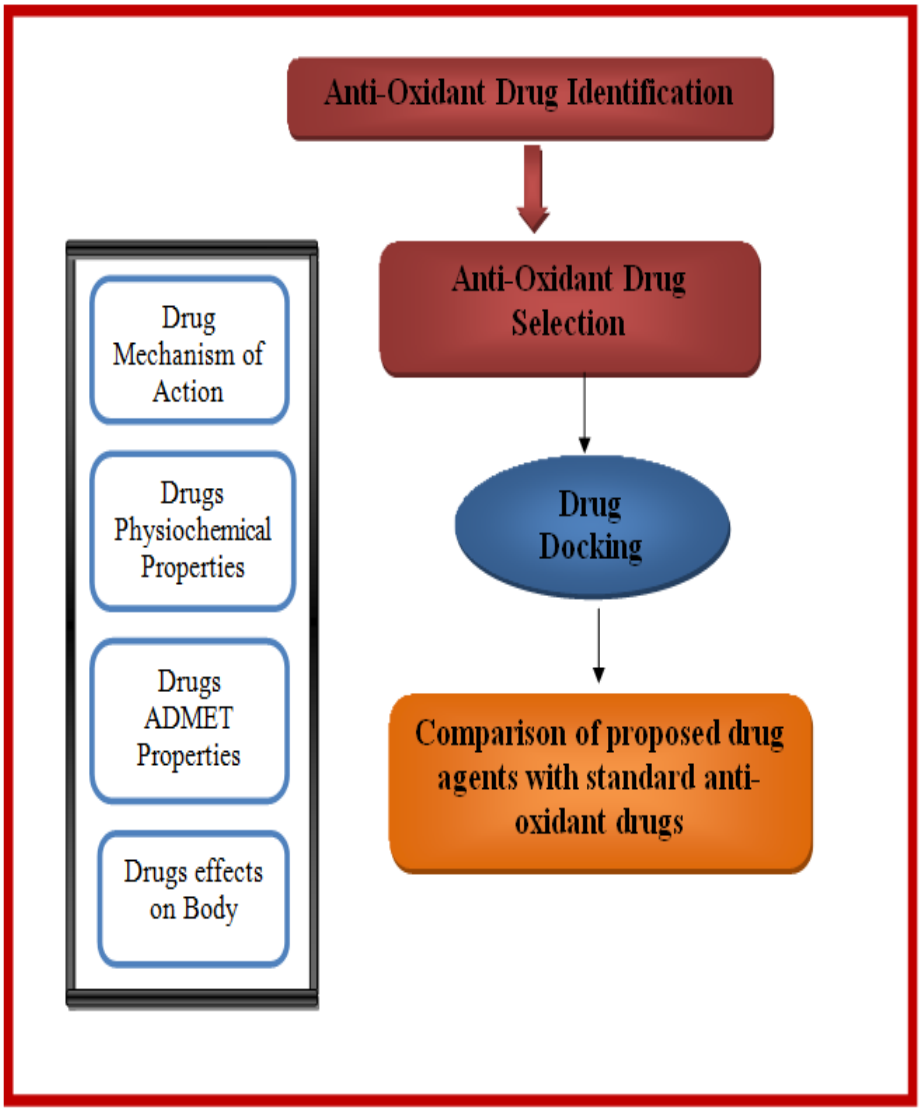

FIGURE 3.2: Flow Chart of Methodology (B).

3.2 Disease Selection

Oxidative stress is the main cause of many human diseases like diabetes, atherosclerosis, cancer, stroke, neurodegenerative diseases, and aging. Antioxidants are well

known as free-radical scavenging molecules not only correct damaged homeostasis, and prevent the onset of chronic diseases but also used as treatment of disease caused or progressed due to free radicals and oxidative stress. Beside these roles antioxidants also involve in the biosynthesis of defense enzymes [101].

3.3 Selection of Receptors

It is possible to prevent and cure chronic diseases related with oxidative stress with natural exogenous antioxidants which enrich body system and first line defense enzymes. These enzymes like Superoxide dismutase (SOD), Glutathione peroxidase (GPX), and Catalase (CAT) are selected as receptors in this research work. These human specific proteins have codes 2P4K, 2F8A, and 1DGH are available in the protein data bank (PDB) [102].

3.4 Primary Sequence Retrieval

The primary sequence of target proteins (2P4K, 2F8A, and 1DGH)was taken in FASTA format from protein sequence database UniProt (https://www.uniprot.org) under accession numbers P04179, P07203, and P04040 with residue length of 222, 203, and 527 amino acids respectively [103].

3.5 Analysis of Physiochemical Properties

Physiochemical properties are vital in determination of the functional role of protein. These properties of 2P4K, 2F8A, and 1DGH was predicted by a computational tool ProtParam [104]. Physiochemical properties such as molecular weight, theoretical pI, amino acid composition, total number of negatively and positively charged residues, atomic composition, total number of atoms, extinction coefficients, estimated half-life, instability index, aliphatic index, and grand average of

hydropathicity (GRAVY) were computed through ProtParam (http://web.expasy.org/protparam/) [105].

3.6 Functional Domain Identification of Targeted Proteins

Data base Interpro (https://www.ebi.ac.uk/interpro/) was used to identify the domains and functional sites of 2P4K, 2F8A,and 1DGH [106]. Interpro is a resource for functional analysis of protein sequences. Conserved domains are involved in sequence/structure/relationship [107].

3.7 3D Structure Predictions of Protein

3D Structures of targeted proteins were downloaded from RCSB PDB(www.rcsb.org) in PDB format. Protein Data Bank is a three-dimensional database of complex molecules of living organisms, such as proteins and nucleic acids.

3.8 Refining of Receptors

All extra water molecules, atoms, ions, and residues were removed from receptors Superoxide dismutase, SOD2 (2P4K), Glutathione peroxidase ,GPX1 (2F8A) ,and Catalase, CAT(1DGH) by using PYMOL software (v1.7.4.5) [108].

3.9 Retrieval of Chemical Structure of Ligands

Ligands (compounds of the selected plant) were searched out from PubChem, which is the World's largest repository of freely accessible chemical information database[109]. Their 3-D structures were downloaded from PubChem in SDF

format. Selected compounds were representing all the classes of compounds like phenols, terpenoids, essential oils, and steroids, etc.

3.10 Energy Minimization of Ligands

Energy minimization of ligands were carried out by chem pro software(chem 3D v 12.0.2) [109]. This was a mandatory step in the preparation of ligands for docking because unstable ligands will show unreliable vina scores in docking results.

3.11 Bioactivity Analysis of Ligands and Toxicity Measurement

Chemical compounds that were used as ligands follow the Lipinski's rule of five and likely to be used as active drug in humans [110]. The efficacy of a compound depends on its ADMET properties. pkCSM (http://biosig.unimelb.edu.au/pkcsm/prediction) is an online tool that helps to search out ADMET properties of the compounds [111]. The rules of five (all numbers are 5 or multiple of 5) are as under:

- The log P (octanol-water partition coefficient) value does not exceed 5.
- A molecular mass less than 500 daltons.
- No more than 5 hydrogen bond donors .
- No more than 10 hydrogen bond acceptors (all nitrogen or oxygen atoms).

3.12 Molecular Docking

Molecular docking is a structure-based drug design method that predicts the binding affinity and mode between receptors and ligands and simulates the molecular

interactions. Now, this technology is extensively used in the drug design research field. After preparing proteins and ligands ready for docking, docking were performed by CB dock which is a well trusted online blind auto docking tool [112]. The results and time required for docking is depend upon structures of receptors, ligands, refinements, and net speed. It may take several hours for a single result so patience was shown while doing docking. CB dock gave us five possible posses and receptor models and among these posses best one was selected by observing certain properties like vena score and size of cavity etc.

3.13 Interactions of Receptors and Ligands

After getting docking results, their interactions were predicted by ligplot software [113]. Before loading structures (best pose of docking and receptor) into ligplot plus (version.1.4.5), these were combined in pymol and their combined form was saved in a file with a proper name for later identification.

This file was browsed into ligplot and certain commands were given in order to get specific interactions of receptor and ligand. Ligplot then show hydrophobic and hydrophilic interactions along with hydrogen bonds and actively participating residues. Furthermore, bond lengths were also be predicted by ligplot. This software automatically generates diagrams of the protein-ligand interactions of the ligands provided in the PDB file [114].

3.14 Ligand ADME Properties

pkCSM is a freely accessible web server (http://structure.bioc.cam.ac.uk/pkcsm), which uses graph-based signatures to develop analytical models of ADMET properties for development of drug. This server rapidly evaluate pharmacokinetic and toxicity properties of selected ligands [115].

3.15 Lead Compound Identification

In this research work after completion of docking, toxicity studies and result analysis, most potential antioxidants in each case of proteins were identified as "lead compounds".

3.16 Antioxidant Drug Identification

The antioxidant drug identification means identification of drugs that are used for oxidative stress and related diseases inhibition, prevention, and treatment. Drug bank, Uni Prot (Uni Prot KB), and KEGG databases are used for this purpose. KEGG (Kyoto Encyclopedia of genes and genomes) is a database resource (http://www.genome.ad.jp/kegg/) which has GENES, PATHWAY, and LIGAND databases. LIGAND database is about chemical compounds, enzyme molecules and enzymatic reactions [116].

3.17 Antioxidant Drug Selection

The identified drugs are filtered to select most effective drug. Drug physiochemical properties, ADMET properties, side effects and mechanism of action were collected from PubChem, pkCSM, Drug bank, and KEGG databases, respectively [117].

3.18 Antioxidant Drug Docking

The selected antioxidant drugs are docked with SOD,GPX, and CAT proteins to identify the antioxidative potential. Docking is done by CB Dock (cavity-detection blind docking) which is an online docking server [112].

3.19 FDA Approved Drug-Proposed Antioxidant Agent Comparison

The comparison between selected antioxidant drugs and proposed antioxidant agents is done by comparing docking results, physiochemical properties and ADMET properties [118]. The comparison is made easy by Byju's "Greater Than Calculator" online learning app (byjus.com/greater-than-calculator/) which helps in identifying smaller and greater values.

Chapter 4

Results and Discussions

4.1 Structure Modeling

4.1.1 Primary Sequence Retrieval

Primary sequence of target proteins (SOD2, GPX1, and CAT) are taken in FASTA format from Uniprot database (http://www.uniprot.org) under accession number P04179, P07203, P04040 with 222, 203, and 527 residues length.

>sp |P04040| CATA-HUMAN Catalase OS=Homo sapiens OX=9606 GN=CAT PE=1 SV=3

MADSRDPASDQMQHWKEQRAAQKADVLTTGAGNPVGDKLNVITVGPRGP
LLVQDVVFTDEMAHFDRERIPERVVHAKGAGAFGYFEVTHDITKYSKAKVF
EHIGKKTPIAVRFSTVAGESGSADTVRDPRGFAVKFYTEDGNWDLVGNNTP
IFFIRDPILFPSFIHSQKRNPQTHLKDPDMVWDFWSLRPESLHQVSFLFSDRG
IPDGHRHMNGYGSHTFKLVNANGEAVYCKFHYKTDQGIKNLSVEDAARLSQ
EDPDYGIRDLFNAIATGKYPSWTFYIQVMTFNQAETFPFNPFDLTKVWPHK
DYPLIPVGKLVLNRNPVNYFAEVEQIAFDPSNMPPGIEASPDKMLQGRLFAY
PDTHRHRLGPNYLHIPVNCPYRARVANYQRDGPMCMQDNQGGAPNYYPN

SFGAPEQQPSALEHSIQYSGEVRRFNTANDDNVTQVRAFYVNVLNEEQRKR
LCENIAGHLKDAQIFIQKKAVKNFTEVHPDYGSHIQALLDKYNAEKPKNAIH
TFVQSGSHLAAREKANL.

>sp |P04179| SODM-HUMAN Superoxide dismutase [Mn], mitochondrial OS=Homo sapiens OX=9606 GN=SOD2 PE=1 SV=3

MLSRAVCGTSRQLAPVLGYLGSRQKHSLPDLPYDYGALEPHINAQIMQLHHSK
HHAAYVNNLNVTEEKYQEALAKGDVTAQIALQPALKFNGGGHINHSIFWTNL
SPNGGGEPKGELLEAIKRDFGSFDKFKEKLTAASVGVQGSGWGWLGFNKER
GHLQIAACPNQDPLQGTTGLIPLLGIDVWEHAYYLQYKNVRPDYLKAIWNV
INWENVTERYMACKK.

>sp |P07203| GPX1-HUMAN Glutathione peroxidase 1 OS=Homo sapiens OX=9606 GN=GPX1 PE=1 SV=4

MCAARLAAAAAAAQSVYAFSARPLAGGEPVSLGSLRGKVLLIENVASLUGTTV
RDYTQMNELQRRLGPRGLVVLGFPCNQFGHQENAKNEEILNSLKYVRPGGGF
EPNFMLFEKCEVNGAGAHPLFAFLREALPAPSDDATALMTDPKLITWSPVCRN
DVAWNFEKFLVGPDGVPLRRYSRRFQTIDIEPDIEALLSQGPSCA.

Superoxide dismutase 2 (SOD2), Glutathione peroxidase 1(GPX1),and Catalase (CAT) are selected as the target proteins and Phenols (Quinic acid, Cynaroside, kaempferol,Luteolin, Quercetin, Coumarin), Flavonoids(Rutin, Apigenin, Isorhamnetin, Mearnsetin, Artemetin, Casticin, Chrysosplenol D, Quercetagetin, Retusin), Sesquiterpenes (Artemisinin, Arteannuin B, Artesunate, Artemisinic acid), Monoterpenes (Limonene, Myrtenol, Alpha-terpinene), Triterpenoid (Friedelin, Epi-friedelanol), Umbelliferone (Scopolin, Scopoletin), Coumarins (Scoparone), Steroid derivative (Stigmasterol), Artemisinin derivatives (Arteether, Artemether, Artemetin, Deoxy artemisinin) and Essential oils (Camphor, Germacrene D, Trans-pinocarveol, Beta-selinene, Beta-caryophyllene, Artemisia ketone) are selected as the ligands.

4.1.2 Physiochemical Characterization of SOD2, GPX1, and CAT

ProtParam is a tool of Expasy which is used online for the computation of various physical and chemical parameters for a given protein stored in Swiss-prot or TrEMBL or for a user entered protein sequence. The computed parameters include the molecular weight, amino acid composition, theoretical pl, atomic composition, extinction coefficient, estimated half-life, instability index, aliphatic index and grand average of hydropathicity (GRAVY). The calculated pl greater than 7 represents the basic nature of the protein while less than 7 shows acidic nature of protein. Extinction coefficient represents light absorption. Instability index if less than 40 shows stability of the protein while greater than 40 indicates the instability of protein [119]. The physiochemical properties of Superoxide dismutase 2, Glutathione peroxidase 1 and Catalase are shown in Table 4.1, 4.2, and 4.3 respectively.

Table 4.1: Physiochemical Properties of Superoxide Dismutase (SOD2).

MW	**PI**	**NR**	**PR**	
24750.14	8.35	20	22	
Ext.Co1	**Ext.Co2**	**Instability index**	**Aliphatic index**	**GRAVY**
48025	47900	40.26	84.41	-0.407

Table 4.2: Physiochemical Properties of Glutathione Peroxidase (GPX1).

MW	**PI**	**NR**	**PR**	
22088.17	6.15	21	20	
Ext.Co1	**Ext.Co2**	**Instability index**	**Aliphatic index**	**GRAVY**
17210	16960	47.96	86.11	-0.070

TABLE 4.3: Physiochemical Properties of Catalase (CAT).

MW	**PI**	**NR**	**PR**	
59756.17	6.90	61	59	
Ext.Co1	**Ext.Co2**	**Instability index**	**Aliphatic index**	**GRAVY**
64540	64290	30.15	68.29	-0.586

The aliphatic index represents the aliphatic content of a protein. The high value of the aliphatic index indicates the thermo stability of the protein. Molecular weight contains both positive and negative charged residues of protein.

At 280nm the ranging extinction coefficient of 73980, 67965, 20105, and 112270 indicates Tyr and Trp high concentration [120]. Low GRAVY shows better interaction with water molecules. All these parameters which are selected for this research work are taken according to previous research work.

MW stands for molecular weight, pl for theoretical isoelectric point (pH at which protein is neutral, without any charge), NR for total number of negatively charged residues (Asp + Glu),PR for total number of positively charged residues (Arg + Lys), Ext.Co1 for extinction coefficients when assuming all pairs of Cys residues form cystines, Ext.Co2 for extinction coefficients when assuming all Cys residues are reduced, and GRAVY for grand average of hydropathicity.

4.1.3 3D Structure Predictions of Protein

3D Structures of targeted proteins were downloaded from RCSB PDB in PDB format. Protein Data Bank is a three-dimensional database of complex molecules of living organisms, such as proteins and nucleic acids.

I-TASSER (Iterative threading ASSEmbly Refinement) is a hierarchical approach to protein structure prediction and structure-based function annotation. This

online server firstly identifies the structural templates from the PDB by multiple threading approach LOMETS, with full-length atomic models that are constructed by iterative template-based fragment assembly simulations. This server has been widely used for protein structure and function predictions in biological and biomedical investigations.

I-TASSER predicts regions of secondary structure like alpha helix, beta sheet and coils from the amino acid sequence [121]. I-TASSER server team mails complete results of job id with five models and on the basis of c-score best 3D structural model can be easily selected.

4.1.4 Functional Domain Identification of Proteins

Data base Interpro was used to identify the domains and functional sites of 2P4K, 2F8A,and 1DGH. Interpro is a resource for functional analysis of protein sequences. Conserved domains are involved in sequence/structure/relationship. Proteins can have more than one functional domain that perform different functions.

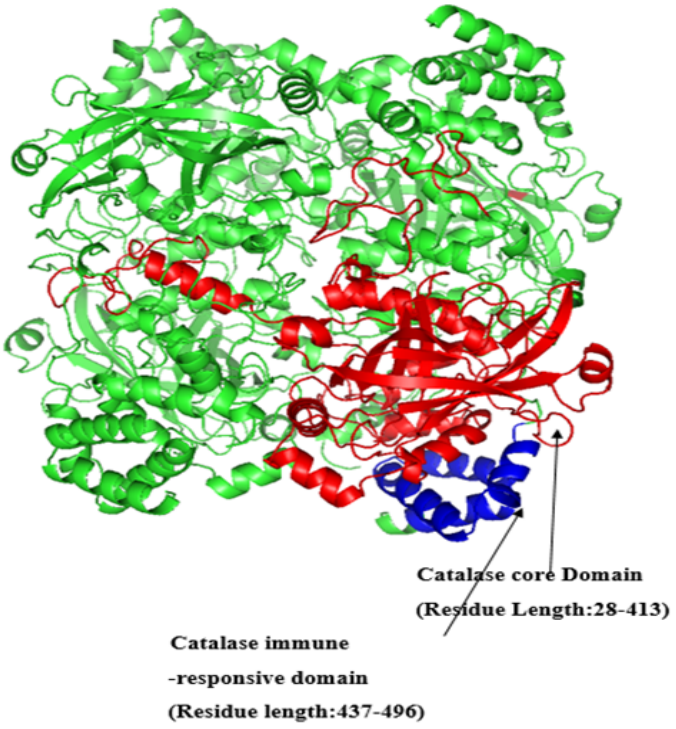

FIGURE 4.1: Functional Domains of CAT With Residue Lengths.

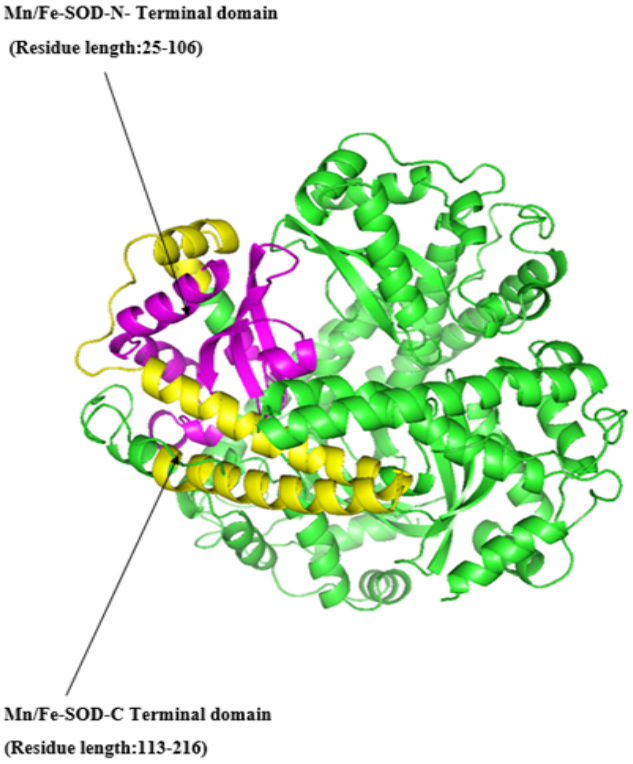

FIGURE 4.2: Functional Domains of SOD2 With Residue Lengths.

FIGURE 4.3: Functional Domains of GPX1 With Residue Lengths.

Functional domain is the active part of a protein that is involved in interactions of proteins with other substances. Catalase has two functional domains that are catalase core domain and catalase immune-responsive domain starting from 28 and 437 amino acids and ending at 413 and 496 amino acids sequence respectively (Fig 4.1).

Superoxide dismutase 2 also has two functional domains which are Mn/Fe-SOD-C Terminal domain with residue length 113-216 and Mn/Fe-SOD-N Terminal domain with residue length 25-106 (Fig 4.2). Glutathione peroxidase 1 belongs to Glutathione peroxidase family having a functional domain GSH-Peroxidase with 15-192 residue length (fig.4.3 & table 4.4).

TABLE 4.4: Functional domain identification of Superoxide Dismutase, Catalase Glutathione Peroxidase 1.

S.No	**Name**	**Domain**	**Start**	**End**
1	Superoxide Dismutase 2	Mn/Fe-SOD-N & Mn/Fe-SOD-C	25&113	106 & 216
2	Catalase	Catalase core domain & Catalase immune- responsive domain	28&437	413 & 496
3	Glutathione Peroxidase 1	GSH-Peroxidase	15	192

4.1.5 Template Selection

The 3 D structures of the selected templates are taken from the protein data bank (PDB) and listed in table 4.5.

TABLE 4.5: Selected PDB Templates Structures

S.No	Templates	Resolution	PDB ID	Structure
1	Contribution to Structure and Catalysis of Tyrosine 34 in Human Manganese Superoxide Dismutase	1.48 Å	2P4K	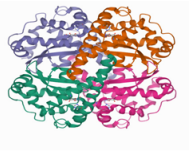
2	Human Erythrocyte Catalase 3-Amino-1,2,4-Triazole Complex.	2.00 Å	1Z9H	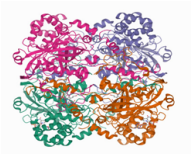
3	Crystal structure of the selenocysteine to glycine mutant of human glutathione peroxidase 1.	1.50 Å	2F8A	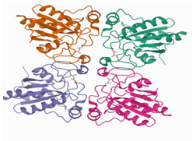

4.1.6 Structure of Proteins Refined for Docking

The selected 3D structures are refined by pymol for docking are shown in figure 4.4, 4.5 & 4.6 respectively.

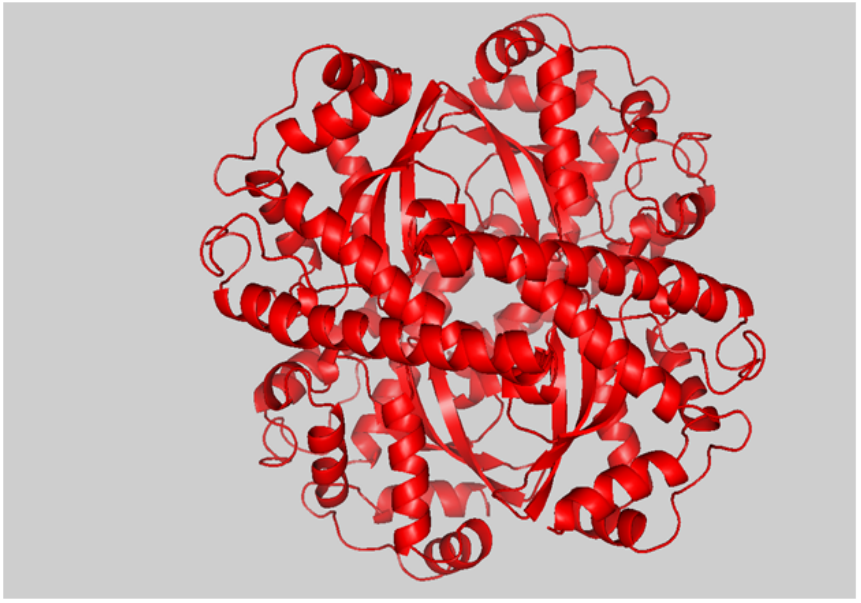

FIGURE 4.4: Refined 3D Structure of 2P4K (SOD2).

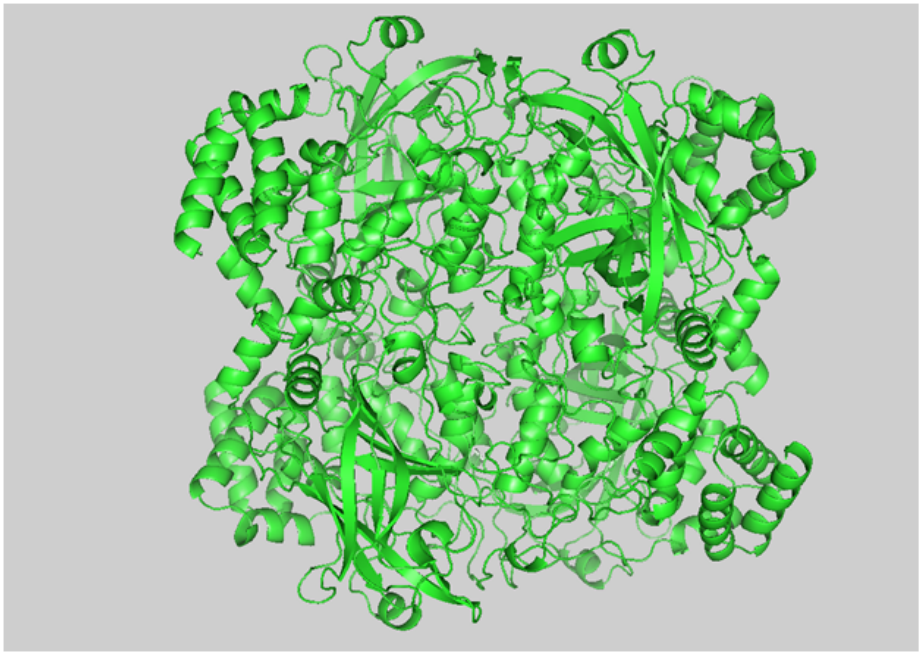

FIGURE 4.5: Refined 3D Structure of 1DGH (CAT).

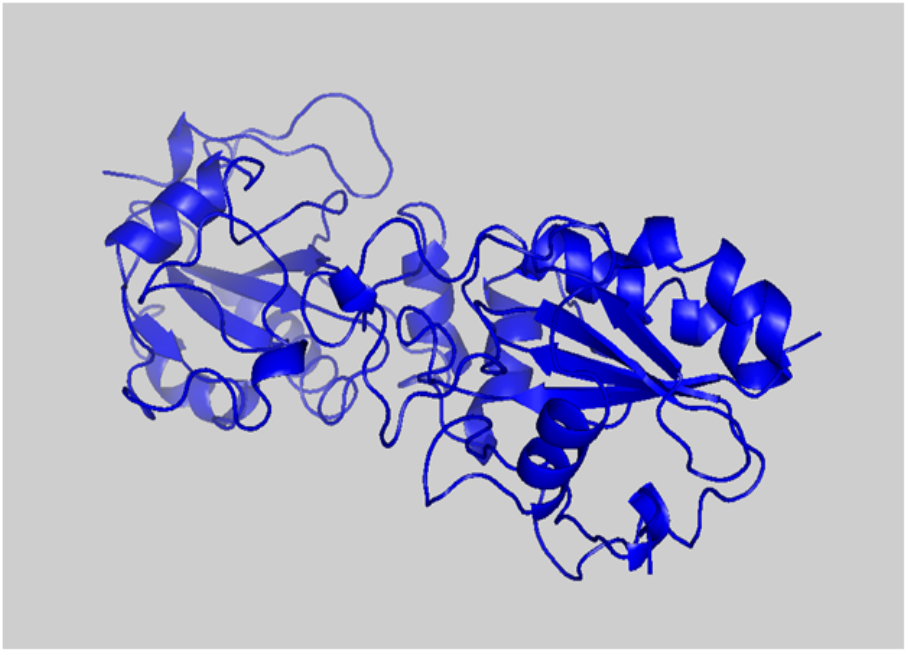

FIGURE 4.6: Refined 3D Structure of 2F8A (GPX1).

4.2 Ligand Selection

Protein data bank contains a large amount of protein ligand complex, especially for the protein target. Therefore, the selection of ligands is based on the best resolution of the structure, the chemical class of the co-crystal ligand bound to the protein structure and the best binding anity. Conformational selection is a process in which ligand selectively binds to one of these conformers, strengthening it and increasing its population with respect to the total population of the protein is ultimately resulting in the final observed complex.

Ligands (compounds of the selected plant) were searched out from PubChem, which is the world's largest freely accessible chemical information database. Their 3-D structures were downloaded from PubChem in SDF format. Selected compounds were representing all the classes of compounds like phenols, terpenoids, essential oils, and steroids, etc.

After selection of ligands then we do energy minimization of ligands which were carried out by chem pro software(chem 3D v 12.0.2). This was a mandatory step in the preparation of ligands for docking because unstable ligands will show unreliable vina scores in docking results. Bioactive antioxidant compounds of Artemisia annua are selected as ligands for the present study (Table 4.6, 4.7, 4.8 & 4.9).

The 3 D structures and information of selected ligands that are Alpha terpinene, Apigenin, Arteannuin B, Arteether, Artemether, Artemetin, Artemisia ketone, Artemisinin, Artemisinic acid, Artesunate, Beta caryophyllene, Beta selinene, Camphor, Casticin, Chrysosplenol D, Coumarin, Cynaroside, Deoxy artemisinin, Epifriedelanol, Friedelin, Germacrene D, Isorhamnetin, Kaempferol, Limonene, Luteolin, Mearnsetin, Myrtenol, Quercetagetin, Quercetin, Quinic acid, Retusin, Rutin, Scoparone, Scopoletin, Scopolin, Stigmasterol, Transpinocarveol are downloaded from PubChem. This database (https://pubchem.ncbi.nlm.nih.gov) is a public repository for information on chemical substances and their biological activities [122].

TABLE 4.6: Selected Ligands With Structural Information.

S.No	Name	Molecular Formula	Molecular Weight	Structure
1	Alpha-Terpinene	$C_{10}H_{16}$	136.23 g/mol	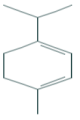
2	Apigenin	$C_{15}H_{10}O_5$	270.24 g/mol	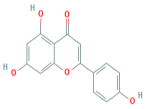
3	Arteannuin B	$C_{15}H_{20}O_3$	248.32 g/mol	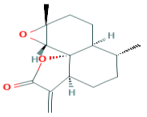
4	Arteether	$C_{17}H_{28}O_5$	312.4 g/mol	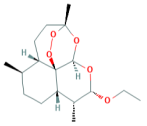
5	Artemether	$C_{16}H_{26}O_5$	298.3 g/mol	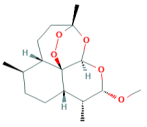
6	Artemetin	$C_{20}H_{20}O_8$	388.4 g/mol	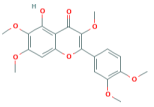
7	Artemisia Ketone	$C_{10}H_{16}O$	152.23 g/mol	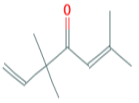
8	Artemisinic Acid	$C_{15}H_{22}O_2$	234.33 g/mol	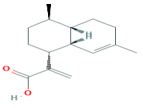
9	Artemisinin	$C_{15}H_{22}O_5$	282.33 g/mol	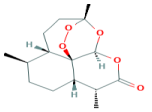
10	Artesunate	$C_{19}H_{28}O_8$	384.4 g/mol	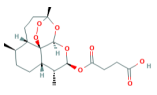

TABLE 4.7: Selected Ligands With Structural Information.

S.No	Name	Molecular Formula	Molecular Weight	Structure
11	Beta-Caryophyllene	$C_{15}H_{24}$	204.35 g/mol	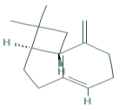
12	Beta-Selinene	$C_{15}H_{24}$	204.35 g/mol	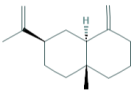
13	Camphor	$C_{10}H_{16}O$	152.23 g/mol	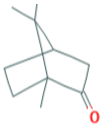
14	Casticin	$C_{19}H_{18}O_8$	374.3 g/mol	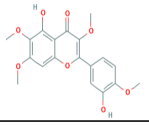
15	Chrysosplenol D	$C_{18}H_{16}O_8$	360.3 g/mol	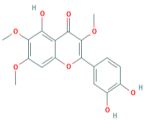
16	Coumarin	$C_9H_6O_2$	146.14 g/mol	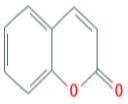
17	Cynaroside	$C_{21}H_{20}O_{11}$	448.4 g/mol	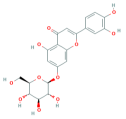
18	Deoxyartemisinin	$C_{15}H_{22}O_4$	266.33 g/mol	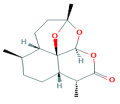
19	Epifriedelanol	$C_{30}H_{52}O$	428.7 g/mol	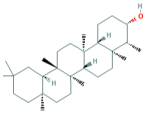
20	Friedelin	$C_{30}H_{50}O$	426.7 g/mol g/mol	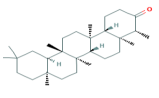

TABLE 4.8: Selected Ligands With Structural Information.

S.No	Name	Molecular Formula	Molecular Weight	Structure
21	Germacrene D	$C_{15}H_{24}$	204.35 g/mol	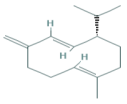
22	Isorhamnetin	$C_{15}H_{12}O_7$	316.26 g/mol	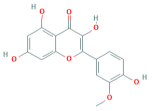
23	Kaempferol	$C_{15}H_{10}O_6$	286.24 g/mol	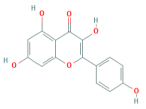
24	Limonene	$C_{10}H_{16}$	136.23 g/mol	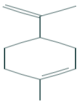
25	Luteolin	$C_{15}H_{10}O_6$	286.24 g/mol	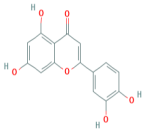
26	Mearnsetin	$C_{16}H_{12}O_8$	332.26 g/mol	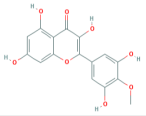
27	Myrtenol	$C_{10}H_{16}O$	152.23 g/mol	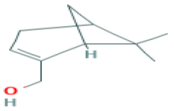
28	Quercetagetin	$C_{15}H_{10}O_8$	318.23 g/mol	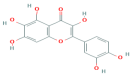
29	Quercetin	$C_{15}H_{10}O_7$	302.23 g/mol	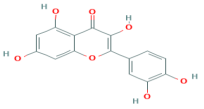
30	Quinic Acid	$C_7H_{12}O_6$	192.17 g/mol	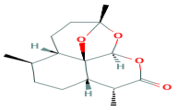
31	Retusin	$C_{19}H_{18}O_7$	358.3 g/mol	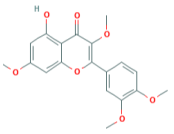
32	Rutin	$C_{27}H_{30}O_{16}$	610.5 g/mol	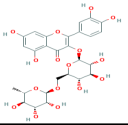

TABLE 4.9: Selected Ligands With Structural Information.

S.No	Name	Molecular Formula	Molecular Weight	Structure
33	Scoparone	$C_{11}H_{10}O_4$	206.19 g/mol	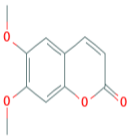
34	Scopoletin	$C_{10}H_8O$	192.17 g/mol	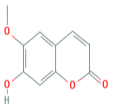
35	Scopolin	$C_{16}H_{18}O_9$	354.31 g/mol	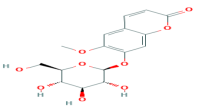
36	Stigmasterol	$C_{29}H_{48}O$	412.7 g/mol	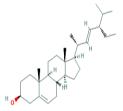
37	TransPinocarveol	$C_{10}H_{16}O$	152.23 g/mol	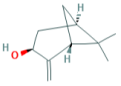

4.3 Virtual Screening and Toxicity Prediction

Drug like and non-drug like compounds are separated by following certain parameters like Lipinski's rule of five, and ADMET properties test [123]. The original rules of five deals with four physicochemical parameters (MWT $\leq$ 500, log P$\leq$ 5, H-bond donors $\leq$ 5, H-bond acceptors $\leq$ 10) which are associated with orally active compounds. The meaning of drug like is dependent on mode of administration [110]. A compound considered as drug likeness if it complying with three or more of the RO5. If a compound violates more than two of these rules ,it is assumed to be poorly absorbed [124]. Table 4.10 & 4.11 shows the applicability of Lipinski's rule of five on selected ligands. All ligands follow these rules. Some ligands complying with 3 rules like Epifriedelanol , Stigmasterol, and Friedelin have log P value more than 5 and Quercetagetin has 6 H- bond donors. There are two

ligands who complying with only 1 and 2 rules, these are Rutin and Cynaroside respectively. Rutin has M.W 610 dalton, 16 H-bond acceptors and 10 H-bond donors. Cynaroside has 11 H-bond acceptors and 7 H-bond donors. Rutin is not considered a drug likeness compound.

Table 4.10: Applicability of Lipinski Rule on Ligands.

S.No	**Ligand**	**logP Value**	**Molecular Weight**	**H-Bond Acceptor**	**H-bond Donor**
1	Alpha Terpinene	3.3089	136.238 g/mol	0	0
2	Apigenin	2.5768	270.24 g/mol	5	3
3	Arteannuin B	2.4518	248.322 g/mol	3	0
4	Arteether	3.2309	312.406 g/mol	5	0
5	Artemether	2.8408	298.379 g/mol	5	0
6	Artemetin	3.2086	388.372 g/mol	8	1
7	Artemisia Ketone	2.7339	152.237 g/mol	1	0
8	Artemisinic acid	3.6458	234.339 g/mol	1	1
9	Artemisinin	2.3949	282.336 g/mol	5	0
10	Artesunate	2.6024	384.425 g/mol	7	1
11	Beta Caryophyllene	4.7252	204.357 g/mol	0	0
12	Beta Selinene	4.7252	204.357 g/mol	0	0
13	Camphor	2.4017	152.237 g/mol	1	0
14	Casticin	2.9056	374.345 g/mol	8	2
15	Chrysosplenol-D	2.6026	360.318 g/mol	8	3
16	Coumarin	1.793	146.145 g/mol	2	0
17	Cynaroside	-0.2445	448.38 g/mol	11	7

TABLE 4.11: Applicability of Lipinski Rule on Ligands.

S.No	Ligand	logP Value	Molecular Weight	H-Bond Acceptor	H-bond Donor
18	Deoxyartemisinin	2.4633	266.337 g/-mol	4	0
19	Epifriedelanol B	8.2488	428.745 g/-mol	1	1
20	Friedelin	8.457	426.729 g/-mol	1	0
21	Germacrene-D	4.8913	204.357 g/-mol	0	0
22	Isorhamnetin	2.291	316.265 g/-mol	7	4
23	Kaempferol	2.2824	152.237 g/-mol	6	4
24	Limonene	3.3089	136.238 g/-mol	0	0
25	Luteolin	2.2824	286.239 g/-mol	6	4
26	Mearnsetin	1.9966	332.264 g/-mol	8	5
27	Myrtenol	1.9711	152.237 g/-mol	1	1
28	Quercetagetin	1.6936	318.237 g/-mol	8	6
29	Quercetin	1.988	302.238 g/-mol	7	5
30	Quinic acid	-2.3214	192.167 g/-mol	5	5
31	Retusin	3.2	358.346 g/-mol	7	1
32	Rutin	-1.6871	610.521 g/-mol	16	10
33	Scparone	1.8102	206.197 g/-mol	4	0
34	Scopoletin	1.5072	192.17 g/mol	4	1
35	Scopolin	-1.0197	354.311 g/-mol	9	4
36	Stigmasterol	7.8008	412.702 g/-mol	1	1
37	Transpinocarveol	1.9695	152.237 g/-mol	1	1

4.3.1 Toxicity Prediction

PkCSM is an online tool used to find the ADMET (Absorption, Distribution, Metabolism, Excretion, and Toxicity) properties of bioactive compounds and drugs. The maximum tolerated dose (MRTD) provides a measure of toxic chemical limits on individuals. This will help in directing the first recommended dose of the treatment regimen in phase 1 clinical trials. MRTD is expressed in the form of logarithms (log mg / kg / day). In a given compound MRTD less than or equal to 0.477log (mg / kg / day) is considered to be lower and higher if it is higher than 0.477 log (mg / kg / day).

The hERG I & II inhibitors model is said to cause the inhibition of potassium channels induced by the h ERG (human ether-a-go-go gene) are the main causes of the development of chronic QT syndrome leading to fatal ventricular arrhythmia. The inhibition of h ERG channels has led to the withdrawal of many items from the pharmaceutical market. LD50 is the quantity of a compound that causes the deaths of 50% of experimental animals (mice).

The LD50 (mol / kg) predicts toxicity of a probable compound where as LOAEL aims to identify the lowest dosage of a compound with a significant adverse effect. Exposure to low to moderate chemical doses for a long time is very important in medicine and is expressed in a log (mg / kg-bw / day).

Hepatotoxicity reveals drug-induced liver damage and is a major safety concern for drug development. Skin sensitivity is a potential adverse effect of skin care & applied products. T. pyriformis is a protozoans bacteria, whose toxin is often used as a toxic endpoint (IGC50) and inhibits 50% growth. p IGC50 (negative concentration logarithm required to prevent 50% growth) in log ug / L predicted value $>$ - 0.5 log ug / L is considered toxic. The lethal concentrations (LC50) represent the concentration of molecules needed to cause the death of 50% of Flathead Minnows (small bait fishes). In Minnow toxicity LC50 values below 0.5 m M (log LC 50 $<$-0.3) are regarded as high acute toxicity [125]. Toxicity predicted values of selected ligands were listed in tables 4.12 to 4.48.

4.3.1.1 Alpha Terpinene, Apigenin and Arteannuin B

Alpha Terpinene shows high Max. tolerated dose (human) 0.756 log mg/kg/day which is greater than 0.477 log mg/kg/day standard max. tolerated dose. Apigenin & Arteannuin B shows low Max. tolerated doses.

All the three ligands are supporters of potassium channels and non-hepatotoxic. T.pyriforms & Minnow toxicity are also within recommended range. Toxicity predicted values of Alpha Terpinene, Apigenin and Arteannuin B. are shown in Table 4.12, 4.13 & 4.14.

Table 4.12: The Toxicity Values of Alpha Terpinene

S.No	Model Name	Predicted Values
1	Max.tolerated dose (human)	0.756 mg/Kg
2	hERG I inhibitor	No
3	hERG II inhibitor	No
4	Oral rat acute toxicity	1.766 mol/Kg
5	Oral rat chronic toxicity	2.394 mg/Kg
6	Hepatoxicity	No
7	Skin sensitisation	No
8	t.pyriformis toxicity	0.627 log ug/L
9	Minnow toxicity	0.906 log mM

Table 4.13: The Toxicity Values of Apigenin.

S.No	Model Name	Predicted Values
1	Max.tolerated dose (human)	0.328 mg/Kg
2	hERG I inhibitor	No
3	hERG II inhibitor	No
4	Oral rat acute toxicity	2.45 mol/Kg
5	Oral rat chronic toxicity	2.298 mg/Kg
6	Hepatoxicity	No
7	Skin sensitisation	No
8	t.pyriformis toxicity	0.38 log ug/L
9	Minnow toxicity	2.432 log mM

Table 4.14: The Toxicity Values of Arteannuin B.

S.No	Model Name	Predicted Values
1	Max.tolerated dose (human)	0.195 mg/Kg
2	hERG I inhibitor	No
3	hERG II inhibitor	No
4	Oral rat acute toxicity	2.052 mol/Kg
5	Oral rat chronic toxicity	1.589 mg/Kg
6	Hepatoxicity	No
7	Skin sensitisation	No
8	t.pyriformis toxicity	0.45 log ug/L
9	Minnow toxicity	1.53 log mM

4.3.1.2 Arteether, Artemether and Artemetin

All these compounds shows their predicted values of all the nine models within safe region. Their max. tolerated doses are also low. Toxicity predicted values of Arteether, Artemether and Artemetin are shown in Table 4.15, 4.16 & 4.17.

Table 4.15: The Toxicity Values of Arteether.

S.No	Model Name	Predicted Values
1	Max.tolerated dose (human)	0.019 mg/Kg
2	hERG I inhibitor	No
3	hERG II inhibitor	No
4	Oral rat acute toxicity	2.32 mol/Kg
5	Oral rat chronic toxicity	0.952 mg/Kg
6	Hepatoxicity	No
7	Skin sensitisation	No
8	t.pyriformis toxicity	0.347 log ug/L
9	Minnow toxicity	1.799 log mM

Table 4.16: The Toxicity Values of Artemether.

S.No	Model Name	Predicted Values
1	Max.tolerated dose (human)	0.074 mg/Kg
2	hERG I inhibitor	No
3	hERG II inhibitor	No
4	Oral rat acute toxicity	2.429 mol/Kg
5	Oral rat chronic toxicity	1.043 mg/Kg
6	Hepatoxicity	No
7	Skin sensitisation	No
8	t.pyriformis toxicity	0.304 log ug/L
9	Minnow toxicity	0.587 log mM

Table 4.17: The Toxicity Values of Artemetin.

S.No	Model Name	Predicted Values
1	Max.tolerated dose (human)	0.335 mg/Kg
2	hERG I inhibitor	No
3	hERG II inhibitor	No
4	Oral rat acute toxicity	2.36 mol/Kg
5	Oral rat chronic toxicity	1.025 mg/Kg
6	Hepatoxicity	No
7	Skin sensitisation	No
8	t.pyriformis toxicity	0.332 log ug/L
9	Minnow toxicity	1.842 log mM

4.3.1.3 Artemisia Ketone, Artemisinic Acid and Artemisinin

Artemisia ketone shows high maximum tolerated dose in humans and act as a sensitizing substance. Artemisinic acid and Artemisia Ketone also have potential to cause a delayed hyper-sensitivity reaction. All other predicted values are within normal range. Predicted values of Artemisinin are normal. Artemisia Ketone, Artemisinic acid and Artemisinin are shown in Table 4.18, 4.19 and 4.20.

Table 4.18: Toxicity prediction of Artemisia Ketone

S.No	Model Name	Predicted Values
1	Max.tolerated dose (human)	0.816 mg/Kg
2	hERG I inhibitor	No
3	hERG II inhibitor	No
4	Oral rat acute toxicity	1.825 mol/Kg
5	Oral rat chronic toxicity	2.045 mg/Kg
6	Hepatoxicity	No
7	Skin sensitisation	Yes
8	t.pyriformis toxicity	0.672 log ug/L
9	Minnow toxicity	1.158 log mM

Table 4.19: Toxicity prediction of Artemisinic acid

S.No	Model Name	Predicted Values
1	Max.tolerated dose (human)	0.403 mg/Kg
2	hERG I inhibitor	No
3	hERG II inhibitor	No
4	Oral rat acute toxicity	1.747 mol/Kg
5	Oral rat chronic toxicity	2.251 mg/Kg
6	Hepatoxicity	No
7	Skin sensitisation	Yes
8	t.pyriformis toxicity	0.541 log ug/L
9	Minnow toxicity	0.541 log mM

Table 4.20: Toxicity prediction of Artemisinin

S.No	Model Name	Predicted Values
1	Max.tolerated dose (human)	0.065 mg/Kg
2	hERG I inhibitor	No
3	hERG II inhibitor	No
4	Oral rat acute toxicity	2.459 mol/Kg
5	Oral rat chronic toxicity	1 mg/Kg
6	Hepatoxicity	No
7	Skin sensitisation	No
8	t.pyriformis toxicity	0.322 log ug/L
9	Minnow toxicity	1.406 log mM

4.3.1.4 Artesunate, Beta Caryophyllene and Beta Selinene

Artesunate predicted values of nine models are within safe range whereas Beta Caryophyllene and Beta Selinene shows positive skin sensitization.

Table 4.21: The Toxicity Values of Artesunate

S.No	Model Name	Predicted Values
1	Max.tolerated dose (human)	0.256 mg/Kg
2	hERG I inhibitor	No
3	hERG II inhibitor	No
4	Oral rat acute toxicity	3.112 mol/Kg
5	Oral rat chronic toxicity	1.549 mg/Kg
6	Hepatoxicity	No
7	Skin sensitisation	No
8	t.pyriformis toxicity	0.285 log ug/L
9	Minnow toxicity	1.499 log mM

Table 4.22: The Toxicity Values of Beta Caryophyllene

S.No	Model Name	Predicted Values
1	Max.tolerated dose (human)	0.351 mg/Kg
2	hERG I inhibitor	No
3	hERG II inhibitor	No
4	Oral rat acute toxicity	1.617 mol/Kg
5	Oral rat chronic toxicity	1.416 mg/Kg
6	Hepatoxicity	No
7	Skin sensitisation	Yes
8	t.pyriformis toxicity	1.401 log ug/L
9	Minnow toxicity	0.504 log mM

Table 4.23: The Toxicity Values of Beta Selinene

S.No	Model Name	Predicted Values
1	Max.tolerated dose (human)	-0.03 mg/Kg
2	hERG I inhibitor	No
3	hERG II inhibitor	No
4	Oral rat acute toxicity	1.581 mol/Kg
5	Oral rat chronic toxicity	1.511 mg/Kg
6	Hepatoxicity	No
7	Skin sensitisation	Yes
8	t.pyriformis toxicity	1.736 log ug/L
9	Minnow toxicity	-0.078 log mM

4.3.1.5 Camphor, Casticin and Chrysosplenol D

Camphor shows itself as sensitizing substance whereas its other model values are normal. The other two ligands exhibited all model values are within safe range.

Table 4.24: The Toxicity Values of Camphor

S.No	Model Name	Predicted Values
1	Max.tolerated dose (human)	0.473 mg/Kg
2	hERG I inhibitor	No
3	hERG II inhibitor	No
4	Oral rat acute toxicity	1.653 mol/Kg
5	Oral rat chronic toxicity	1.981 mg/Kg
6	Hepatoxicity	No
7	Skin sensitisation	Yes
8	t.pyriformis toxicity	0.233 log ug/L
9	Minnow toxicity	1.458 log mM

Table 4.25: The Toxicity Values of Casticin

S.No	Model Name	Predicted Values
1	Max.tolerated dose (human)	0.47 mg/Kg
2	hERG I inhibitor	No
3	hERG II inhibitor	No
4	Oral rat acute toxicity	2.302 mol/Kg
5	Oral rat chronic toxicity	1.768 mg/Kg
6	Hepatoxicity	No
7	Skin sensitisation	No
8	t.pyriformis toxicity	0.317 log ug/L
9	Minnow toxicity	2.233 log mM

Table 4.26: The Toxicity Values of Chrysosplenol D

S.No	Model Name	Predicted Values
1	Max.tolerated dose (human)	0.284 mg/Kg
2	hERG I inhibitor	No
3	hERG II inhibitor	No
4	Oral rat acute toxicity	2.345 mol/Kg
5	Oral rat chronic toxicity	2.658 mg/Kg
6	Hepatoxicity	No
7	Skin sensitisation	No
8	t.pyriformis toxicity	0.323 log ug/L
9	Minnow toxicity	2.254 log mM

4.3.1.6 Coumarin, Cynaroside and Deoxyartemisinin

Cynaroside shows high maximum tolerated dose while other two ligands shows low doses. Remaining 8 models predicted values are normal for all three compounds.

Table 4.27: The Toxicity Values of Coumarin

S.No	Model Name	Predicted Values
1	Max.tolerated dose (human)	0.435 mg/Kg
2	hERG I inhibitor	No
3	hERG II inhibitor	No
4	Oral rat acute toxicity	2.112 mol/Kg
5	Oral rat chronic toxicity	1.903 mg/Kg
6	Hepatoxicity	No
7	Skin sensitisation	No
8	t.pyriformis toxicity	0.365 log ug/L
9	Minnow toxicity	1.555 log mM

Table 4.28: The Toxicity Values of Cynaroside

S.No	Model Name	Predicted Values
1	Max.tolerated dose (human)	0.584 mg/Kg
2	hERG I inhibitor	No
3	hERG II inhibitor	No
4	Oral rat acute toxicity	2.547 mol/Kg
5	Oral rat chronic toxicity	4.279 mg/Kg
6	Hepatoxicity	No
7	Skin sensitisation	No
8	t.pyriformis toxicity	0.285 log ug/L
9	Minnow toxicity	6.342 log mM

Table 4.29: The Toxicity Values of Deoxyartemisinin

S.No	Model Name	Predicted Values
1	Max.tolerated dose (human)	0.174 mg/Kg
2	hERG I inhibitor	No
3	hERG II inhibitor	No
4	Oral rat acute toxicity	2.161 mol/Kg
5	Oral rat chronic toxicity	1.506 mg/Kg
6	Hepatoxicity	No
7	Skin sensitisation	No
8	t.pyriformis toxicity	0.363 log ug/L
9	Minnow toxicity	1.538 log mM

4.3.1.7 Epifriedelanol, Friedelin and Germacrene D

Germacrene D shows slightly high maximum tolerated dose and positive skin sensitization. Epifriedelanol and Friedelin predicted values shows hERG-II inhibitors.

Table 4.30: The Toxicity Values of Epifriedelanol

S.No	Model Name	Predicted Values
1	Max.tolerated dose (human)	-0.518 mg/Kg
2	hERG I inhibitor	No
3	hERG II inhibitor	Yes
4	Oral rat acute toxicity	2.675 mol/Kg
5	Oral rat chronic toxicity	0.883 mg/Kg
6	Hepatoxicity	No
7	Skin sensitisation	No
8	t.pyriformis toxicity	0.303 log ug/L
9	Minnow toxicity	-1.78 log mM

Table 4.31: The Toxicity Values of Friedelin

S.No	Model Name	Predicted Values
1	Max.tolerated dose (human)	-0.213 mg/Kg
2	hERG I inhibitor	No
3	hERG II inhibitor	Yes
4	Oral rat acute toxicity	2.64 mol/Kg
5	Oral rat chronic toxicity	0.909 mg/Kg
6	Hepatoxicity	No
7	Skin sensitisation	No
8	t.pyriformis toxicity	0.3 log ug/L
9	Minnow toxicity	-2.384 log mM

Table 4.32: The Toxicity Values of Germacrene D

S.No	Model Name	Predicted Values
1	Max.tolerated dose (human)	0.497 mg/Kg
2	hERG I inhibitor	No
3	hERG II inhibitor	No
4	Oral rat acute toxicity	1.634 mol/Kg
5	Oral rat chronic toxicity	1.413 mg/Kg
6	Hepatoxicity	No
7	Skin sensitisation	Yes
8	t.pyriformis toxicity	1.671 log ug/L
9	Minnow toxicity	0.257 log mM

4.3.1.8 Isorhamnetin, Kaempferol and Limonene

All these three above mentioned compounds have high maximum tolerated dose. Limonene shows positive skin sensitization.

Table 4.33: The Toxicity Values of Isorhamnetin

S.No	Model Name	Predicted Values
1	Max.tolerated dose (human)	0.576 mg/Kg
2	hERG I inhibitor	No
3	hERG II inhibitor	No
4	Oral rat acute toxicity	2.407 mol/Kg
5	Oral rat chronic toxicity	2.499 mg/Kg
6	Hepatoxicity	No
7	Skin sensitisation	No
8	t.pyriformis toxicity	0.296 log ug/L
9	Minnow toxicity	2.206 log mM

Table 4.34: The Toxicity Values of Kaempferol

S.No	Model Name	Predicted Values
1	Max.tolerated dose (human)	0.531 mg/Kg
2	hERG I inhibitor	No
3	hERG II inhibitor	No
4	Oral rat acute toxicity	2.449 mol/Kg
5	Oral rat chronic toxicity	2.505 mg/Kg
6	Hepatoxicity	No
7	Skin sensitisation	No
8	t.pyriformis toxicity	0.312 log ug/L
9	Minnow toxicity	2.885 log mM

Table 4.35: The Toxicity Values of Limonene

S.No	Model Name	Predicted Values
1	Max.tolerated dose (human)	0.777 mg/Kg
2	hERG I inhibitor	No
3	hERG II inhibitor	No
4	Oral rat acute toxicity	1.88 mol/Kg
5	Oral rat chronic toxicity	2.336 mg/Kg
6	Hepatoxicity	No
7	Skin sensitisation	Yes
8	t.pyriformis toxicity	0.579 log ug/L
9	Minnow toxicity	1.203 log mM

4.3.1.9 Luteolin, Mearnsetin and Myrtenol

Luteolin and Mearnsetin shows high maximum tolerated doses whearas Myrtenol shows positive skin sensitization.

Table 4.36: The Toxicity Values of Luteolin

S.No	Model Name	Predicted values
1	Max.tolerated dose (human)	0.499 mg/Kg
2	hERG I inhibitor	No
3	hERG II inhibitor	No
4	Oral rat acute toxicity	2.455 mol/Kg
5	Oral rat chronic toxicity	2.409 mg/Kg
6	Hepatoxicity	No
7	Skin sensitisation	No
8	t.pyriformis toxicity	0.326 log ug/L
9	Minnow toxicity	3.169 log mM

Table 4.37: The Toxicity Values of Mearnsetin

S.No	Model Name	Predicted values
1	Max.tolerated dose (human)	0.5 mg/Kg
2	hERG I inhibitor	No
3	hERG II inhibitor	No
4	Oral rat acute toxicity	2.462 mol/Kg
5	Oral rat chronic toxicity	2.622 mg/Kg
6	Hepatoxicity	No
7	Skin sensitisation	No
8	t.pyriformis toxicity	0.286 log ug/L
9	Minnow toxicity	3.205 log mM

Table 4.38: The Toxicity Values of Myrtenol

S.No	Model Name	Predicted values
1	Max.tolerated dose (human)	0.439 mg/Kg
2	hERG I inhibitor	No
3	hERG II inhibitor	No
4	Oral rat acute toxicity	1.746 mol/Kg
5	Oral rat chronic toxicity	1.8 mg/Kg
6	Hepatoxicity	No
7	Skin sensitisation	Yes
8	t.pyriformis toxicity	0.262 log ug/L
9	Minnow toxicity	1.698 log mM

4.3.1.10 Quercetagetin, Quercetin and Quinic acid

All above mentioned compounds shows high maximum tolerated doses. Maximum tolerated dose helps in deciding maximum starting dose in phase I Clinical trials.

Table 4.39: The Toxicity Values of Quercetagetin

S.No	Model Name	Predicted values
1	Max.tolerated dose (human)	0.486 mg/Kg
2	hERG I inhibitor	No
3	hERG II inhibitor	No
4	Oral rat acute toxicity	2.537 mol/Kg
5	Oral rat chronic toxicity	3.185 mg/Kg
6	Hepatoxicity	No
7	Skin sensitisation	No
8	t.pyriformis toxicity	0.285 log ug/L
9	Minnow toxicity	3.475 log mM

Table 4.40: The Toxicity Values of Quercetin

S.No	Model Name	Predicted values
1	Max.tolerated dose (human)	0.499 mg/Kg
2	hERG I inhibitor	No
3	hERG II inhibitor	No
4	Oral rat acute toxicity	2.471 mol/Kg
5	Oral rat chronic toxicity	2.612 mg/Kg
6	Hepatoxicity	No
7	Skin sensitisation	No
8	t.pyriformis toxicity	0.288 log ug/L
9	Minnow toxicity	3.721 log mM

Table 4.41: The Toxicity Values of Quinic acid

S.No	Model Name	Predicted values
1	Max.tolerated dose (human)	1.626 mg/Kg
2	hERG I inhibitor	No
3	hERG II inhibitor	No
4	Oral rat acute toxicity	1.128 mol/Kg
5	Oral rat chronic toxicity	3.529 mg/Kg
6	Hepatoxicity	No
7	Skin sensitisation	No
8	t.pyriformis toxicity	0.285 log ug/L
9	Minnow toxicity	4.869 log mM

4.3.1.11 Retusin, Rutin and Scoparone

Scoparone shows a slightly high 0.494 log mg/kg/day maximum tolerated dose. Rutin value shows hERG II inhibitor which predicts from to be an effective drug.

Table 4.42: The Toxicity Values of Retusin

S.No	Model Name	Predicted values
1	Max.tolerated dose (human)	0.296 mg/Kg
2	hERG I inhibitor	No
3	hERG II inhibitor	No
4	Oral rat acute toxicity	2.23 mol/Kg
5	Oral rat chronic toxicity	1.166 mg/Kg
6	Hepatoxicity	No
7	Skin sensitisation	No
8	t.pyriformis toxicity	0.399 log ug/L
9	Minnow toxicity	1.398 log mM

Table 4.43: The Toxicity Values of Rutin

S.No	Model Name	Predicted values
1	Max.tolerated dose (human)	0.452 mg/Kg
2	hERG I inhibitor	No
3	hERG II inhibitor	Yes
4	Oral rat acute toxicity	2.491 mol/Kg
5	Oral rat chronic toxicity	3.673 mg/Kg
6	Hepatoxicity	No
7	Skin sensitisation	No
8	t.pyriformis toxicity	0.285 log ug/L
9	Minnow toxicity	7.677 log mM

Table 4.44: The Toxicity Values of Scoparone

S.No	Model Name	Predicted values
1	Max.tolerated dose (human)	0.494 mg/Kg
2	hERG I inhibitor	No
3	hERG II inhibitor	No
4	Oral rat acute toxicity	2.345 mol/Kg
5	Oral rat chronic toxicity	2.408 mg/Kg
6	Hepatoxicity	No
7	Skin sensitisation	No
8	t.pyriformis toxicity	0.603 log ug/L
9	Minnow toxicity	1.223 log mM

4.3.1.12 Scopoletin, Scopolin and Stigmasterol

Scopoletin shows high maximum tolerated dose. Stigmasterol exhibit itself as hERG II inhibitor.

Table 4.45: The Toxicity Values of Scopoletin

S.No	Model Name	Predicted values
1	Max.tolerated dose (human)	0.614 mg/Kg
2	hERG I inhibitor	No
3	hERG II inhibitor	No
4	Oral rat acute toxicity	1.95 mol/Kg
5	Oral rat chronic toxicity	1.378 mg/Kg
6	Hepatoxicity	No
7	Skin sensitisation	No
8	t.pyriformis toxicity	0.516 log ug/L
9	Minnow toxicity	1.614 log mM

Table 4.46: The Toxicity Values of Scopolin

S.No	Model Name	Predicted values
1	Max.tolerated dose (human)	0.393 mg/Kg
2	hERG I inhibitor	No
3	hERG II inhibitor	No
4	Oral rat acute toxicity	2.393 mol/L
5	Oral rat chronic toxicity	3.756 mg/Kg
6	Hepatoxicity	No
7	Skin sensitisation	No
8	t.pyriformis toxicity	0.286 log ug/L
9	Minnow toxicity	4.198 log mM

Table 4.47: The Toxicity Values of Stigmasterol

S.No	Model Name	Predicted values
1	Max.tolerated dose (human)	-0.664 mg/Kg
2	hERG I inhibitor	No
3	hERG II inhibitor	Yes
4	Oral rat acute toxicity	2.54 mol/Kg
5	Oral rat chronic toxicity	0.872 mg/Kg
6	Hepatoxicity	No
7	Skin sensitisation	No
8	t.pyriformis toxicity	0.433 log ug/L
9	Minnow toxicity	-1.675 log mM

4.3.1.13 Transpinocarveol

Transpinocarveol predicted category of skin sensitisation shows that this compound can induce allergic contact dermatitis. Skin sensitization is an important safety concern.

Table 4.48: The Toxicity Values of Transpinocarveol

S.No	Model Name	Predicted values
1	Max.tolerated dose (human)	0.402 mg/Kg
2	hERG I inhibitor	No
3	hERG II inhibitor	No
4	Oral rat acute toxicity	1.71 mol/Kg
5	Oral rat chronic toxicity	1.804 mg/Kg
6	Hepatoxicity	No
7	Skin sensitisation	Yes
8	t.pyriformis toxicity	0.268 log ug/L
9	Minnow toxicity	1.865 log mM

4.4 Molecular Docking

Molecular Docking is technique used to estimate the strength of a bond between a ligand and a target protein through a special scoring function and to determine the correct structure of the ligand within the target binding site. The 3D structure of the target proteins and the ligands is taken as the input for docking.

Molecular docking is a structure-based drug design method that predicts the binding affinity and mode between receptors and ligands and simulates the molecular interactions. Now, this technology is extensively used in the drug design research field. It is convenient for researchers to purchase, synthesize, and complete follow-up pharmacological tests by using the compounds database to screen potential pharmacophores. Furthermore, molecular docking greatly improves efficiency and reduces the research cost.

The basic theory of molecular docking is to simulate the optimal conformation according to the complementarity and pre-organization, which could predict and

obtain the binding affinity and interactive mode between receptor and ligand. After preparing proteins and ligands ready for docking, docking were performed by CB dock which is a well trusted online blind auto docking tool. The results and time required for docking is depend upon structures of receptors, ligands, refinements, and net speed.

It may take several hours for a single result so patience was shown while doing docking. CB dock gave us five possible posses and receptor models and among these posses best one was selected by observing certain properties like vena score and size of cavity etc.

Molecular docking without having information of binding sites is performed by using a user- friendly blind docking web server called as CB Dock, which predicts and estimate a binding site for a given protein and calculate centers and sizes with a novel rotation cavity detection method and perform docking with the popular docking program known as Auto dock Vina [126].

Molecular dockings are performed by using SOD2, GPX1 and CAT as receptors and 37 selected compounds as ligands [127]. After submitting input files (receptor file in PDB format & ligand file in SDF format), CB-Dock checks the input files and converts them to pdbqt formatted files using OpenBabel and MGLTools.

After that CB-Dock predicts cavities of the receptor and calculates the centres and sizes of the top N (n=5 by default) cavities. Each center, size and pdbqt files are submitted to Auto Dock Vina for docking. The final results are displayed after the computation of N rounds.

The interactive 3D structures are drawn by NGL viewer [10]. Among 5 best confirmations, best one is selected on the bases of highest affinity score of receptor-ligand interaction. Ligands with best binding score values with SOD2, GPX1 and CAT are shown in Table 4.49 to 4.53.

Table 4.49: A: Ligands With Best Binding Score Values With Catalase, Superoxide Dismutase 2, Glutathione Peroxidase 1

S.No	Compounds	Alpha Terpinene	Apigenin	Arteannuin B	Arteether	Artemether
1	Binding Score	-6	-9.6	-7.9	-7.7	-7.6
2	Cavity size	6031	6031	320	6911	326
3	HBD	0	3	0	0	0
4	HBA	0	5	3	5	5
5	logP	3.3089	2.5768	2.4518	3.2309	2.8408
6	Molecular Weight g/-mol	136.23 g/-mol	270.24 g/mol	248.322 g/mol	312.406 g/mol	298.379 g/mol
7	Rotatable Bonds	1	1	0	2	1
8	Grid Map	34	34	59	72	43
9	Min-energy Kcl/mol	0	0	0	0	0
10	Max-energy Kcl/mol	1.60E+00	1.60E+00	1.60E+00	1.60E+00	1.60E+00

Continued Table 4.49 B: Ligands With Best Binding Score Values With Catalase, Superoxide Dismutase 2, Glutathione Peroxidase 1

S.No	Compounds	Artemetin	Artemisia Ketone	Artemisinic acid	Artemisinin	Artesunate
1	Binding Score	-8.2	-6.3	-8.1	-8.4	-8.6
2	Cavity Size	5536	6031	4846	332	326
3	HBD	1	0	1	0	1
4	HBA	8	1	1	5	7
5	logP	3.2086	2.7339	3.6458	2.3949	2.6024
6	Molecular Weight g/mol	388.372 g/mol	152.237 g/mol	234.339 g/mol	282.336 g/mol	384.425 g/mol
7	Rotatable Bonds	6	3	2	0	4
8	Grid Map	51	34	41	43	43
9	Min-energy Kcl/mol	0	0	0	0	0
10	Max-energy Kcl/mol	1.60E+00	1.60E+00	1.60E+00	1.60E+00	1.60E+00

Table 4.50: A: Ligands With Best Binding Score Values With Catalase, Superoxide Dismutase 2, Glutathione Peroxidase 1

S.No	Compounds	Casticin	Camphor	Beta-Selinene	Beta Caryophyllene	Chrysosplenol D
1	Binding Score	-8.4	-5.7	-7.1	-7.5	-8.4
2	Cavity size	5536	320	6031	6031	5536
3	HBD	2	0	0	0	3
4	HBA	8	1	0	0	8
5	logP	2.9056	2.4017	4.7252	4.7252	2.6026
6	Molecular Weight g/-mol	374.345 g/-mol	152.237 g/mol	204.357 g/mol	204.357 g/mol	360.318 g/mol
7	Rotatable Bonds	5	0	1	0	4
8	Grid Map	51	59	34	34	51
9	Min-energy Kcl/mol	0	0	0	0	0
10	Max-energy Kcl/mol	1.60E+00	1.60E+00	1.60E+00	1.60E+00	1.60E+00

Continued Table 4.50 B: Ligands With Best Binding Score Values With Catalase, Superoxide Dismutase 2, Glutathione Peroxidase 1

S.No	**Compounds**	**Coumarin**	**Cynaroside**	**Epifriede-lanol**	**Friedelin**	**Deoxyart-misinin**
1	Binding Score	-7.6	-10.5	-9.9	-10	-8
2	Cavity Size	6031	6031	326	6911	332
3	HBD	0	7	1	0	0
4	HBA	2	11	1	1	4
5	logP	1.793	-0.2445	8.2488	8.457	2.4633
6	Molecular Weight g/mol	146.145 g/mol	448.38 g/mol	428.745 g/mol	426.729 g/mol	266.337 g/mol
7	Rotatable Bonds	0	4	0	0	0
8	Grid Map	34	34	43	72	43
9	Min-energy Kcl/mol	0	0	0	0	0
10	Max-energy Kcl/mol	1.60E+00	1.60E+00	1.60E+00	1.60E+00	1.60E+00

Table 4.51: A: Ligands With Best Binding Score Values With Catalase, Superoxide Dismutase 2, Glutathione Peroxidase 1

S.No	**Compounds**	**Germacrene D**	**Isorhamnetin**	**Kaempferol**	**Limonene**	**Luteolin**
1	Binding Score	-6.7	-8.9	9.5	-5.8	-9.9
2	Cavity size	332	6911	5536	6031	6031
3	HBD	0	4	4	0	4
4	HBA	0	7	6	0	6
5	logP	4.8913	2.291	2.2824	3.3089	2.2824
6	Molecular Weight g/-mol	204.357 g/-mol	316.265 g/mol	286.239 g/mol	136.238 g/mol	286.239 g/mol
7	Rotatable Bonds	1	2	1	1	1
8	Grid Map	43	72	51	34	34
9	Min-energy Kcl/mol	0	0	0	0	0
10	Max-energy Kcl/mol	1.60E+00	1.60E+00	1.60E+00	1.60E+00	1.60E+00

Continued Table 4.51 B: Ligands With Best Binding Score Values With Catalase, Superoxide Dismutase 2, Glutathione Peroxidase 1

S.No	Compounds	Mearnsetin	Myrtenol	Quercet-agetin	Quercetin	Quinic acid
1	Binding Score	-9.3	-6.2	-9.8	-10	-6.7
2	Cavity Size	7293	4846	5536	5536	6031
3	HBD	5	1	6	5	5
4	HBA	8	1	8	7	5
5	logP	1.9966	1.9711	1.6936	1.988	-2.3214
6	Molecular Weight g/mol	332.264 g/mol	152.237 g/mol	318.237 g/mol	302.238 g/mol	192.167 g/mol
7	Rotatable Bonds	2	1	1	1	1
8	Grid Map	33	41	51	51	34
9	Min-energy Kcl/mol	0	0	0	0	0
10	Max-energy Kcl/mol	1.60E+00	1.60E+00	1.60E+00	1.60E+00	1.60E+00

Table 4.52: Ligands With Best Binding Score Values With Catalase, Superoxide Dismutase 2, Glutathione Peroxidase 1

S.No	Compounds	Retusin	Rutin	Scoparone	Scopoletin	Scopolin
1	Binding Score	-8.9	-10.1	-7.2	-7.3	-8.8
2	Cavity size	6911	7293	6031	6031	6031
3	HBD	1	10	0	1	4
4	HBA	7	16	4	4	9
5	logP	3.2	-1.6871	1.8102	1.5072	-1.0197
6	Molecular Weight g/-mol	358.346 g/-mol	610.521 g/mol	206.197 g/mol	192.17 g/mol	354.311 g/mol
7	Rotatable Bonds	5	6	2	1	4
8	Grid Map	72	33	34	34	34
9	Min-energy Kcl/mol	0	0	0	0	0
10	Max-energy Kcl/mol	1.60E+00	1.60E+00	1.60E+00	1.60E+00	1.60E+00

Table 4.53: Ligands With Best Binding Score Values With Catalase, Superoxide Dismutase 2, Glutathione Peroxidase 1.

S.No	**Compound**	**Stigmasterol**	**Transpinocarveol**
1	Binding Score	-9.1	-5.8
2	HBD	1	1
3	HBA	1	1
4	logP	7.8008	1.9695
5	Molecular Weight g/mol	412.702	152.237
6	Rotatable Bonds	5	0
7	Grid Map	72	43
8	Min-energy Kcl/mol	0.00	0.00
9	Max-energy Kcl/mol	1.60E+00	1.60E+00
10	Cavity Size	6911	326

4.5 Interaction of Ligands and Target Protein

The docking analysis are performed by using Ligplot^{+} (version v.1.4.5) and PyMol Edu (v1.7.4.5). Interactions of ligands and target proteins are predicted by using Ligplot plus (version v.1.4.5). The graphical system of LigPlot + automatically generates multiple 2D diagrams of interactions from 3D coordinates. These 2D diagrams portray the hydrogen-bond interaction pattern and hydrophobic contacts between the ligand and the main-chain or side-chain elements of the protein [128]. The 2D diagrams of the best binding score ligands with respective proteins are shown in Figures 4.7 to 4.43 while their hydrogen bonds and hydrophobic interactions are listed in Table 4.54. Figure 4.7 shows the interaction of Alpha Terpinene with CAT. As evident from 2D diagram ligand show only hydrophobic interactions with protein. Ligand consists on 10 carbons and shows hydrophobic interactions with Gln53, Glu344, Ala345, Met339, Glu420, Leu355 and Val55 residues as evident also from table 4.10. Alpha Terpinene, Beta Caryophyllene, Beta Selinene, Epifriedelanol, Friedelin, Germacrene D, Limonene, Scoparone and Stigmasterol ligands are without hydrogen bonds as it is evident from their 2D structures they are mostly without active oxygen atoms. Epifriedelanol, Friedelin, and Stigmasterol have one oxygen namely as O Alcohol, OCarbonyl and again OAlcohol respectively which does not involve in hydrogen bonding.Scoparone have four oxygen

atoms namely as O1Carboxyl, O2Enol, O3Enol and O4Carbonyl but no one involves in hydrogen bonding.Maximum hydrogen bonds are shown by Scopolin, Rutin, Quinic acid , Isorhamnetin and Cynaroside as 8, 7, 6, 5 & 5 respectively. Rutin also shows maximum hydrophobic interactions with protein residues as it contains 16 oxygens in its structure.

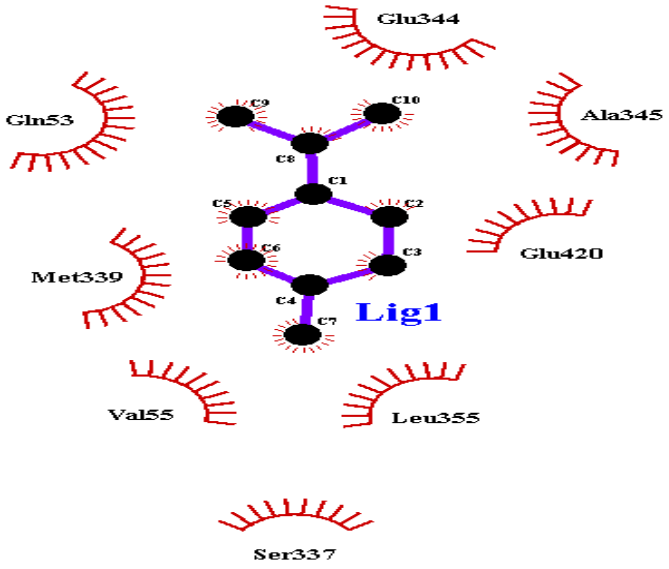

FIGURE 4.7: Interactions of Alpha-Terpinene With CAT By Ligplot.

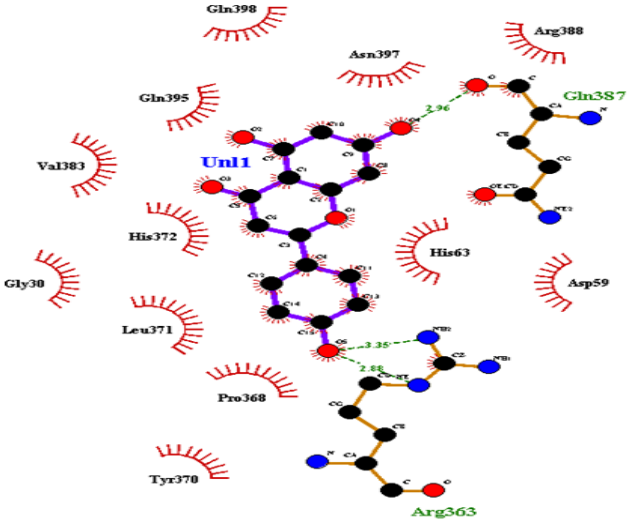

FIGURE 4.8: Interactions of Apigenin With CAT By Ligplot.

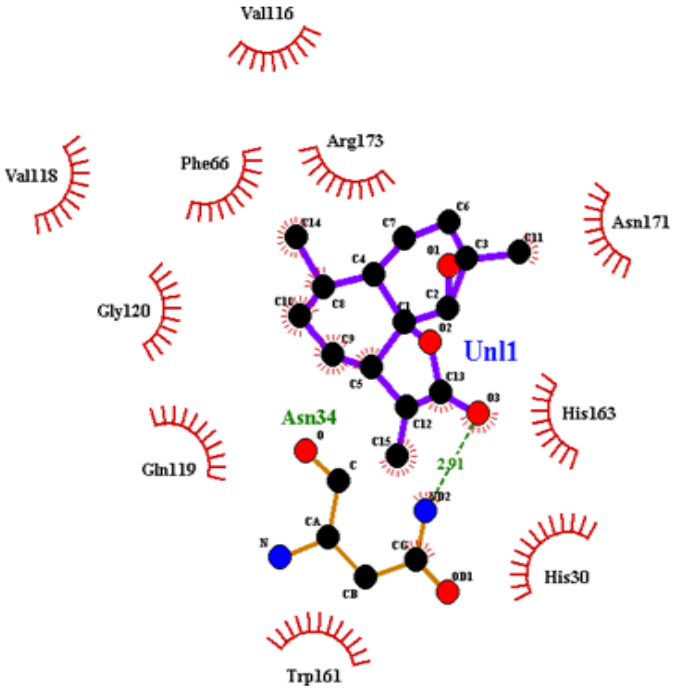

FIGURE 4.9: Interactions of Arteannuin B With SOD2 By Ligplot.

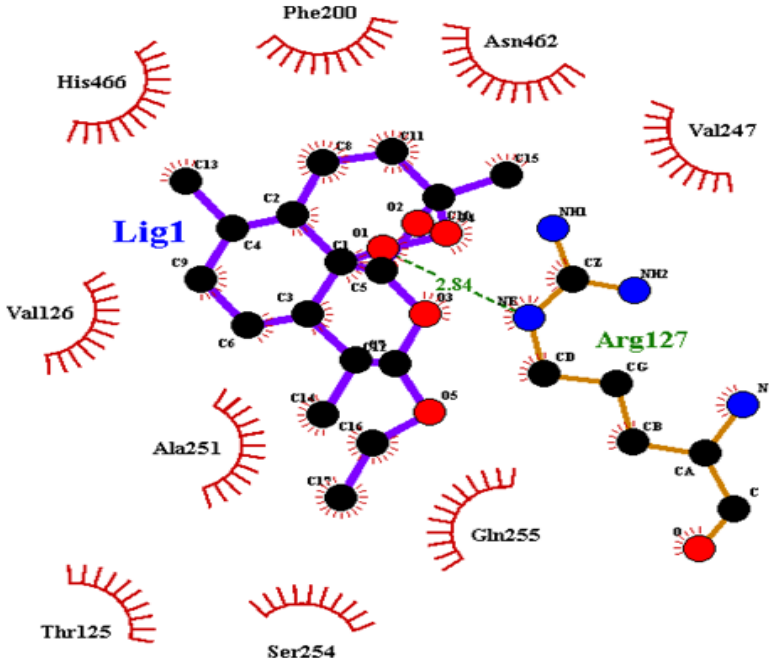

FIGURE 4.10: Interactions of Arteether With CAT By Ligplot.

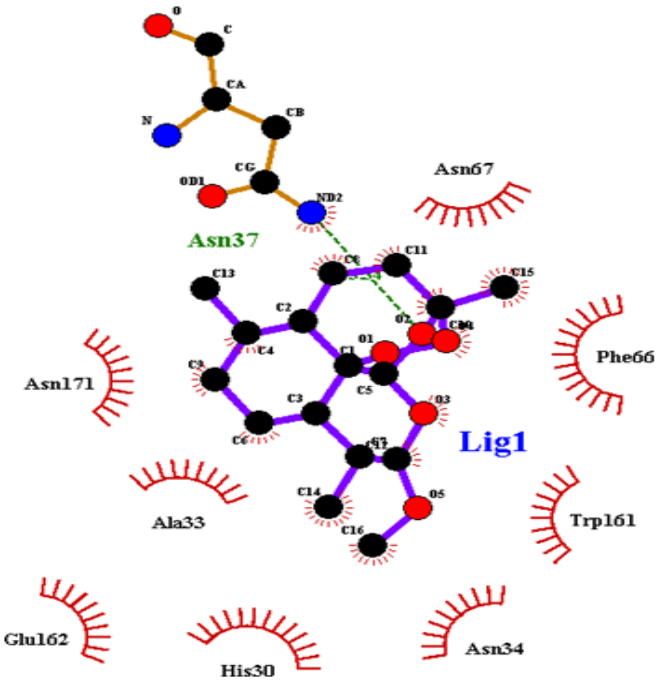

FIGURE 4.11: Interactions of Artemether With SOD2 By Ligplot.

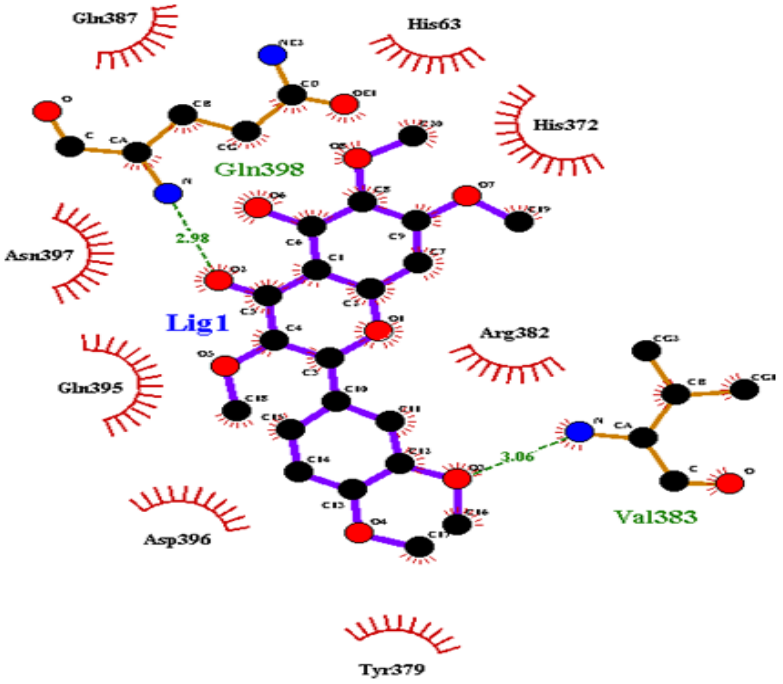

FIGURE 4.12: Interactions of Artemetin With CAT By Ligplot.

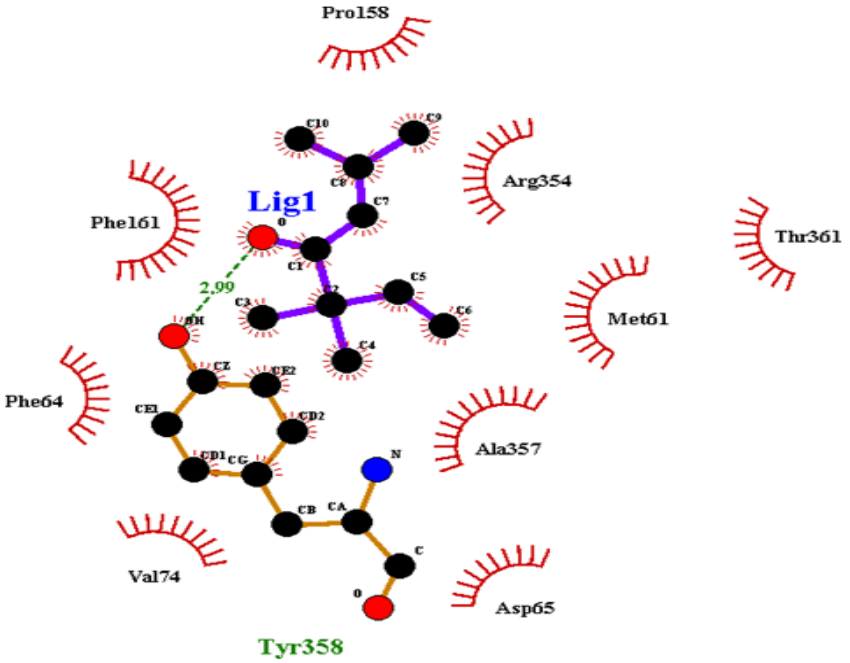

FIGURE 4.13: Interactions of Artemisia Ketone With CAT By Ligplot.

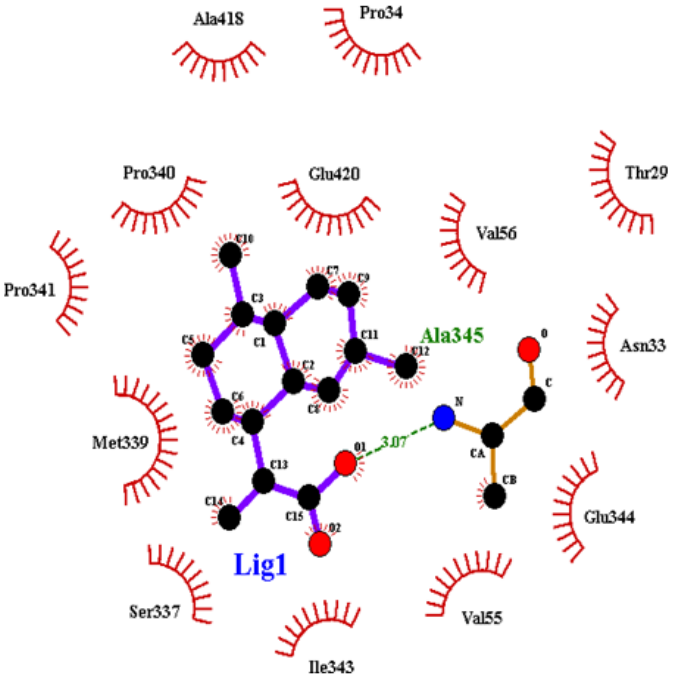

FIGURE 4.14: Interactions of Artemisinic acid With CAT By Ligplot.

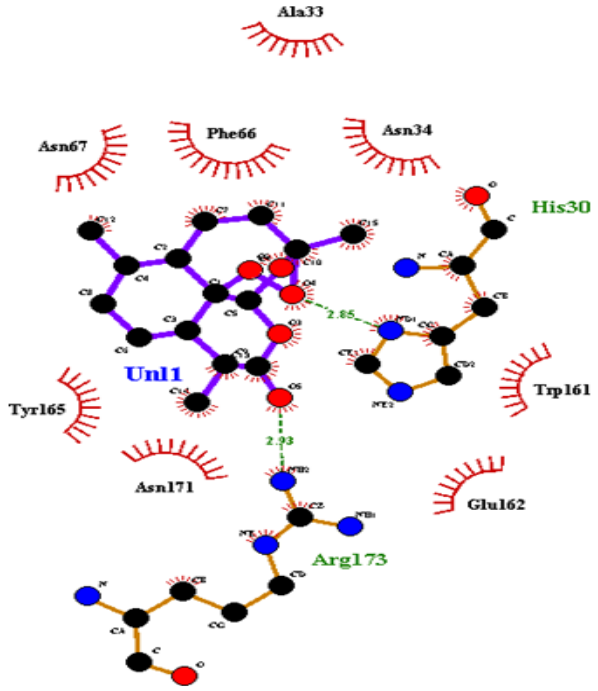

FIGURE 4.15: Interactions of Artemisinin With SOD2 By Ligplot.

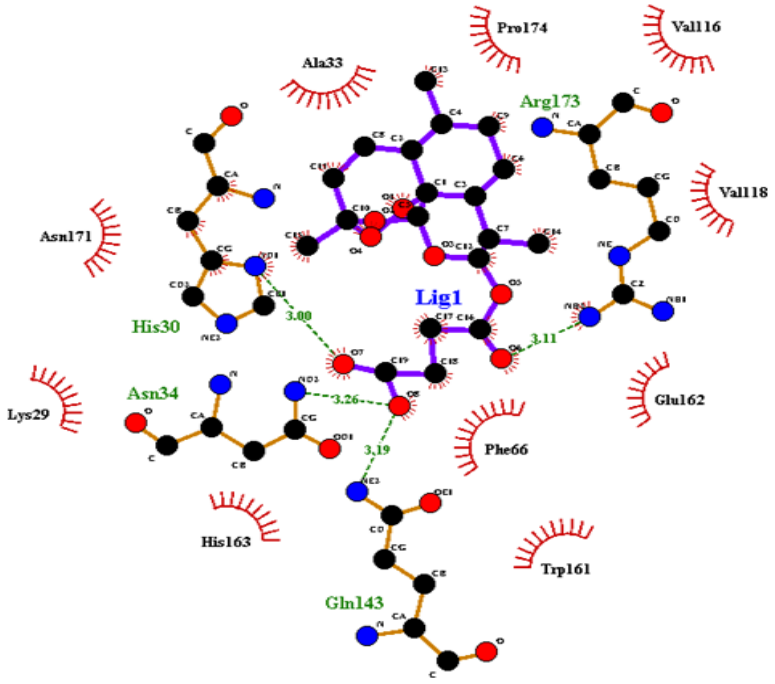

FIGURE 4.16: Interactions of Artesunate With SOD2 By Ligplot.

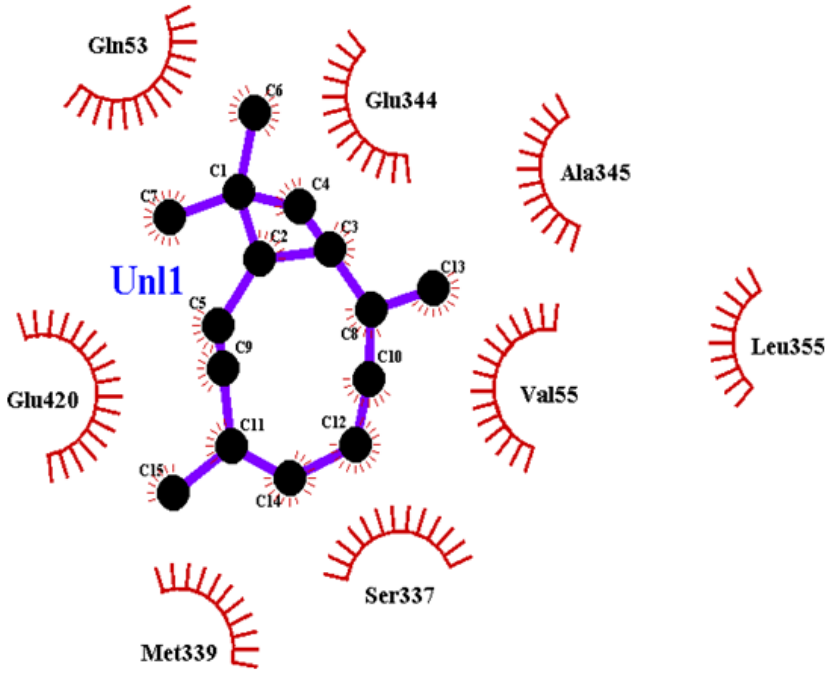

FIGURE 4.17: Interactions of Beta-Caryophyllene With CAT By Ligplot.

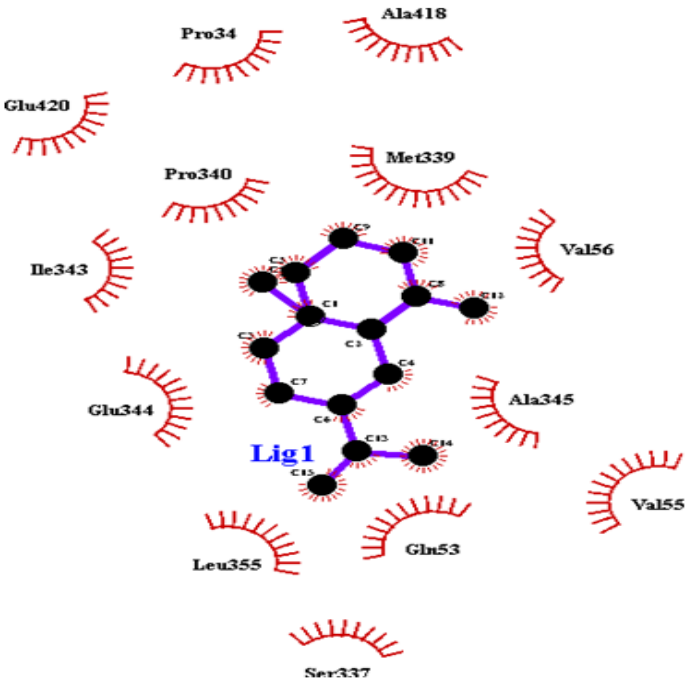

FIGURE 4.18: Interactions of Beta-Selinene With CAT By Ligplot.

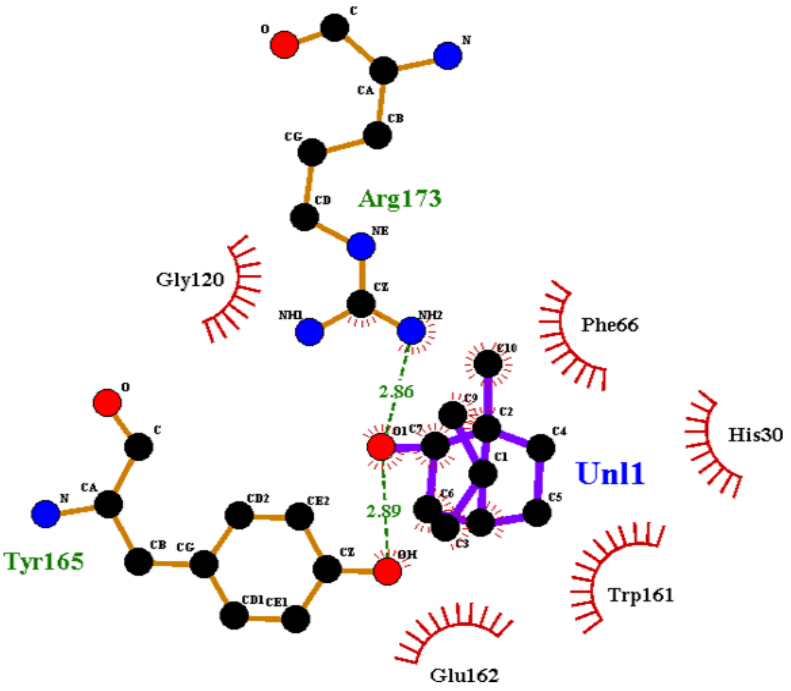

FIGURE 4.19: Interactions of Camphor With SOD2 By Ligplot.

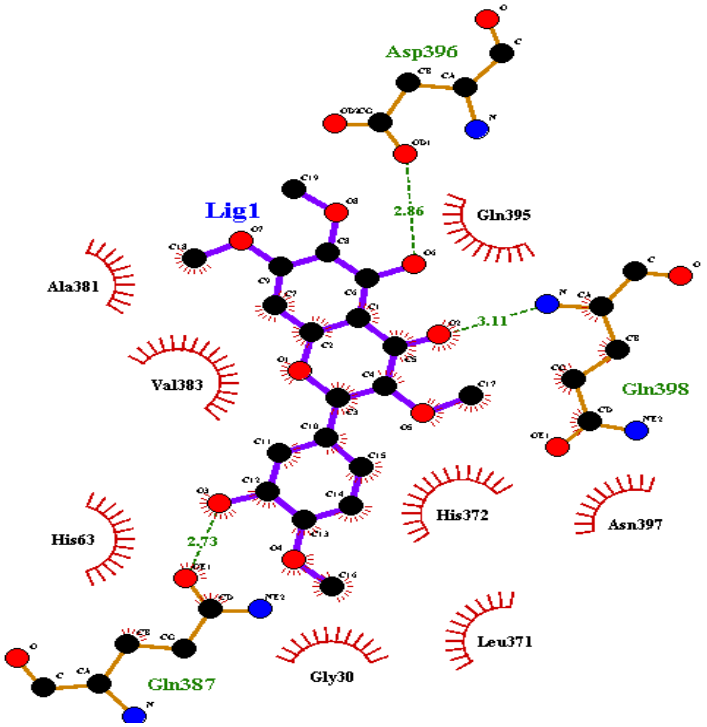

FIGURE 4.20: Interactions of Casticin With CAT By Ligplot.

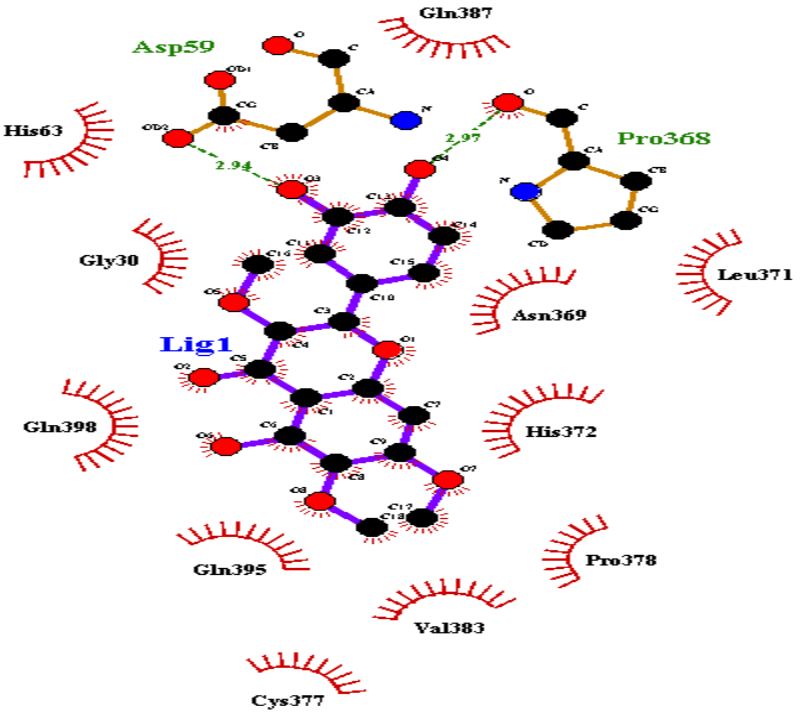

FIGURE 4.21: Interactions of Chrysosplenol-D With CAT By Ligplot.

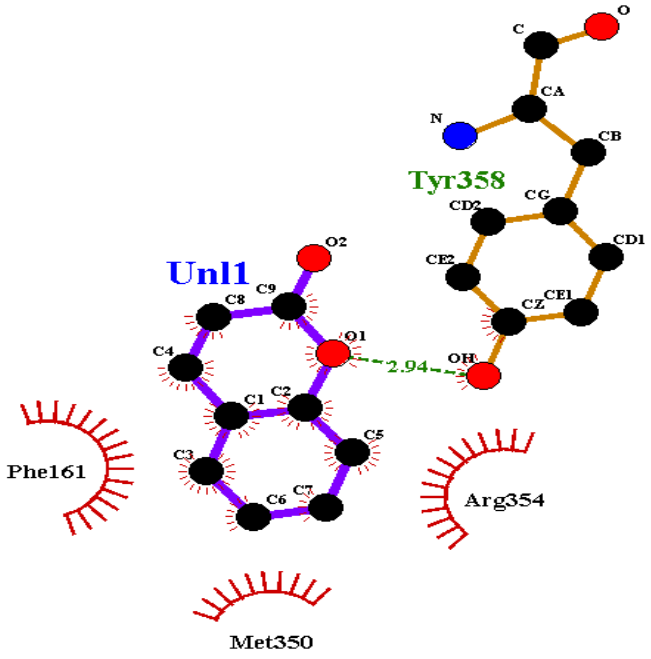

FIGURE 4.22: Interactions of Coumarin With CAT By Ligplot.

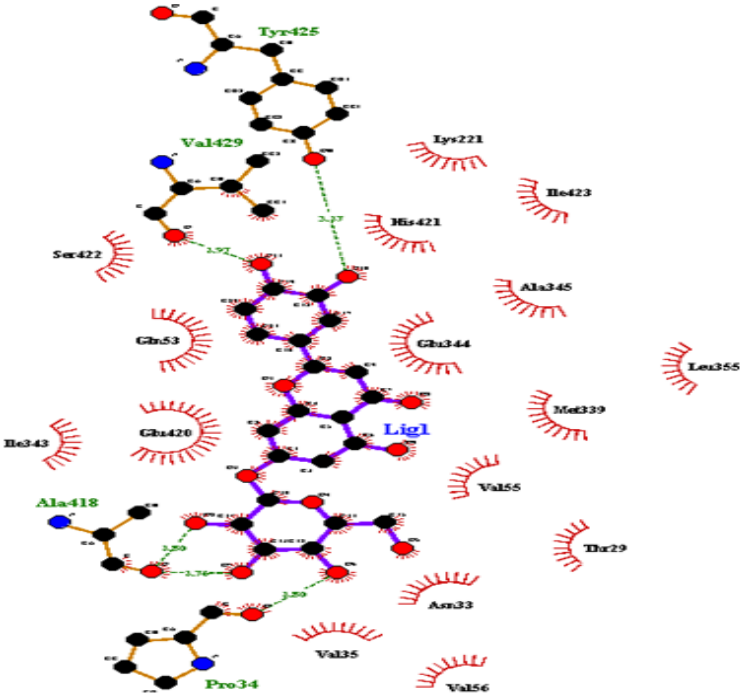

FIGURE 4.23: Interactions of Cynaroside With CAT By Ligplot.

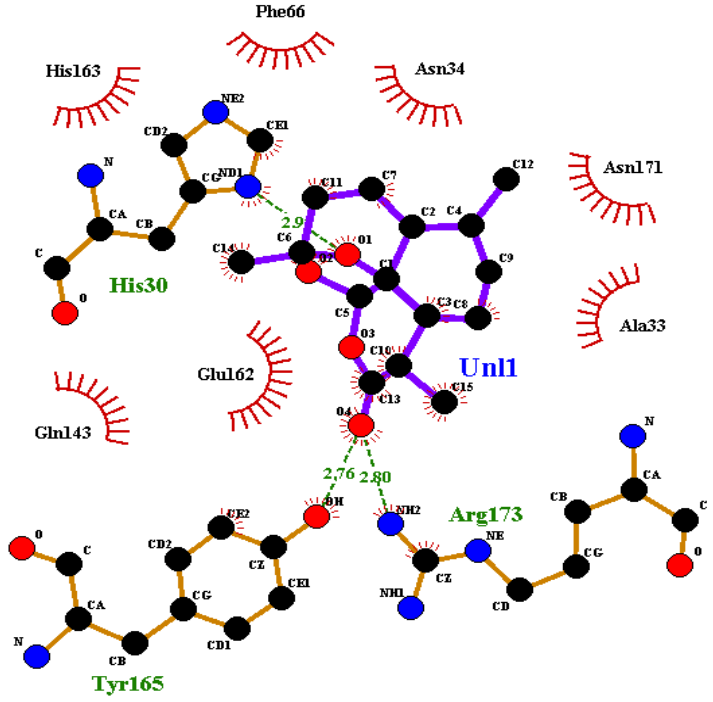

FIGURE 4.24: Interactions of Deoxyartemisinin With SOD2 By Ligplot.

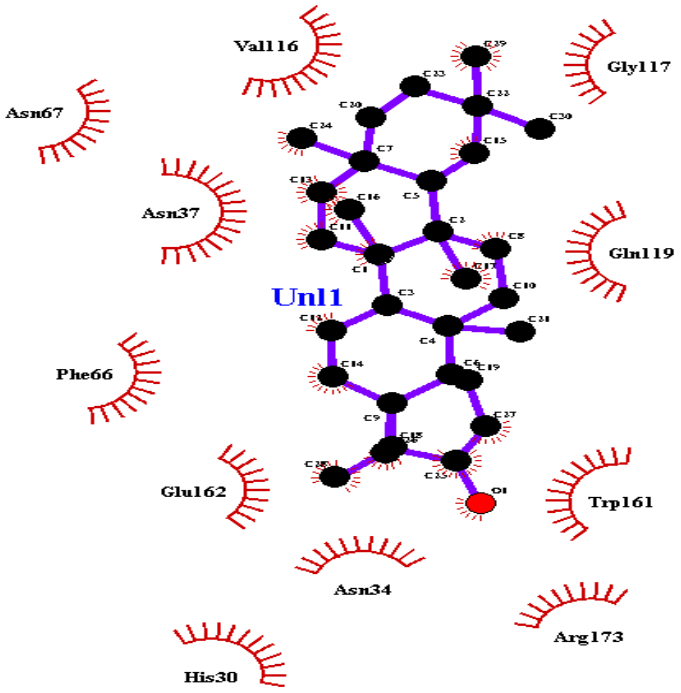

FIGURE 4.25: Interactions of Epifriedelanol With SOD2 By Ligplot.

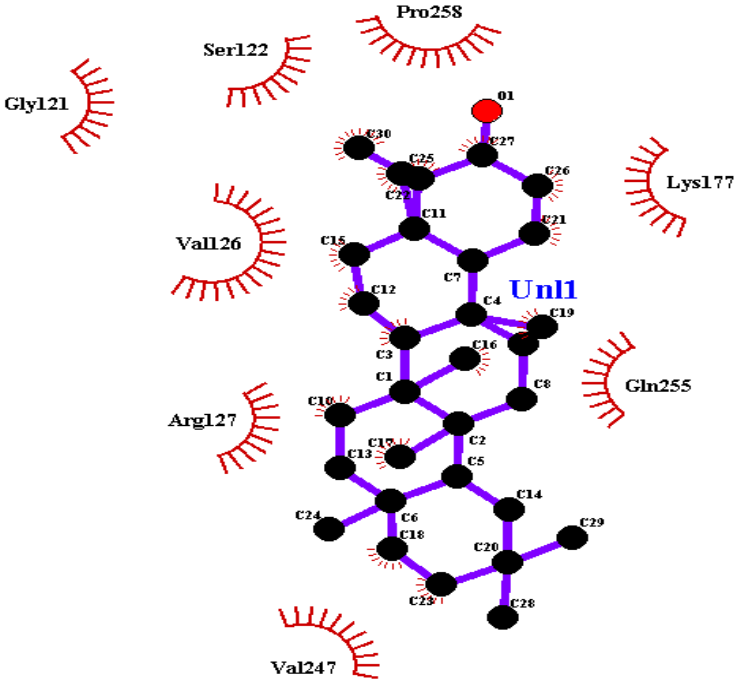

FIGURE 4.26: Interactions of Friedelin With CAT By Ligplot.

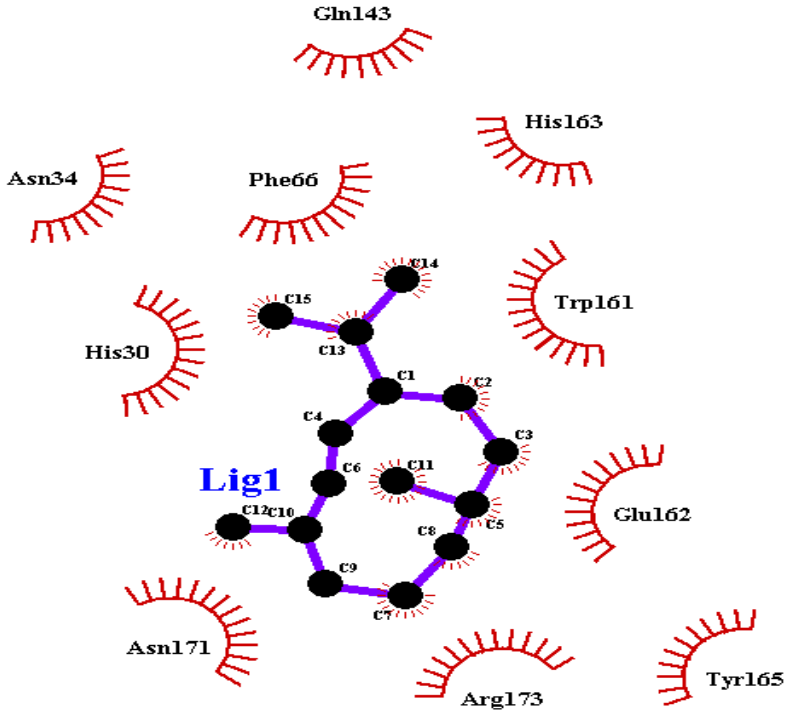

FIGURE 4.27: Interactions of Germacrene-D With SOD2 By Ligplot.

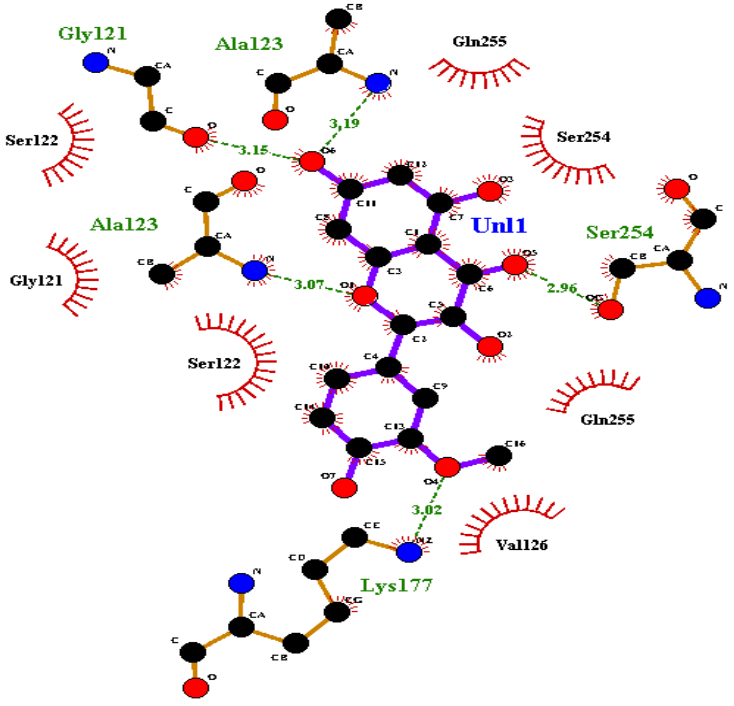

FIGURE 4.28: Interactions of Isorhamnetin With CAT By Ligplot.

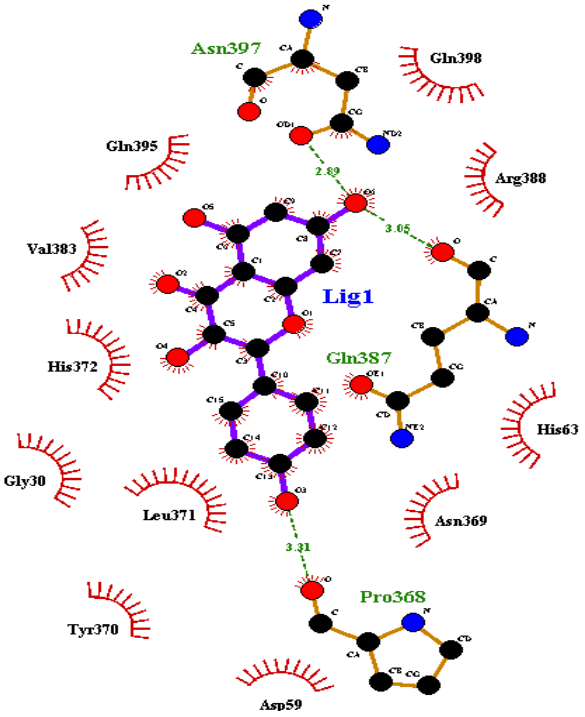

FIGURE 4.29: Interactions of Kaempferol With CAT By Ligplot.

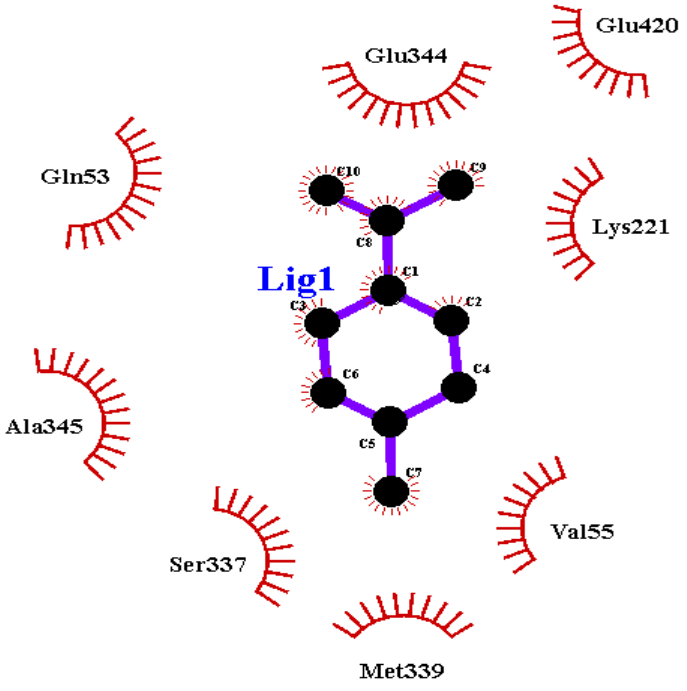

FIGURE 4.30: Interactions of Limonene With CAT By Ligplot.

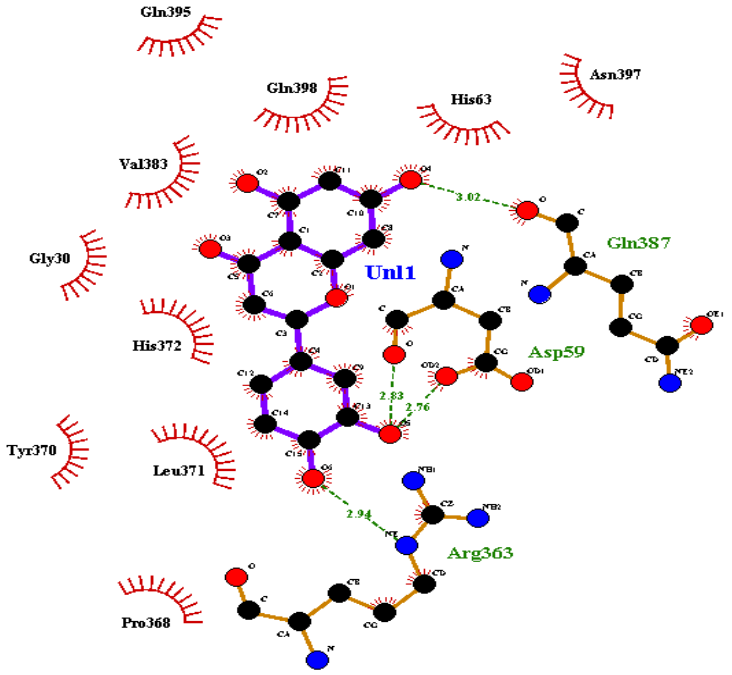

FIGURE 4.31: Interactions of Luteolin With CAT By Ligplot.

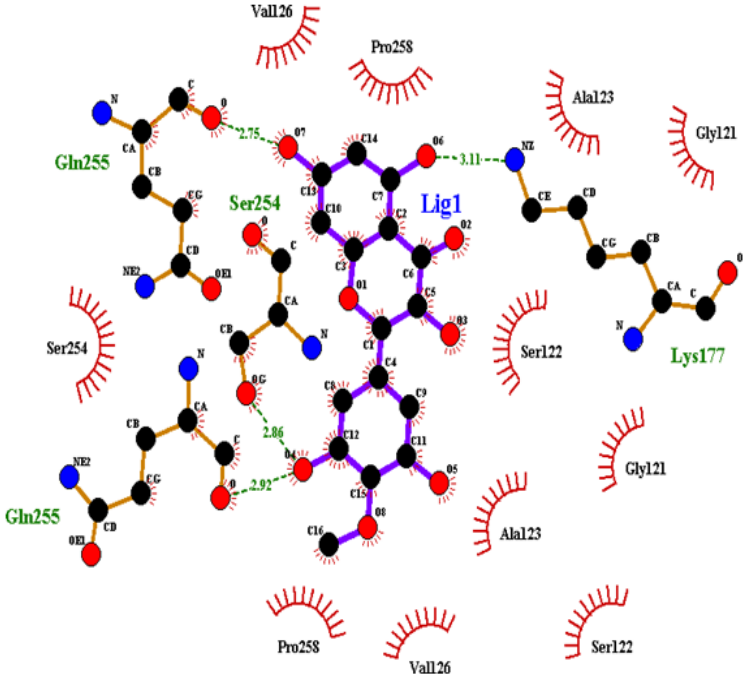

FIGURE 4.32: Interactions of Mearnsetin With CAT By Ligplot.

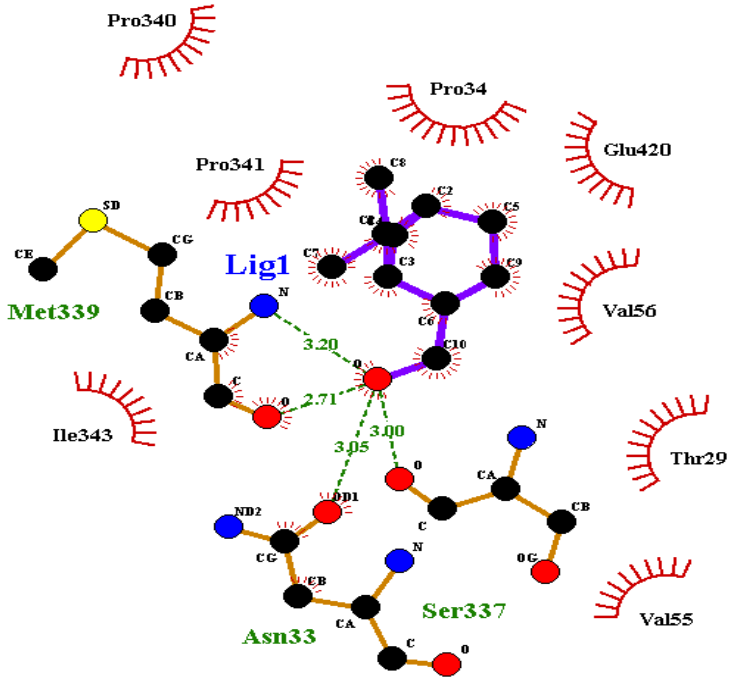

FIGURE 4.33: Interactions of Myrtenol With CAT By Ligplot.

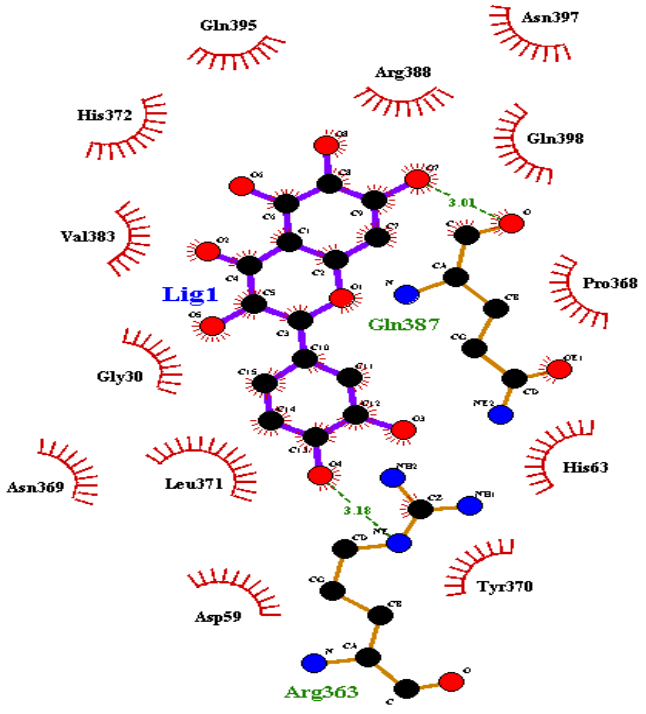

FIGURE 4.34: Interactions of Quercetagetin With CAT By Ligplot.

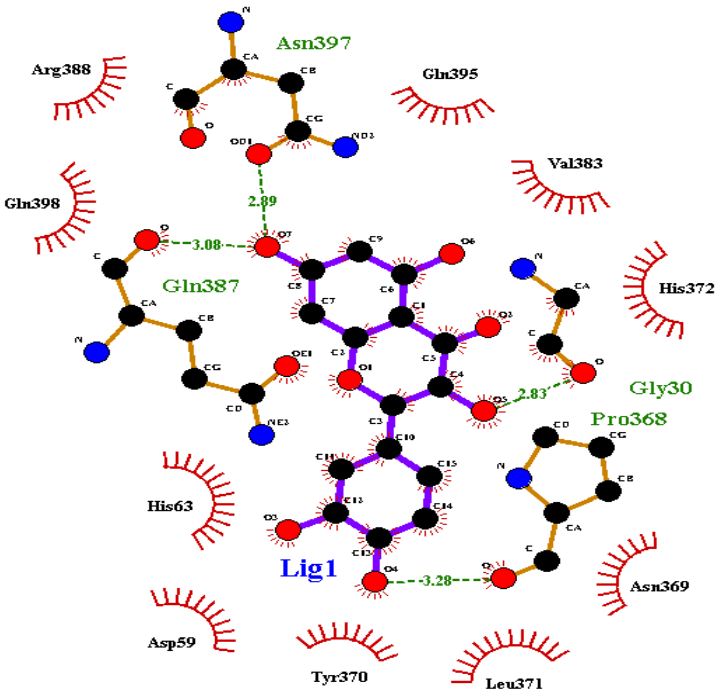

FIGURE 4.35: eractions of Quercetin With CAT By Ligplot.

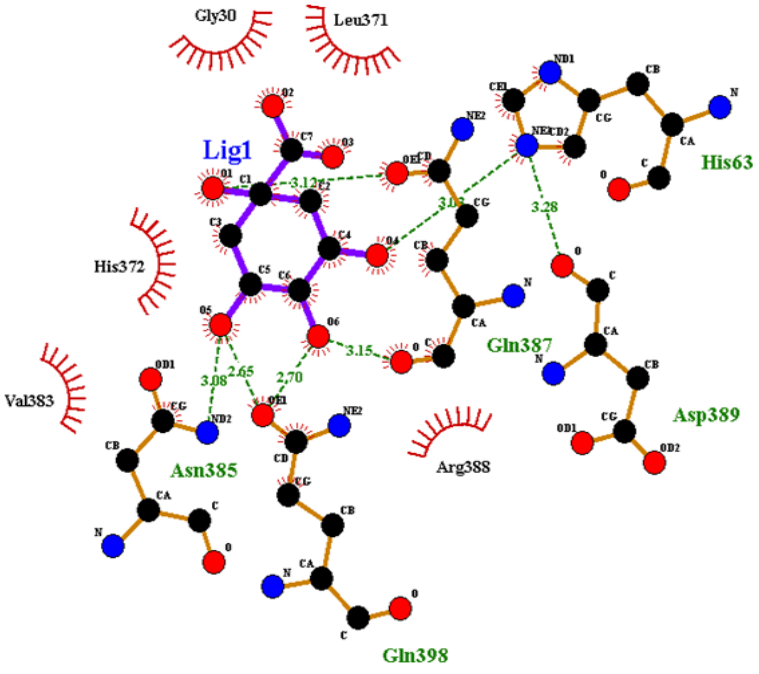

FIGURE 4.36: Interactions of Quinic acid With CAT By Ligplot.

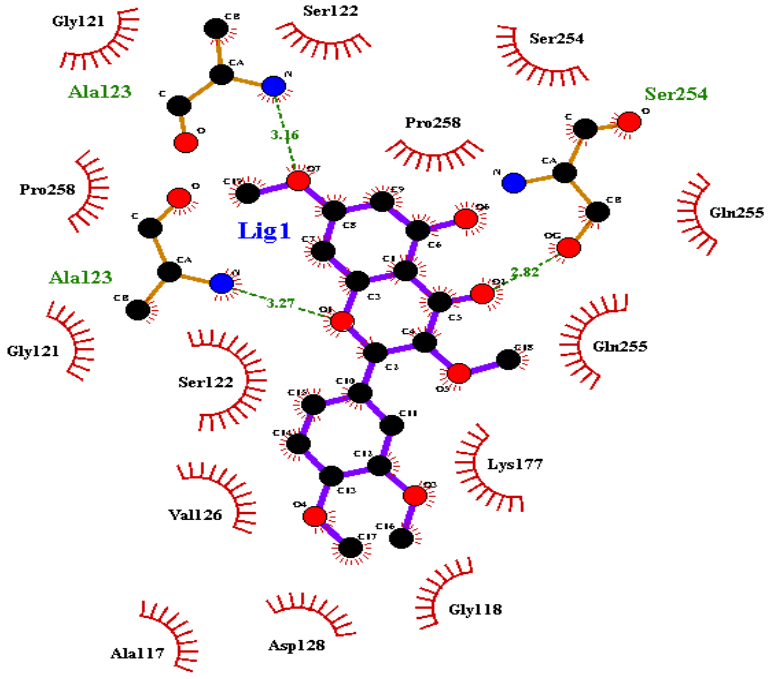

FIGURE 4.37: Interactions of Retusin With CAT By Ligplot.

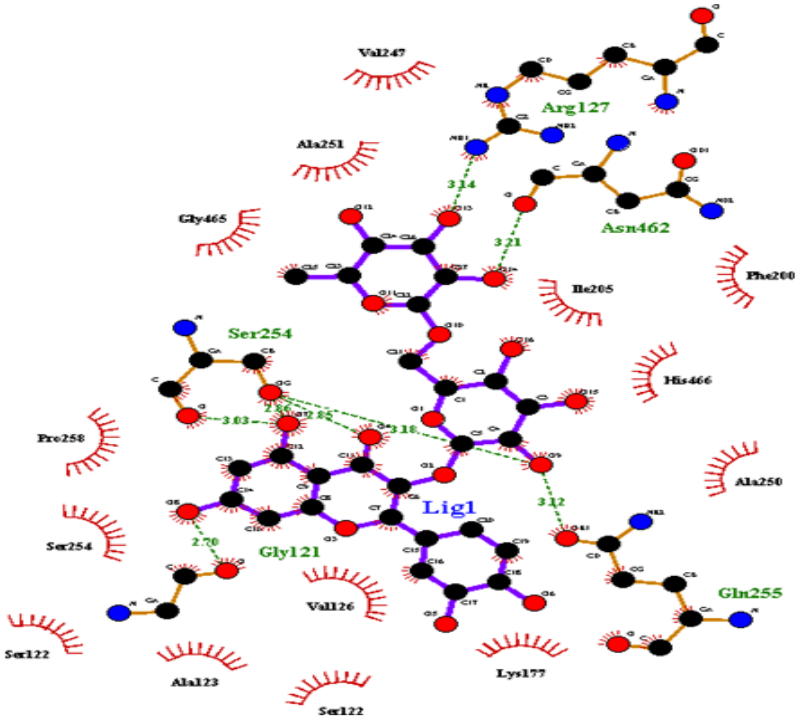

FIGURE 4.38: Interactions of Rutin With CAT By Ligplot.

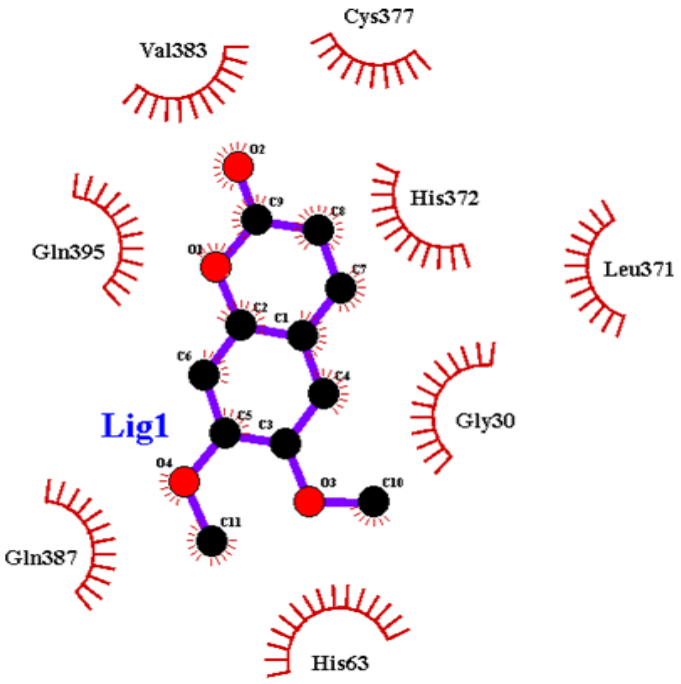

FIGURE 4.39: Interactions of Scoparone With CAT By Ligplot.

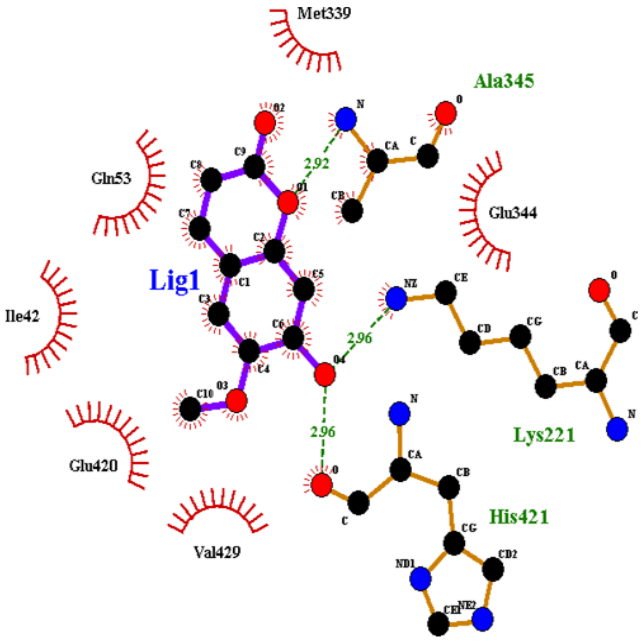

FIGURE 4.40: Interactions of Scopoletin With CAT By Ligplot.

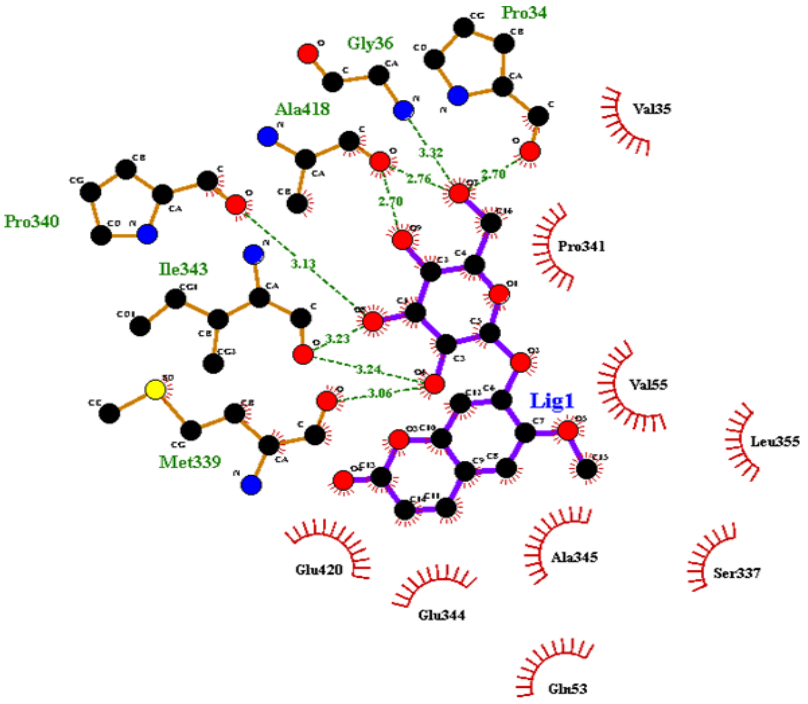

FIGURE 4.41: Interactions of Scopolin With CAT By Ligplot.

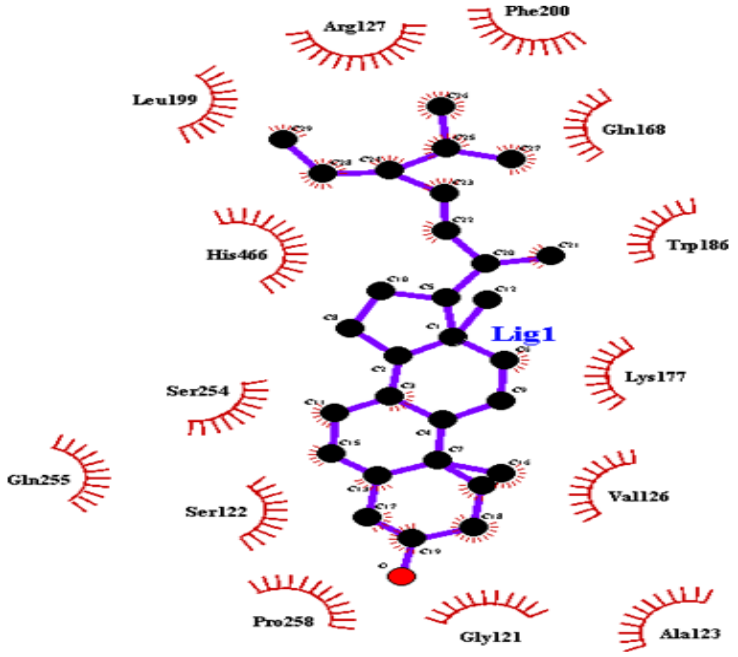

FIGURE 4.42: Interactions of Stigmasterol With CAT By Ligplot.

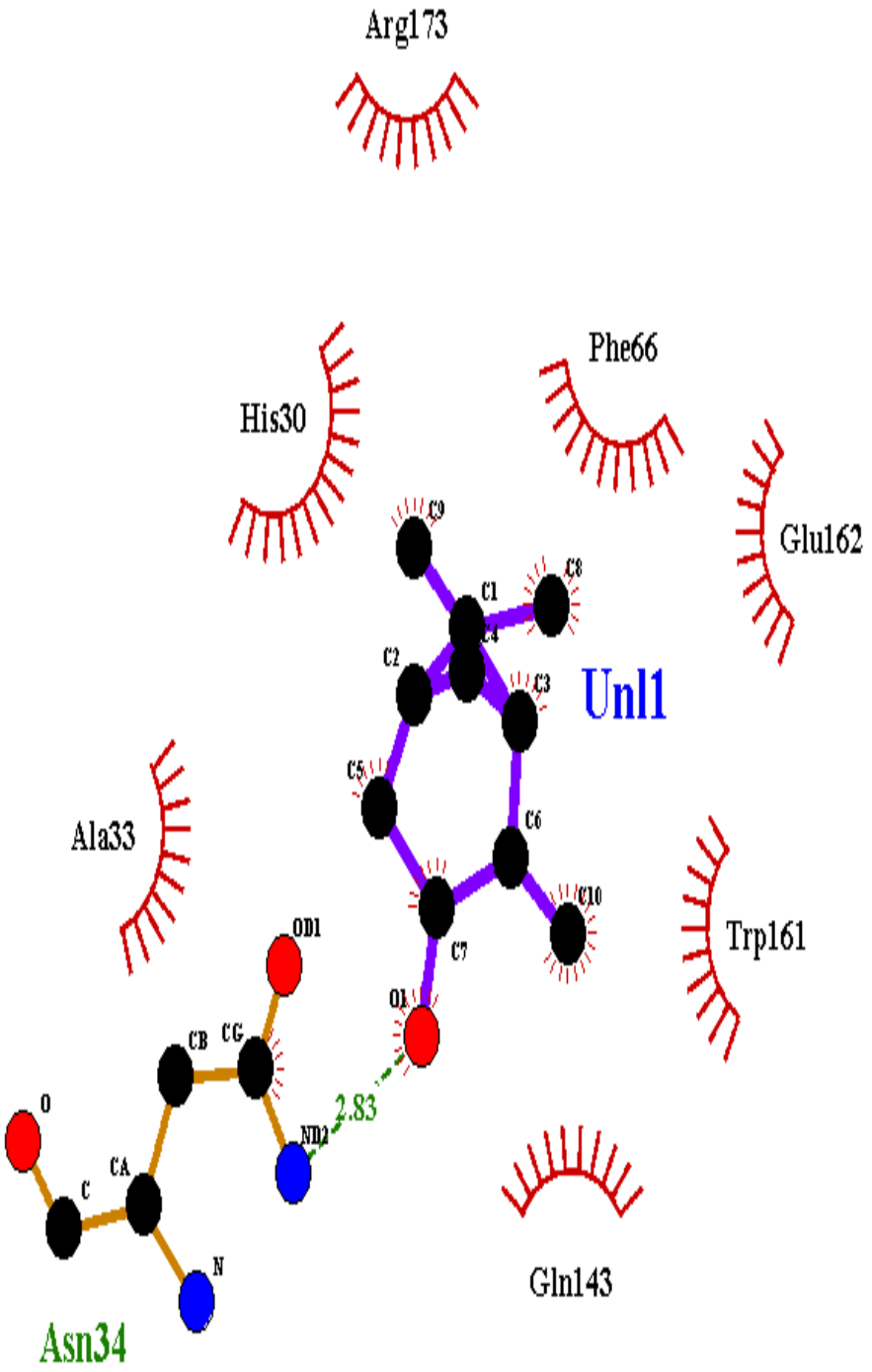

FIGURE 4.43: Interactions of Transpinocarveol With SOD2 By Ligplot.

Table 4.54: Active Ligand Showing Hydrogen and Hydrophobic Interactions

S.No	Ligand Name	Binding Energy	No. of HBs	Hydrogen Bonding Amino Acids	Distance	Hydrophobic Bonding
1	Alpha-Terpinene	-6	0			Gln53 Met339 Val55 Ser337 Glu344 Ala345 Glu420 Leu355
2	Apigenin	-9.5	3	O: Gln: O4 NB2:Arg:O5 NE:Arg:O5	2.96 3.35 2.88	Arg388 Asn397 Glu398 Glu395 Val383 His372 His63 Asp59 Gly30

Continued Table 4.54: Active Ligand Showing Hydrogen and Hydrophobic Interactions.

S.No	Ligand Name	Binding Energy	No. of HBs	Hydrogen Bonding		Hydrophobic Bonding
				Amino Acids	Distance	
						Leu371
3	Arteannuin B	-7.9	1	ND2:Asn:O3	2.91	Trp161 His30 His163 Glu119 Asu171 Gly120 Phe66 Arg173
4	Arteether	-7.6	1	NE:Arg:O1	2.84	Glu255 Ala251 Ser254

Continued Table 4.54: Active Ligand Showing Hydrogen and Hydrophobic Interactions.

S.No	Ligand Name	Binding Energy	No. of HBs	Hydrogen Bonding Amino Acids	Distance	Hydrophobic Bonding
						Val247 Asu462 Phe200 His466
5	Artemether	-7.6	1	ND2:Asn:O2	3.34	Asn67 Phe66 Asn171 Trp161 His30 Glu162
6	Artemetin	-8.2	2	N:Gln:O2 N:Val:O3	2.98 3.06	Arg382 Try379

Continued Table 4.54: Active Ligand Showing Hydrogen and Hydrophobic Interactions.

S.No	Ligand Name	Binding Energy	No. of HBs	Hydrogen Bonding		Hydrophobic Bonding
				Amino Acids	Distance	
						Asp396 Gln395 Asn397 His372 His63 Gln387
7	Artemisia Ketone	-6.3	1	O:Tyr:O	2.99	Pro158 Phe161 Arg354 Met61 Ala357 Phe64

Continued Table 4.54: Active Ligand Showing Hydrogen and Hydrophobic Interactions.

S.No	Ligand Name	Binding Energy	No. of HBs	Hydrogen Bonding Amino Acids	Distance	Hydrophobic Bonding
						Asp65 Val74
8	Artemisinic acid	-8.2	1	N:Ala:O1	3.07	Pro340 Glu420 Val56 Asn33 Pro341 Met339 Glu344 Ser337 Ile343 Val55
9	Artemisinin	-8.4	2	N:His:O4 NB2:Arg:O5	2.85 2.93	Asn67 Phe66 Asn34 Trp161

Continued Table 4.54: Active Ligand Showing Hydrogen and Hydrophobic Interactions.

S.No	Ligand Name	Binding Energy	No. of HBs	Hydrogen Bonding Amino Acids	Distance	Hydrophobic Bonding
						Tyr165 Asn171 Glu162
10	Artesunate	-8.6	4	NB:Arg:O6 NE:Gln:O3 N:Asn:O3 N:His:O7	3.11 3.19 3.26 3.00	Ala33 Pro174 Val116 Val118 Asn171 Lys29 Phe66 Glu162 His163 Trp161
11	Beta-Caryophyllene	-7.5	0			Gln53 Glu344 Ala345

Continued Table 4.54: Active Ligand Showing Hydrogen and Hydrophobic Interactions.

S.No	Ligand Name	Binding Energy	No. of HBs	Hydrogen Bonding Amino Acids	Distance	Hydrophobic Bonding
						Val55 Glu420 Met339 Ser337
12	Beta-Selinene	-7.1	0			Pro340 Met339 Ile343 Val56 Glu344 Ala345 Leu355 Gln53
13	Camphor	-5.7	2	NH2:Arg:O1 OH:Tyr:O1	2.86 2.89	Gly120 Phe66 His30

Continued Table 4.54: Active Ligand Showing Hydrogen and Hydrophobic Interactions.

S.No	Ligand Name	Binding Energy	No. of HBs	Hydrogen Bonding		Hydrophobic Bonding
				Amino Acids	Distance	
						Trp161
						Glu162
14	Casticin	-8.4	3	N:Gln:O2	3.11	Gln395
				OD1:Asp:O6	2.86	Ala381
				OE1:Gln:O3	2.73	Val383
						His372
						Asn397
						Leu371
						Gly30
						Gln387
				O:Pro:O4	2.97	His63
15	Chrysosplenol D	-8.4	2	OD2:Asp:O3	2.94	Gly30
						Leu371
						Asn369
						Gln398
						His372

Continued Table 4.54: Active Ligand Showing Hydrogen and Hydrophobic Interactions.

S.No	Ligand Name	Binding Energy	No. of HBs	Hydrogen Bonding		Hydrophobic Bonding
				Amino Acids	Distance	
						Gln395
						Pro378
						Val383
16	Coumarin	-7.6	1	OH:Tyr:O1	2.94	Arg354
						Phe161
						Met350
						His421
				OH:Tyr:O10	3.37	Glu344
17	Cynaroside	-10.5	5	O:Val:O11	2.97	Gln53
				O:Ala:O3	2.50	Ser422
				O:Ala:O9	2.76	Val55
				O:Pro:O8	2.50	Glu420
						Ile343

Continued Table 4.54: Active Ligand Showing Hydrogen and Hydrophobic Interactions.

S.No	Ligand Name	Binding Energy	No. of HBs	Hydrogen Bonding		Hydrophobic Bonding
				Amino Acids	Distance	
						Val35
18	Deoxy artemisinin	-8	3	ND1:His:O1 OH:Tyr:O4 NH2:Arg:O4	2.9 2.76 2.80	His163 Phe66 Asn34 Asn171 Ala33 Glu162 Gln143
19	Epifriedelanol	-9.9	0			Val116 Asn67 Asn37 Gln119 Phe66 Glu162 Trp161 Asn34

Continued Table 4.54: Active Ligand Showing Hydrogen and Hydrophobic Interactions.

S.No	Ligand Name	Binding Energy	No. of HBs	Hydrogen Bonding Amino Acids	Distance	Hydrophobic Bonding
20	Friedelin	-10	0			Pro258 Ser122 Lys177 Val126 Glu255 Arg127 Val247
21	Germacrene D	-6.7	0			Phe66 His30 Trp161 Glu162 Asn171 Arg173
22	Isorhamnetin	-8.9	5	N:Ala:O6 O:Gly:O6	3.19 3.15	Ser122 Gln255 Ser254

Continued Table 4.54: Active Ligand Showing Hydrogen and Hydrophobic Interactions.

S.No	Ligand Name	Binding Energy	No. of HBs	Hydrogen Bonding		Hydrophobic Bonding
				Amino Acids	Distance	
23	Kaempferol	-9.5	3	N:Ala:O1	3.07	Gly121
				O:Ser:O5	2.96	Ser122
				N:Lys:O4	3.02	Gln255
						Val126
				OD1:Asn:O6	2.89	Gln398
				O:Gln:O6	3.05	Arg388
				O:Pro:O3	3.31	Gln395
						Val383
						His372
						Gly30
						Leu371
						Asn369
						His63
						Asp59
24	Limonene	-5.8	0			Gln53
						Glu344
						Lys221

Continued Table 4.54: Active Ligand Showing Hydrogen and Hydrophobic Interactions.

S.No	Ligand Name	Binding Energy	No. of HBs	Hydrogen Bonding		Hydrophobic Bonding
				Amino Acids	Distance	
						Ala345
						Ser337
						Val55
						Met339
25	Luteolin	-9.8	4	O:Gln:O4	3.02	Gln398
				O:Asp:O5	2.83	His63
				OD2:Asp:O5	2.76	Val383
				NE:Arg:O4	2.94	Gly30
						His372
						Leu371
						Pro368
26	Mearnsetin	-9.3	4	O:Gln:O7	2.75	Val126
				NZ:Lys:O6	3.11	Pro258
				OG:Ser:O4	2.86	Ala123
				O:Gln:O4	2.92	Gly121
						Ser122
						Ser254

Continued Table 4.54: Active Ligand Showing Hydrogen and Hydrophobic Interactions.

S.No	Ligand Name	Binding Energy	No. of HBs	Hydrogen Bonding		Hydrophobic Bonding
				Amino Acids	Distance	
27	Myrtenol	-6.2	4	N:Met:O O:Met:O OD1:Asn:O O:Ser:O	3.20 2.71 3.05 3.00	Pro34 Glu420 Pro341 Val56 Ile343 Thr29 Val55
28	Quercetagetin	-9.8	2	O:Gln:O7 NE:Arg:O4	3.01 3.18	Arg388 Gln398 His372 Val383 Pro368 Gly30 Leu371 His63 Tyr370 Asp59

Continued Table 4.54: Active Ligand Showing Hydrogen and Hydrophobic Interactions.

S.No	Ligand Name	Binding Energy	No. of HBs	Hydrogen Bonding		Hydrophobic Bonding
				Amino Acids	Distance	
29	Quercetin	-10	4	OD1:Asn:O7	2.89	Arg388
				O:Gln:O7	3.08	Gln398
				O:Gly:O5	2.83	Gln395
				O:Pro:O4	3.28	Val383
						His372
						His63
						Asn369
						Asp59
						Tyr370
						Leu371
30	Quinic acid	-6.7	6	NE:His:O4	3.02	Arg388
				OE:Gln:O1	3.12	Val383
				ND2:Asn:O5	3.08	His372
				OE1:Gln:O5	2.65	Gly30
				OE1:Gln:O6	2.70	Leu371
				O:Gln:O6	3.15	

Continued Table 4.54: Active Ligand Showing Hydrogen and Hydrophobic Interactions.

S.No	Ligand Name	Binding Energy	No. of HBs	Hydrogen Bonding		Hydrophobic Bonding
				Amino Acids	Distance	
31	Retusin	-8.8	3	O:Ala:O7	3.16	Gly121
				O:Ser:O2	2.82	Ser122
				N:Ala:O1	3.27	Ser254
						Pro258
						Gln255
						Pro258
						Val126
						Lys177
						Gly118
						Asp128
32	Rutin	-10.1	7	O:Asn:O10	3.21	Val247
				N:Arg:O13	3.14	Ala251
				O:Gln:O9	3.12	Gly465
				O:Ser:O4	2.85	Ile205
				O:Ser:O9	3.18	Phe200
				O:Ser:O7	3.03	His466
				O:Gly:O2	2.70	Pro258

Continued Table 4.54: Active Ligand Showing Hydrogen and Hydrophobic Interactions.

S.No	Ligand Name	Binding Energy	No. of HBs	Hydrogen Bonding Amino Acids	Distance	Hydrophobic Bonding
						Ser254 Ala250 Val126 Lys177 Ser122 Ala123
33	Scoparone	-7.2	0			Val383 Cys377 Gln30 Gln387 His63 His372
34	Scopoletin	-7	3	N:Ala:O1 N:Lys:O4 O:His:O4	2.92 2.96 2.96	Met339 Glu344 Gln53 Ile42 Glu420

Continued Table 4.54: Active Ligand Showing Hydrogen and Hydrophobic Interactions.

S.No	Ligand Name	Binding Energy	No. of HBs	Hydrogen Bonding Amino Acids	Distance	Hydrophobic Bonding
						Val429
35	Scopolin	-8.8	8	O:Pro:O7 N:Gly:O7 O:Ala:O7 O:Ala:O9 O:Pro:O5 O:Ile:O5 O:Ile:O4 O:Met:O4	2.70 3.32 2.76 2.70 3.13 3.23 3.24 3.06	Val35 Pro341 Val55 Glu420 Glu344 Ala345 Leu355 Ser337 Gln53
36	Stigmasterol	-9.1	0			Arg127 Phe200 Leu199 Gln168 His466 Trp186

Continued Table 4.54: Active Ligand Showing Hydrogen and Hydrophobic Interactions.

S.No	Ligand Name	Binding Energy	No. of HBs	Hydrogen Bonding Amino Acids	Distance	Hydrophobic Bonding
						Lys177 Ser254 Ser122 Val126 Pro258 Gly121
37	Transpinocarveol	-5.8	1	N:Asn:O1	2.83	Ala33 Gln143 Trp161 His30 Phe66 Glu162

4.6 ADME Properties of Ligands

Lipinski's five-drug law used as a first step in assessing verbal bioavailability and artificial availability. A second study was performed by calculating the ADMET properties of ligands as a measure of pharmacokinetics using the online tool pkCSM [129]. In pharmacology there are two broad terms the one is pharmacodynamics and the other is pharmacokinetics.

4.6.1 Pharmacodynamics

Pharmacodynamics is a branch of pharmacology in which we study the effect of drugs on the body.

4.6.2 Pharmacokinetics

Pharmacokinetics is a branch of pharmacology in which we study the effect of body on the drugs. In pharmacokinetics we study the absorbtion of drugs, distriburion of drugs, metabolism of the drug and excretion of the drugs.

4.6.3 Absorption

In pharmacology (specifically pharmacokinetics), the transfer of a drug from the bloodstream into the tissues is called absorption. So the chemical composition of a drug, as well as the environment into which a drug is placed, work together to determine the rate and extent of drug absorption.

Absorption is one of ADME properties which predict absorption of orally administered drugs and includes Water solubility, Caco2 permeability, Intestinal absorption, Skin permeability, P-glycoprotein substrate, and P- glycoprotein I & II inhibitors. Water solubility (log S) of a compound predicts its solubility in water

at $25C^0$. It is predicted as a molar concentration logarithm (log mol / L). Lipid soluble drugs are less soluble in water than water-soluble drugs.

The Caco-2 permeability model predicts the logarithm of the apparent permeability coefficient (log Papp; logcm/s). A compound has a high Caco-2 absorbency if it has a Papp $> 8 \times$ 10-6cm /s. Intestinal absorption predicts the percentage that will enter a person's small intestine. A compound with less than 30% absorption is considered to be less absorbent. The skin permeability model predicts the absorbency in log Kp and this model has a special interest in the formation of transdermal drugs. The element with the log Kp > -2.5 means it has low skin penetration.

The P-glycoprotein substrate acts as a natural barrier and removes toxins and xenobiotics from the cells. This model predicts whether the given compound may be P-glycoprotein (Pgp) substratum or not. This means if a compound is a Pgp-substrate (categorically yes), it may be show low oral absorption. P-gp substrates can be easily pumped out of the cells to reduce their absorption.

P-glycoprotein I/II inhibitor model predicts that the compound is likely to be a P-gb I/II inhibitor or not. P-gp inhibitors reduce the pumping activity of P-gp and may have high absorption [130].

4.6.3.1 Absorption Properties of Alpha Terpinene, Apigenin, Arteannuin B, Arteether, & Artemether

All these ligands showed less water solubility. Caco2 permeability in the form of log Papp in 10-6cm/s is within normal range. Their intestinal absorption values are good in the line of 90%, highest among them is 98.347% of Arteannuin B. Apigenin, Arteannuin B, Arteether and Artemether shows low skin permeability values in the form of log Kp. Apigenin predicted as P-glycoprotein substrate while Arteether and Artemether as P-glycoprotein I inhibitor (Table 4.55).

Table 4.55: Absorption Properties of Ligands

S.No	Ligands	Alpha-Terpinene	Apigenin	Arteannuin-B	Arteether	Artemether
1	Water solubility	-3.941 mol/L	-3.329 mol/L	-3.221 mol/L	-3.908 mol/L	-3.927 mol/L
2	Caco2 permeability	1.414 cm/S	1.007 cm/S	1.537 cm/S	1.332 cm/S	1.311 cm/S
3	Intestinal absorption (human)	96.219 %	93.25 %	98.347 %	96.488 %	96.855 %
4	Skin Permeability	-1.489 log Kp	-2.735 log Kp	-3.322 log Kp	-3.345 log Kp	-2.929 log Kp
5	P-glycoprotein substrate	No	Yes	No	No	No
6	P-glycoprotein I inhibitor	No	No	No	Yes	Yes
7	P-glycoprotein II inhibitor	No	No	No	No	No

4.6.3.2 Absorption Properties of Artemetin, Artemisia Ketone, Artemisinic acid, Artemisinin & Artesunate

Artemetin showed low water solubility and normal Caco2 permeability with 100% intestinal absorption. Its skin permeability is low and shows positive result as P-glycoprotein substrate and as P gp I/II inhibitor. Artesunate also shows positive predicted result as Pgp substrate. All these compounds show low water solubility and skin permeability except Artemisia Ketone (log Kp-1.796) (Table 4.56).

Table 4.56: Absorption Properties of Ligands

S.No	Ligands	Artemetin	Artemisia-Ketone	Artemisinin	Artemisinic acid	Artesunate
1	Water solubility	-4.326 mol/L	-2.456 mol/L	-3.678 mol/L	3.632 mol/L	-3.097 mol/L
2	Caco2 permeability	1.424 cm/S	1.32 cm/S	1.295 cm/S	1.6 cm/S	0.863 cm/S
3	Intestinal absorption (human)	100 %	97.196 %	97.543 %	95.706 %	72.19 %
4	Skin Permeability	-2.747 log Kp	-1.796 log Kp	-3.158 log Kp	-2.699 log Kp	-2.735 log Kp
5	P-glycoprotein substrate	Yes	No	No	No	Yes
6	P-glycoprotein I inhibitor	Yes	No	No	No	No
7	P-glycoprotein II inhibitor	Yes	No	No	No	No

4.6.3.3 Absorption Properties of Beta Caryophyllene, Beta Selinene, Camphor, Casticin & Chrysosplenol D

All these compounds showed low water solubility. Casticin and Chrysosplenol D Positive for model Pgp substrate and Pgp II inhibitor (Table 4.57).

Table 4.57: Absorption Properties of Ligands

S.No	Ligands	Casticin	Beta-Selinene	Camphor	Beta Caryophyllene	Chrysos-plenol D
1	Water solubility	-3.599 mol/L	-6.439 mol/L	-2.895 mol/L	-5.555 mol/L	-3.328 mol/L
2	Caco2 permeability	1.39 cm/S	1.429 cm/S	1.499 cm/S	1.423 cm/S	0.402 cm/S
3	Intestinal absorption (human)	96.91 %	95.574 %	95.965 %	94.845 %	81.386 %
4	Skin Permeability	-2.744 log Kp	-1.702 log Kp	-2.002 log Kp	-1.58 log Kp	-2.735 log Kp
5	P-glycoprotein substrate	Yes	No	No	No	Yes
6	P-glycoprotein I inhibitor	No	No	No	No	No
7	P-glycoprotein II inhibitor	Yes	No	No	No	Yes

4.6.3.4 Absorption Properties of Coumarin, Cynaroside, Deoxy artemisinin, Epifriedelanol & Friedelin

Cynaroside shows 37.55% intestinal absorption and positive predicted value of model Pgp substrate. Epifriedelanol and Friedelin exhibited as Pgp I/II inhibitors. Such compounds if used as drugs must be given in small oral doses (<50mg) because they are not easily pumped out of the cells to reduce their absorption. (Table 4.58).

Table 4.58: Absorption Properties of Ligands

S.No	Ligands	Coumarin	Cynaroside	Deoxy-artemisinin	Epifriedelanol	Friedelin
1	Water solubility	-1.517 mol/L	-2.716 mol/L	-3.396 mol/L	-5.572 mol/L	-5.514 mol/L
2	Caco2 permeability	1.649 cm/S	0.248 cm/S	1.318 cm/S	1.22 cm/S	1.266 cm/S
3	Intestinal absorption (human)	97.344 %	37.556 %	97.828 %	95.938 %	98.736 %
4	Skin Permeability	-1.921 log Kp	-2.735 log Kp	-3.279 log Kp	-2.732 log Kp	-2.605 log Kp
5	P-glycoprotein substrate	No	Yes	No	No	No
6	P-glycoprotein I inhibitor	No	No	No	Yes	Yes
7	P-glycoprotein II inhibitor	No	No	No	Yes	Yes

4.6.3.5 Absorption Properties of Germacrene D, Isorhamnetin, Kaempferol, Limonene & Luteolin

All compounds show good intestinal absorption, furthermore all these ligands predict as positive for model Pgp substrate except Germacrene D. If a compound is positive for Pgp substrate then its means that it can be easily pumped out of the cells to reduce its absorption (Table 4.59).

Table 4.59: Absorption Properties of Ligands

S.No	Ligands	Limonene	Luteolin	Kaempferol	Germacrene D	Isorhamnetin
1	Water solubility	-3.568 mol/L	-3.094 mol/L	-3.04 mol/L	-5.682 mol/L	-3 mol/L
2	Caco2 permeability	1.401 cm/S	0.096 cm/S	0.032 cm/S	1.436 cm/S	-0.003 cm/S
3	Intestinal absorption (human)	95.898 %	81.13 %	74.29 %	95.59 %	76.014 %
4	Skin Permeability	-1.721 log Kp	-2.735 log Kp	-2.735 log Kp	-1.429 log Kp	-2.735 log Kp
5	P-glycoprotein substrate	Yes	Yes	Yes	No	Yes
6	P-glycoprotein I inhibitor	No	No	No	No	No
7	P-glycoprotein II inhibitor	No	No	No	No	No

4.6.3.6 Absorption Properties of Mearnsetin, Myrtenol, Quercetagetin, Quercetin & Quinic acid

Quinic acid predicts 32% intestinal absorption which is near to poorly absorbed substances (30%). Mearnsetin, Quercetagetin, and Quercetin predicted as Pgp substrates (Table 4.60).

Table 4.60: Absorption Properties of Ligands

S.No	Ligands	Mearnsetin	Myrtenol	Quercetagetin	Quercetin	Quinic acid
1	Water solubility	-2.913 mol/L	-2.382 mol/L	-2.904 mol/L	-2.925 mol/L	-1.119 mol/L
2	Caco2 permeability	0.337 cm/S	1.464 cm/S	-1.488 cm/S	-0.229 cm/S	-0.258 cm/S
3	Intestinal absorption (human)	68.476 %	94.34 %	62.773 %	77.207 %	32.274 %
4	Skin Permeability	-2.735 log Kp	-2.347 log Kp	-2.735 log Kp	-2.735 log Kp	-2.737 log Kp
5	P-glycoprotein substrate	Yes	No	Yes	Yes	No
6	P-glycoprotein I inhibitor	No	No	No	No	No
7	P-glycoprotein II inhibitor	No	No	No	No	No

4.6.3.7 Absorption Properties of Retusin, Rutin, Scoparone, Scopoletin, and Scopolin

Rutin was the first compound in this study which shows poor intestinal absorption (23.44%). It is also predicted as Pgp substrate. Retusin and Scopolin also predicted as Pgp substrates. Retusin exhibit itself as Pgp I/II inhibitor (Table 4.61).

Table 4.61: Absorption Properties of Ligands

S.No	Ligands	Retusin	Rutin	Scoparone	Scopoletin	Scopolin
1	Water solubility	-4.152 mol/L	-2.892 mol/L	-1.976 mol/L	-2.504 mol/L	-2.21 mol/L
2	Caco2 permeability	1.198 cm/S	-0.949 cm/S	1.298 cm/S	1.184 cm/S	0.377 cm/S
3	Intestinal absorption (human)	95.257 %	23.446 %	97.879 %	95.277 %	48.119 %
4	Skin Permeability	-2.729 log Kp	-2.735 log Kp	-2.346 log Kp	-2.944 log Kp	-2.822 log Kp
5	P-glycoprotein substrate	Yes	Yes	No	No	Yes
6	P-glycoprotein I inhibitor	Yes	No	No	No	No
7	P-glycoprotein II inhibitor	Yes	No	No	No	No

4.6.3.8 Absorption Properties of Stigmasterol & Transpinocarveol

Stigmasterol shows poor water solubility and good intestinal absorption. It also predicted as Pgp I/II inhibitor (Table 4.62 & 4.63).

Table 4.62: Absorption Properties of Ligands

S.No	Ligands	Stigmasterol
1	Water solubility	-6.682 mol/L
2	Caco2 permeability	1.213 cm/S
3	Intestinal absorption (human)	94.97 %
4	Skin Permeability	-2.783 log Kp
5	P-glycoprotein substrate	No
6	P-glycoprotein I inhibitor	Yes
7	P-glycoprotein II inhibitor	Yes

Table 4.63: Absorption Properties of Ligands

S.No	Ligands	Transpinocarveol
1	Water solubility	-2.43 mol/L
2	Caco2 permeability	1.465 cm/S
3	Intestinal absorption (human)	93.456 %
4	Skin Permeability	-2.361 log Kp
5	P-glycoprotein substrate	No
6	P-glycoprotein I inhibitor	No
7	P-glycoprotein II inhibitor	No

4.6.4 Distribution

Distribution in pharmacology is a branch of pharmacokinetics which deals with the movement of drug within the body from one location to another location. Distribution as one of ADME property includes four models namely as Volume of distribution in human (VDss expressed as log L/kg)), Fraction unbound in humans (Fu), Blood brain barrier (BBB) permeability expressed as log BB, and Central nervous system permeability (CNS permeability) expressed as log PS [131].

Model-1 explains the theoretical volume that the total amount of drug will need to be evenly distributed to provide the same concentration as in blood plasma. VDss is considered low if it is less than 0.71 L / kg (log VDss < 0.15) and higher if it is above 2.81L / kg (log VDss> 0.45). If VDss is high, it means that more of the drug is still distributed to the tissues than to plasma.

If a compound shows more Fu value, its mean it is more effective. BBB protects the brain from exogenous compounds so BBB permeability is an important parameter. If predicted value of log BB >0.3 then its mean given substance can cross BBB and if value <-1 then no harm to brain. Log PS is the product of blood-brain permeability and surface area, and its value >-2 considered to penetrate the Central Nervous System (CNS), and <-3 considered as safe.

Among selected compounds, Apigenin, Beta-caryophyllene, Beta Selinene, Cynaroside, Germacrene D, Isorhamnetin, Kaempferol, Luteolin, Mearnsetin, Quercetagetin, Quercetin, and Rutin showed high VDss value.

Alpha terpinene, Arteannuin B, Artemether, Artemisia Ketone, Beta Caryophyllene, Beta Selinene, Camphor, Epifriedelanol, Friedelin, Germacrene D, Limonene, and Myrtenol showed log BB>0.3. Log PS in -1 for Beta Selinene, Coumarin, Epifriedelanol, Friedelin, and Stigmasterol (Table 4.64 to 4.71).

Table 4.64: The Distribution of Ligands

S.No	Ligands	Arteether	Apigenin	Arteannuin B	Alpha Terpinene	Artemether
1	VDss (human)	0.448 L/Kg	0.822 L/Kg	0.401 L/Kg	0.412 L/Kg	0.412 L/Kg
2	Fraction unbound (human)	0.376 Fu	0.147 Fu	0.426 Fu	0.42 Fu	0.42 Fu
3	BBB permeability	0.253 log BB	-0.734 log BB	0.434 log BB	0.754 log BB	0.754 log BB
4	CNS permeability	-3.359 log PS	-2.061 log PS	-2.951 log PS	-2.049 log PS	-2.049 log PS

Table 4.65: The Distribution of Ligands

S.No	Ligands	Artemetin	Artemisia Ketone	Artemisinic Acid	Artemisinin	Artesunate
1	VDss (human)	-0.244 L/Kg	0.069 L/Kg	-0.449 L/Kg	0.457 L/Kg	0.172 L/Kg
2	Fraction unbound (human)	0.123 Fu	0.499 Fu	0.302 Fu	0.4 Fu	0.36 Fu
3	BBB permeability	-1.152 log BB	0.597 log BB	0.323 log BB	0.235 log BB	-0.954 log BB
4	CNS permeability	-3.156 log PS	-2.307 log PS	-2.314 log PS	-2.909 log PS	-3.039 log PS

Table 4.66: The Distribution of Ligands

S.No	Ligands	Casticin	Beta Selinene	Camphor	Beta Caryophyllene	Chryosplenol-D
1	VDss (human)	-0.176 L/Kg	0.639 L/Kg	0.331 L/Kg	0.652 L/Kg	0.287 L/Kg
2	Fraction unbound (human)	0.103 Fu	0.089 Fu	0.459 Fu	0.263 Fu	0.093 Fu
3	BBB permeability	-1.053 log BB	0.816 log BB	0.612 log BB	0.733 log BB	-1.607 log BB
4	CNS permeability	-3.209 log PS	-1.461 log PS	-2.158 log PS	-2.172 log PS	-3.298 log PS

Table 4.67: The Distribution of Ligands

S.No	Ligands	Coumarin	Cynaroside	Deoxyartemisinin	Epifriedelanol	Friedelin
1	VDss (human)	-0.143 L/Kg	0.884 L/Kg	0.356 L/Kg	-0.082 L/Kg	-0.272 L/Kg
2	Fraction unbound (human)	0.367 Fu	0.224 Fu	0.411 Fu	0 Fu	0 Fu
3	BBB permeability	-0.007 log BB	-1.564 log BB	0.28 log BB	0.7 log BB	0.72 log BB
4	CNS permeability	0.72 log PS	-3.93 log PS	-2.999 log PS	-1.674 log PS	-1.555 log PS

Table 4.68: The Distribution of Ligands

S.No	Ligands	Limonene	Isorhamnetin	Kaempferol	Germacrene D	Luteolin
1	VDss (human)	0.396 L/Kg	1.123 L/Kg	1.274 L/Kg	0.544 L/Kg	1.153 L/Kg
2	Fraction unbound (human)	0.48 Fu	0.091 Fu	0.178 Fu	0.261 Fu	0.168 Fu
3	BBB permeability	0.732 log BB	-1.135 log BB	-0.939 log BB	0.723 log BB	-0.907 log BB
4	CNS permeability	-2.37 log PS	-3.188 log PS	-2.228 log PS	-2.138 log PS	-2.251 log PS

Table 4.69: The Distribution of Ligands

S.No	Ligands	Mearnsetin	Myrtenol	Quercetagetin	Quercetin	Quinic Acid
1	VDss (human)	1.437 L/Kg	0.488 L/Kg	1.424 L/Kg	1.559 L/Kg	-0.217 L/Kg
2	Fraction unbound (human)	0.133 Fu	0.499 Fu	0.246 Fu	0.206 Fu	0.821 Fu
3	BBB permeability	-1.252 log BB	0.773 log BB	-1.664 log BB	-1.098 log BB	-0.894 log BB
4	CNS permeability	-3.448 log PS	-2.511 log PS	-3.362 log PS	-3.065 log PS	-3.667 log PS

Table 4.70: The Distribution of Ligands

S.No	Ligands	Retusin	Rutin	Scoparone	Scopoletin	Scopolin
1	VDss (human)	-0.211 L/Kg	1.663 L/Kg	-0.344 L/Kg	0.034 L/Kg	-0.611 L/Kg
2	Fraction unbound (human)	0.138 Fu	0.187 Fu	0.298 Fu	0.363 Fu	0.397 Fu
3	BBB permeability	-0.94 log BB	-1.899 log BB	0.177 log BB	-0.299 log BB	-1.286 log BB
4	CNS permeability	-3.036 log PS	-5.178 log PS	-2.328 log PS	-2.32 log PS	-3.954 log PS

Table 4.71: The Distribution of Ligands

S.No	Ligands	Stigmasterol	Transpinocarveol
1	VDss (human)	0.178 L/Kg	0.464 L/Kg
2	Fraction unbound (human)	0 Fu	0.497 Fu
3	BBB permeability	0.771 log BB	0.756 log BB
4	CNS permeability	-1.652 log PS	-2.438 log PS

4.6.5 Metabolism

CYP1A2, CYP2C19, CYP2C9, CYP2D6, and CYP3A4 models of the various isoforms of Cytochrome P450 which is an important cleansing enzyme found in the liver. This enzyme reacts to xenobiotics to facilitate their release. Some drugs are triggered by this enzyme while most drugs are neutralized by it [115]. Metabolic properties of ligands were given below in Table 4.72 to 4.79.

Table 4.72: Metabolic Properties of Ligands

S.No	Ligands	Artemether	Apigenin	Arteannuin-B	Arteether	Alpha Terpinene
1	CYP2D6 substrate	No	No	No	No	No
2	CYP3A4 substrate	Yes	No	Yes	Yes	No
3	CYP1A2 inhibitior	Yes	Yes	Yes	No	No
4	CYP2C19 inhibitior	No	Yes	No	No	No
5	CYP2C9 inhibitior	No	No	No	No	No
6	CYP2D6 inhibitior	No	No	No	No	No
7	CYP3A4 inhibitior	No	No	No	No	No

Table 4.73: Metabolic Properties of Ligands

S.No	Ligands	Artemetin	Artemisia Ketone	Artemisinic Acid	Artemisinin	Artesunate
1	CYP2D6 substrate	No	No	No	No	No
2	CYP3A4 substrate	Yes	No	No	Yes	Yes
3	CYP1A2 inhibitior	Yes	No	No	Yes	No
4	CYP2C19 inhibitior	Yes	No	No	No	No
5	CYP2C9 inhibitior	Yes	No	No	No	No
6	CYP2D6 inhibitior	No	No	No	No	No
7	CYP3A4 inhibitior	No	No	No	No	No

Table 4.74: Metabolic Properties of Ligands

S.No	Ligands	Casticin	Camphor	Beta Selinene	Beta Caryophyllene	Chrysosplenol D
1	CYP2D6 substrate	No	No	No	No	No
2	CYP3A4 substrate	Yes	No	Yes	No	Yes
3	CYP1A2 inhibitior	Yes	No	Yes	No	Yes
4	CYP2C19 inhibitior	Yes	No	No	No	No
5	CYP2C9 inhibitior	No	No	No	No	No
6	CYP2D6 inhibitior	No	No	No	No	No
7	CYP3A4 inhibitior	Yes	No	No	No	No

Table 4.75: Metabolic Properties of Ligands

S.No	Ligands	Coumarin	Cynaroside	Friedelin	Deoxyartemisinin	Epifriedelanol
1	CYP2D6 substrate	No	No	No	No	No
2	CYP3A4 substrate	No	No	Yes	Yes	Yes
3	CYP1A2 inhibitior	Yes	No	No	Yes	No
4	CYP2C19 inhibitior	No	No	No	No	No
5	CYP2C9 inhibitior	No	No	No	No	No
6	CYP2D6 inhibitior	No	No	No	No	No
7	CYP3A4 inhibitior	No	No	No	No	No

Table 4.76: Metabolic Properties of Ligands

S.No	Ligands	Limonene	Luteolin	Kaempferol	Germacrene D	Isorhamnetin
1	CYP2D6 substrate	No	No	No	No	No
2	CYP3A4 substrate	No	No	No	No	Yes
3	CYP1A2 inhibitior	No	Yes	Yes	No	Yes
4	CYP2C19 inhibitior	No	No	No	No	No
5	CYP2C9 inhibitior	No	Yes	No	No	No
6	CYP2D6 inhibitior	No	No	No	No	No
7	CYP3A4 inhibitior	No	No	No	No	No

Table 4.77: Metabolic Properties of Ligands

S.No	Ligands	Mearnsetin	Quercetagetin	Myrtenol	Quercetin	Quinic acid
1	CYP2D6 substrate	No	No	No	No	No
2	CYP3A4 substrate	No	No	No	No	No
3	CYP1A2 inhibitior	No	Yes	No	Yes	No
4	CYP2C19 inhibitior	No	No	No	No	No
5	CYP2C9 inhibitior	No	No	No	No	No
6	CYP2D6 inhibitior	No	No	No	No	No
7	CYP3A4 inhibitior	No	No	No	No	No

Table 4.78: Metabolic Properties of Ligands

S.No	Ligands	Retusin	Rutin	Scoparone	Scopoletin	Scopolin
1	CYP2D6 substrate	No	No	No	No	No
2	CYP3A4 substrate	Yes	No	No	No	No
3	CYP1A2 inhibitior	Yes	No	Yes	Yes	No
4	CYP2C19 inhibitior	Yes	No	No	No	No
5	CYP2C9 inhibitior	No	No	No	No	No
6	CYP2D6 inhibitior	No	No	No	No	No
7	CYP3A4 inhibitior	Yes	No	No	No	No

TABLE 4.79: Metabolic Properties of Ligands

S.No	Ligands	Stigmasterol	Transpinocarveol
1	CYP2D6 substrate	No	No
2	CYP3A4 substrate	Yes	No
3	CYP1A2 inhibitior	No	No
4	CYP2C19 inhibitior	No	No
5	CYP2C9 inhibitior	No	No
6	CYP2D6 inhibitior	No	No
7	CYP3A4 inhibitior	No	No

4.6.6 Excretion

The organs involved in drug excretion are the kidneys, which play important role in excretion (renal excretion) and the liver (biliary excretion). Other organs may also be involved in excretion, such as the lungs for volatile or gaseous agents. Drugs can also be excreted in sweat, saliva and tears. Models of Excretion property are Total Clearance (CLtot) expressed as log (CL tot) in ml/min/kg and second one is Renal OCT2 substrate which predicts results as Yes /No. OCT2 (organic cation transporter 2) is a renal uptake transporter that plays role in disposition and renal clearance of drugs [132].

All ligands showed negative result for model Renal OCT2 substrate. Only two compounds namely as Friedelin and Rutin exhibit poor total clearance. Excretory properties are listed in Table 4.80 to 4.87.

Table 4.80: Excretory Properties of Ligands

S.No	Ligands	Alpha Terpinene	Apigenin	Arteether	Arteannuin B	Artemether
1	Total Clearance	0.223 ml/Kg	0.566 ml/Kg	1.068 ml/Kg	0.965 ml/Kg	1.031 ml/Kg
2	Renal OCT2 substrate	No	No	No	No	No

Table 4.81: Excretory Properties of Ligands

S.No	Ligands	Artemetin	Artemisia Ketone	Artemisinic-acid	Artemisinin	Artesunate
1	Total Clearance	0.706 ml/Kg	0.435 ml/Kg	0.639 ml/Kg	0.98 ml/Kg	0.969 ml/Kg
2	Renal OCT2 substrate	No	No	No	No	No

Table 4.82: Excretory Properties of Ligands

S.No	Ligands	Beta-Caryophyllene	Casticin	Camphor	Chrysosplenol-D	Beta-Selinene
1	Total Clearance	1.088 ml/Kg	0.628 ml/Kg	0.109 ml/Kg	0.502 ml/Kg	1.174 ml/Kg
2	Renal OCT2 substrate	No	No	No	No	No

Table 4.83: Excretory Properties of Ligands

S.No	Ligands	Epifriedelanol	Coumarin	Friedelin	Deoxy artemisinin	Cynaroside
1	Total Clearance	0.015 ml/Kg	0.97 ml/Kg	-0.04 ml/Kg	0.803 ml/Kg	0.478 ml/Kg
2	Renal OCT2 substrate	No	No	No	No	No

Table 4.84: Excretory Properties of Ligands

S.No	Ligands	Isorhamnetin	Limonene	Kaempferol	Germacrene D	Luteolin
1	Total Clearance	0.508 ml/Kg	0.213 ml/Kg	0.477 ml/Kg	1.42 ml/Kg	0.495 ml/Kg
2	Renal OCT2 substrate	No	No	No	No	No

Table 4.85: Excretory Properties of Ligands

S.No	Ligands	Mearnsetin	Quercetagetin	Myrtenol	Quercetin	Quinic acid
1	Total Clearance	0.47 ml/Kg	0.307 ml/Kg	0.054 ml/Kg	0.407 ml/Kg	0.639 ml/Kg
2	Renal OCT2 substrate	No	No	No	No	No

Table 4.86: Excretory Properties of Ligands

S.No	Ligands	Retusin	Rutin	Scoparone	Scopoletin	Scopolin
1	Total Clearance	0.738 ml/Kg	-0.369 ml/Kg	0.793 ml/Kg	0.73 ml/Kg	0.716 ml/Kg
2	Renal OCT2 substrate	No	No	No	No	No

Table 4.87: Excretory Properties of Ligands

S.No	Ligands	Stigmasterol	Transpinocarveol
1	Total Clearance	0.618 ml/Kg	0.034 ml/Kg
2	Renal OCT2 substrate	No	No

4.7 Lead Compound Identification

Physicochemical and Pharmacokinetics properties determine the final destiny of compounds as drug or non-drug compounds. Physicochemical properties or Lipinski's rule of five works as primary filter and Pharmacokinetics studies as secondary filter in screening of potential compounds. Rutin and Cynaroside not obey Lipinski's rule of five, so they knock out in primary screening while Epifriedelanol, Stigmasterol, and Friedelin not totally comply with RO5 (All these three compounds have log p >5). Pharmacokinetic studies of these compounds screen out Alpha terpinene, Arteannuin B, Artemether, Artemisia Ketone, Beta Caryophyllene, Camphor, and Germacrene D (log BB > 0.3), Epifriedelanol, and Friedelin (log BB >0.3 & log PS >-2), Beta Selinene, Coumarin, and Stigmasterol (log PS> -2). Best five compounds (Hit compounds on the basis of primary and secondary filters, toxicity predicted values and binding score) are Quercetin, Luteolin, Apigenin, Kaempferol, and Mearnsetin (Binding scores with all three receptors shown in Table 4.88). Lead Compound of this research work is Quercetin.

Table 4.88: Hit Compounds With Binding Scores.

S.No	**Name of Potential-Compound**	**Binding Score with CAT**	**Binding Score with SOD2**	**Binding Score with GPX1**
1	Quercetin	-10	-8.4	-6.5
2	Luteolin	-9.8	-8	-6.4
3	Apigenin	-9.5	-7.8	-6
4	Kaempferol	-9.5	-8.2	-5.9
5	Mearnsetin	-9.3	-8.6	-6.4

4.8 Anti-Oxidant Drug Identification

The docking results of these 37 compounds were compared with 12 FDA approved & investigational drugs namely Alpha- tocopherol, Ascorbic acid, Allopurinol, Beta Carotene, Catechin, Carvedilol, Metformin, Methionine, N-Acetyl cysteine, Nebivolol, Resveratrol, and Serotonin. I have downloaded their structures from Pubchem database and minimized their energy by Chem 3D Pro (version 12.0) and save them in sdf format. The docking of these drugs as ligands against CAT, SOD2, and GPX1 as receptors was performed by CB dock. Among these 12 drugs, Carvedilol screen out due to its size, 18.6KB, (because CB dock accepts files up to 15KB). The remaining 11 drugs shows their 5 best poses with selected receptors. Mechanism of these 11 selected drugs with references are shown in Table 4.89.

Table 4.89: Drugs And Their Mechanism of Action

S.No	Drugs	Mechanism of action	References
1	Alpha-Tocopherol	Alpha-Tocopherol prevent endothelial impairment initiated by oxidative damage in heart failure, diabetes, and hypercholesterolemia.	[133,135]
2	Ascorbic acid	Ascorbic acid, a potent water-soluble antioxidant works as enzyme manager increasing eNOS activity and decreasing the amounts of ROS sources.	[136]
3	Allopurinol	Allopurinol works as xanthine oxidase inhibitor, diminish oxidative stress and high blood pressure and enhance endothelial function.	[137]
4	Beta carotene	Beta carotene combine and neutralize peroxyl radicals before they produce lipid peroxidation.	[138,139]
5	Catechin	Catechin influences sympathetic nervous system (SNS) activity, increasing energy expenditure and promoting the lipid oxidation.	[140]
6	Metformin	Metformin activates the cellular energy sensor AMP-activated protein kinase (AMPK) which restore energy homeostasis.	[141]

Continue Table 4.89: Drugs And Their Mechanism of Action

S.No	Drugs	Mechanism of action	References
7	Methionine	Methionine activates the protein kinase mTOR and enhance the expression of the transcription factor Myc, also involves in expansion of T cells.	[142]
8	N-Acetyl cysteine	N-Acetylcysteine (NAC) inhibit oxidative stress via NO dependent mechanism and prevent oxidative damage by reducing lipid peroxidation and ROS scavenging.	[143,144]
9	Nebivolol	Nebivolol involves in the inhibition of the expression and activity of NADPH oxidase and prevention of endothelial dysfunction. Furthermore, nebivolol increases e NOS generation by promoting e NOS activity.	[145,146]
10	Resveratrol	Beta carotene combine and neutralize Resveratrol stimulates the production of endothelial nitric oxide, reduces oxidative stress, restrains vascular inflammation and prevents platelet aggregation.	[147]
11	Serotonin	Serotonin acts as neurotransmitter, and immunomodulator, downregulating the inflammatory response by central and peripheral mechanisms.	[148]

4.9 Selection of Antioxidant Drugs

For the selection of most efficient drug, physiochemical parameters including molecular formula, molecular weight, absorption, water solubility, log P, H-bond donors and acceptors, bioavailability, polarizability, ADMET probability (must be less than 1) and side effects of these drugs were studied by using PubChem, and Drug bank databases and pkCSM online tool. Physiochemical properties of drugs are listed in Table 4.90 to Table 4.93.

Table 4.90: Physiochemical Properties of Drugs.

S.No	Properties	Alpha-Tocopherol	Ascorbic acid	Allopurinol
1	Chemical formula	$C_{29}H_{50}O_2$	$C_6H_8O_6$	$C_5H_4N_4O$
2	Absorption	10-33% in the small intestine,9.7 hours.	70-90%.	90% from the gastrointestinal tract,1.5 hours.
3	Water solubility mg/ml	7.0406	245.0	22.0
4	logP	8.84026	-1.6	-0.41
5	H-bond donor	1	4	2
6	H-bond Acceptor	2	5	4
7	Bioavailability	0	1	1
8	Polarizability	55.29 $Å^3$	14.93 $Å^3$	11.7 $Å^3$
9	ADMET probability	0.9795	0.6559	0.997
10	Side Effects	Dizziness, Fatigue, Headaches, Weakness, Blurred vision, Abdominal pain, Diarrhea & Nausea.	Nausea, Vomiting, Heartburn, Stomach cramps & Headache.	Skin rash, Diarrhea, Nausea, Changes in Liver function-test (LFT) & Gout-flare-up.

Table 4.91: Physiochemical Properties of Drugs.

S.No	Properties	Beta carotene	Catechin	Metformin
1	Chemical formula	$C_{40}H_{56}$	$C_{15}H_{14}O_6$	$C_4H_{11}N_5$
2	Absorption	6-7hours	6-7 hours	4-8 hours
3	Water solubility mg/ml	0.000391	0.645	1.38
4	logP	9.72	1.02	-1.8
5	H-bond donor	0	5	4
6	H-bond Acceptor	0	6	5
7	Bioavailability	0	1	1
8	Polarizability	71.84 $Å^3$	27.89 $Å^3$	13.43 $Å^3$
9	ADMET probability	0.917	0.68	0.9156
10	Side Effects	Renal or hepatic impairment & Carotenoderma (yellow skin).	Nausea, Dry mouth, Constipation, Diarrhea, Difficulty in sleeping & Fatigue.	Heart burn, Gas, Stomach pain, Nausea or Vomiting, Constipation & Diarrhea.

Table 4.92: Physiochemical Properties of Drugs.

S.No	Properties	Methionine	N-Acetyl cysteine	Nebivolol
1	Chemical formula	$C_5H_{11}NO_2S$	$C_5H_9NO_3S$	$C22H_{25}F_2NO_4$
2	Absorption	Absorbed from lumen of small intestine into the enterocytes.	6-10% By oral administration.	1.5-4hours.
3	Water solubility mg/ml	23.9	5.09	0.0403
4	logP	-1.8	-0.03	2.44
5	H-bond donor	2	3	3
6	H-bond Acceptor	3	3	7
7	Bioavailability	1	1	1
8	Polarizability	15.5 $Å^3$	15.34 $Å^3$	41.98 $Å^3$
9	ADMET probability	0.9797	0.77	0.8483
10	Side Effects	Headache, Drowsiness, Diarrhea, Heartburn & Nausea.	Nausea, Vomiting & Diarrhea or Constipation.	Dizziness, Feeling tired, Nausea, Headaches & prohibited in pregnancy & breastfeeding.Serious side effects may include heart failure & bronchospasm.

Table 4.93: Physiochemical Properties of Drugs.

S.No	Properties	Resveratrol	Serotonin
1	Chemical formula	$C_{14}H_{12}O_3$	$C_{10}H_{12}N_2O$
2	Absorption	High absorption	Take 15-20 min
3	Water solubility mg/ml	0.0688	2.5
4	logP	2.57	0.56
5	H-bond donor	3	3
6	H-bond Acceptor	3	2
7	Bioavailability	1	1
8	Polarizability	24.55 $Å^3$	19.31 $Å^3$
9	ADMET probability	0.9952	0.913
10	Side Effects	Slow blood clotting, increase risk of bleeding & Might act like estroge [149].	Nausea, Dry mouth, Constipation, Loss of appetite, Tiredness, Drowsiness or increased sweating.

4.9.1 Nebivolol

After docking and physiochemical properties analyses, Nebivolol was selected as standard for comparison with lead compound (figure 4.44). Nebivolol exhibit best binding interactions and minimized score among all selected drugs (Table 4.94). Nebivolol is widely used in the clinical practice for the curement of hypertension and heart failure and proves itself as highly selective beta-blocker with additional vasodilator properties [150].

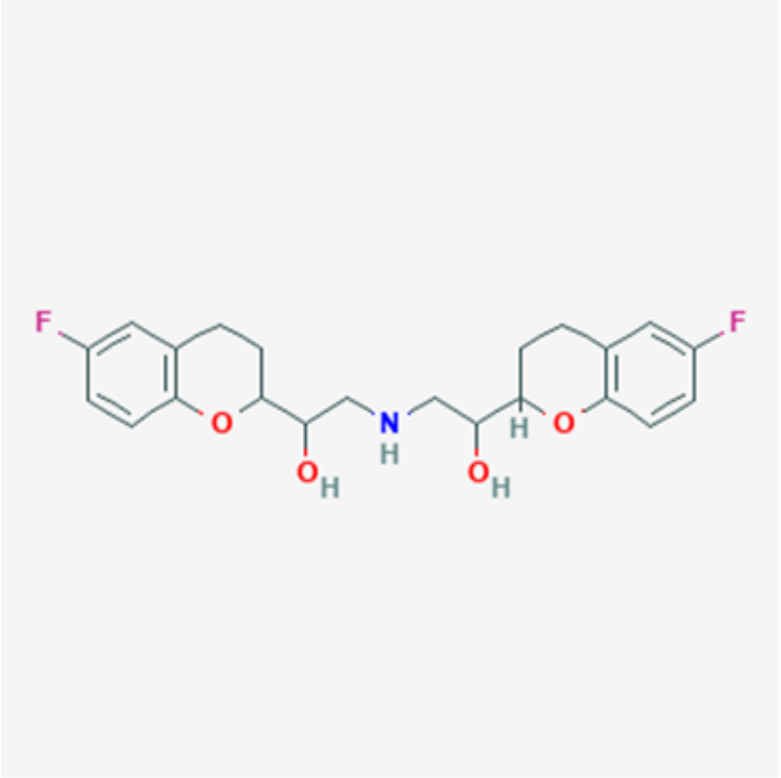

FIGURE 4.44: 2D Structure of Nebivolol Drug- PubChem.

TABLE 4.94: Physiochemical Properties of Nebivolol

logP value	**Rotatable bonds**	**H-bond acceptor**	**H-bond donor**	**Molecular Formula**	**Molecular Weight**
2.44	6	7	3	$C_{22}H_{25}F_2NO_4$	405.4

4.10 Drug ADMET Properties

ADMET properties (Absorption, Distribution, Metabolism, Excretion & Toxicity) of reference drug (Nebivolol) were explored by pkCSM online prediction tool.

4.10.1 Toxicity Prediction of Reference Drug

The predicted toxicity values of reference drug are listed in Table 4.95. The maximum tolerated dose value is low as shown as -0.098 whereas this drug predicts itself as hERG II inhibitor that's means it inhibits potassium channels. LD50 predicts toxic potency of drug and LOAEL tells about lowest dose that causing adverse effects. Nebivolol also shows itself as hepatotoxic that's means it induced liver injury. T. pyriformis toxicity used as toxic end point. pIGC50 (negative logarithm of the concentration required to stop 50% growth >-0.5 considered as toxic. Nebivolol predicts pIGC50 out of this range. The last model named as Minnow toxicity predicts LC50 in m M which represents the lethal concentration of a molecule sufficient to cause death of 50% flathead minnows (small bait fishes). Nebivolol predicts minnow toxicity value as 1.419m M.

Table 4.95: Toxicity Values of Nebivolol

S.No	Model Name	Predicted values
1	Max.tolerated dose(human)	-0.098 mg/Kg
2	hERG I inhibitor	No
3	hERG II inhibitor	Yes
4	Oral rat acute toxicity	2.566 mol/Kg
5	Oral rat chronic toxicity	1.526 mg/Kg
6	Hepatoxicity	Yes
7	Skin sensitization	No
8	t.pyriformis toxicity	1.608 log ug/L
9	Minnow toxicity	1.419 log mM

4.10.2 Absorption Properties

Nebivolol shows absorption properties as shown in Table 4.96. As clear from table, nebivolol is less soluble in water and has 90% absorption in small intestine of human. Skin permeability is low and shows positive result as Pgp-substrate, and PdpI/II inhibitor. Its means standard drug has low oral absorption. Pgp-I/II inhibitor 'YES' means nebivolol has reduced pumping activity to pump out xenobiotics from cell and have high absorption.

Table 4.96: Absorption Properties of Nebivolol.

S.No	Model Name	Value
1	Water solubility	-3.123 mol/L
2	Caco2 permeability	1.15 cm/S
3	Intestinal absorption (human)	90.554 %
4	Skin Permeability	-2.879 log Kp
5	P-glycoprotein substrate	Yes
6	P-glycoprotein I inhibitor	Yes
7	P-glycoprotein II inhibitor	Yes

4.10.3 Distribution Properties

Distribution properties consists of four models, among them first one is volume of distribution in human (VDss) expressed as log L/kg. Nebivolol shows high VDss which means more of the drug is distributed in tissue rather than plasma. Fu (fraction unbound) predicts the unbounded friction in plasma, if it is more than drug may be more effective. Our standard drug has 0.283 Fu predicted value. Third model BBB permeability (blood brain barrier permeability) expressed as log BB shows value of -0.888 is less than -1 and considered as safe for brain. Last model named as CNS permeability (central nervous system permeability) expressed as log PS <-3 considered as safe while nebivolol shows logPS=-3.083. The distribution properties of standard drug are listed in Table 4.97.

Table 4.97: Distribution Properties of Nebivolol.

S.No	Model Name	Value
1	VDss (human)	0.993 L/Kg
2	Fraction unbound (human)	0.283 Fu
3	BBB permeability	-0.888 log BB
4	CNS permeability	-3.083 log PS

4.10.4 Metabolic Properties

Reference drug's metabolic properties are given below in Table 4.98. Cytochrome P450 is a detoxification enzyme present in liver and plays role in excretion of exogenous compounds by oxidizing them. CYP2D6 & CYP3A4 are two main isoforms of cytochrome P450. First & second model result shows that nebivolol is metabolized by cytochrome P450. Model no 3-6 shows that drug is not an inhibitor for these isoforms of cytochrome P450 whereas model 7 named as CYP3A4 shows nebivolol as inhibitor for this isoform which changes the pharmacokinetics of nebivolol.

Table 4.98: Metabolic Properties of Nebivolol.

S. No	Model Name	Predicted Value
1	CYP2D6 substrate	Yes
2	CYP3A4 substrate	Yes
3	CYP1A2 inhibitor	No
4	CYP2C19 inhibitor	No
5	CYP2C9 inhibitor	No
6	CYP2D6 inhibitor	No
7	CYP3A4 inhibitor	Yes

4.10.5 Excretion Properties

The predicted values of excretion of reference drug are given in Table 4.99. Total clearance expressed as log (CL tot) value is 0.89 ml/min/kg which indicates the hepatic and renal clearance of nebivolol. OCT2 is an organic cation transporter 2 that plays role in disposition and renal clearance of drugs. Nebivolol predicts

Renal OCT2 substrate 'No' which means it is not interfering in the functioning of OCT2 in the cell.

Table 4.99: The Excretion Properties of Nebivolol.

S.No	Model Name	Predicted Value
1	Total Clearance	0.89 ml/Kg
2	Renal OCT2 substrate	No

4.11 Nebivolol Mechanism of Action

Nebivolol (D05127, DG 00319) is an antihypertensive, vasodilator, and beta-andenergic receptor antagonist (https://www.genome.jp/kegg/). Nebivolol acts on cardiac muscle of heart and targets Beta- 1 adrenergic receptor which mediate the catecholamine-induced activation of adenylate cyclase through the action of G proteins.Beta-1 adrenergic receptor have equal affinity for epinephrine and norepinephrine [151]. Nebivolol competes with epinephrine or other beta-1 adrenergic receptor activator and binds with beta-1 adrenergic receptor and inhibit it in muscle and heart. In this way drug (Nebivolol) reduces the heart rate and blood pressure. Nebivolol also reduced the constriction of blood vessels by preventing the release of renin (a hormone from kidneys) [152]. Renin decreased by inhibition of aldosterone, and beta-1 antagonism in the juxtaglomerular apparatus in kidney by nebivolol, which results in decreased aldosterone and renin. First one decrease leads to decreased blood volume while second one leads to reduced vasoconstriction [153]. Nebivolol acts on cardiac muscle and skeletal muscle by inhibiting beta-1 adrenergic receptor by activating G-protein signaling cascade. Myosin with an ADP and phosphate binds to actin and forms a bridge. Myosin performs a power stroke and drawing the actin filaments together. Muscle contractions occur due to pulling action of many actin filaments (Fig 4.45).

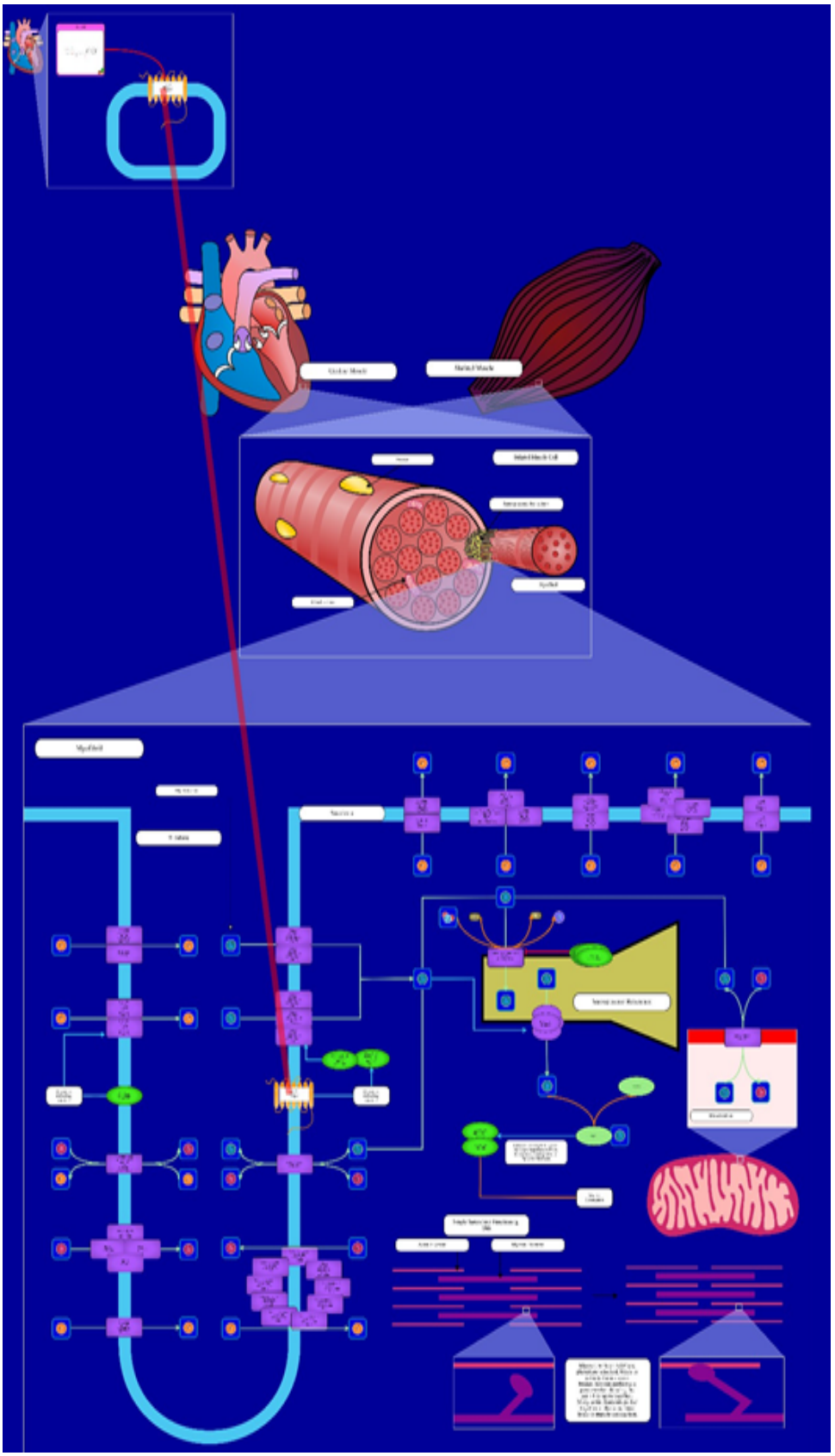

FIGURE 4.45: Mechanism of Action of Nebivolol From Drug Bank.

4.12 Nebivolol Effects on Body

Nebivolol is a beta-1 adrenergic receptor blocker with extra vasodilation properties and widely used in the clinical practice for the treatment of hypertension and heart failure [150]. Some common effects of nebivolol are headache, paresthesia, fatigue, bradycardia, vomiting, rhinitis, and dizziness [154]. Cardiac failure, bronchospasm, hypoglycemia, and heart block are adverse effects of above-mentioned drug. This drug has long duration of action even after 48 hours of stopping the medication so abrupt stopping of this drug results in exacerbation of coronary artery disease. If nebivolol users are also diabetic patients then must monitor their glucose levels as beta blockers can mask symptoms of hypoglycemia [155].

4.13 Nebivolol Docking

Nebivolol as ligand was docked with drug targets by an online automatic docking tool that is CB dock. Drug targets were Catalase (CAT), Superoxide dismutase 2 (SOD 2) and Glutathione Peroxidase 1 (GPX1) in this research work. Best docking score was -9.4 with CAT receptor. Molecular docking interactions of docked drug with target are listed below in Table 4.100.

Table 4.100: Nebivolol Docking Score via CB Dock

S.No	**Compound**	**Nebivolol**
1	Binding Score	-9.4
2	HBD	3
3	HBA	7
4	logP	2.44
5	Molecular Weight g/mol	405.4
6	Rotatable Bonds	6
7	Grid Map	33
8	Min-energy Kcl/mol	0
9	Max-energy Kcl/mol	1.60E+00
10	Cavity Size	7293

4.14 Nebivolol and Antioxidant Agent Comparison

The standard drug and lead compound was compared for their physiochemical and pharmacokinetic properties to assess their bioavailability, drug likeness, efficacy and safety. Both of these compounds passed the drug likeness criteria (Lipinski's rule of five). However, quercetin has low molecular weight and log P value than nebivolol and shows 5 H-BD whereas nebivolol shows 3 H-BD. Molar refractivity of quercetin also high than nebivolol (Table 4.101).

Table 4.101: Nebivolol and Quercetin Lipinski Rule of Five.

S.No	**Name of compound**	**Log P value**	**Molecular Weight**	**H-bond donor**	**H-bond acceptor**	**Molar refractivity**
1	Nebivolol	2.44	405.4 g/mol	3	7	71A$^{\circ 2}$
2	Quercetin	1.988	302.238 g/-mol	5	7	127 A$^{\circ 2}$

4.14.1 ADMET Properties Comparison

Pharmacokinetics properties include absorption, distribution, metabolism, excretion, and toxicity (ADMET) properties plays critical role in screening of compounds as drug candidates. ADMET properties were compared by using Byju's 'Greater Than Calculator 'learning app. Pharmacokinetic properties of reference drug and lead compound are listed in Table 4.105 to

4.14.1.1 Toxicity Comparison

Toxicity is the most important parameter of pharmacokinetic (ADMET) properties which consists on 9 models. Maximum tolerated dose helps to set maximum recommended tolerated dose which shows negative value for nebivolol (log mg/kg/-day as-0.098) and log mg/kg/day=0.499 for quercetin which shows bio compound is ahead in safety than reference drug. The models h ERG I/II inhibitors predicts about either analyzed compounds are inhibitors of potassium channels or not. If answer is 'yes' then compound may not be fit for drug. From table 4.29, it is evident that nebivolol shows itself as h ERG II inhibitor. Mostly h ERG I/II inhibitors are withdrawal from the pharmaceutical market. The model named as oral rat acute toxicity (LD50) expressed as mol/kg is the amount of drug that can cause the death of 50% rats (test animals). LD 50 value of nebivolol is slightly higher than quercetin. Oral rat chronic toxicity (LOAEL) determines the lowest dose of drug which can produce adverse effects over long duration usage (chronic use) of drug. LOAEL predicted value of nebivolol is less than quercetin which shows its potency to be more toxic than bio compound. Hepatotoxicity simply indicates the injury to liver which shows result in two categories yes/no. Nebivolol predicted result shows it as hepatotoxic whereas quercetin is not a hepatotoxic compound (table 4.29). Both of these compounds not cause any allergic reactions. T. pyriformis toxicity expressed as negative logarithm of the concentration required to inhibit 50% growth (p IGC50). T. pyriformis toxicity predicted value of nebivolol is higher than quercetin which is again goes in favor of quercetin. Minnow toxicity is the lethal concentration values (LC50 expressed as log LC50

in m M) of a compound which is necessary to cause the death of 50% minnows (small bait fishes). Nebivolol predicted value is 1.416m M, whereas 3.721m M is the predicted value of quercetin. It is clear that less quantity of reference drug than quercetin is enough to cause death of 50% minnows, which again shows standard drug's toxicity and highlights the efficacy and safety of lead compound. All the 9 models of toxicity show quercetin as safe compound than nebivolol (table 4.102).

Table 4.102: Toxicity Values of Nebivolol & Quercetin.

S.No	**Model Name**	**Predicted Values**	
		Nebivolol	**Quercetin**
1	Max.tolerated dose(human)	-0.098 mg/Kg	0.499 mg/Kg
2	hERG I inhibitor	No	No
3	hERG II inhibitor	Yes	No
4	Oral rat acute toxicity	2.566 mol/Kg	2.471 mol/Kg
5	Oral rat chronic toxicity	1.608 mg/Kg	2.612 mg/Kg
6	Hepatoxicity	Yes	No
7	Skin sensitization	No	No
8	t.pyriformis toxicity	0.365	0.288
9	Minnow toxicity	1.419	3.721

4.14.1.2 Absorption Properties Comparison

Water solubility of standard drug is less than lead compound. Caco2 permeability predicts about the absorption of orally administered drugs. Predicted values of this earlier mention model are within safe range for both compounds but quercetin shows more less value than nebivolol. Model intestinal absorption in humans predicts 77% & 90.5% values for quercetin and nebivolol respectively. Both of these compounds predict low skin permeability. Nebivolol falls in 'Yes' category for P-gp substrate and P-gp I/II inhibitors while quercetin stands in 'No' category for all these three models. This means nebivolol as P-gp substrate shows low oral absorption and as P-gp I/II inhibitor reduce the pumping out of xenobiotics and toxins activity of P-gp from cell and may have high absorption (Table 4.103).

Table 4.103: Absorption Properties of Standard Drug and Lead Compound.

S.No	Ligand	Nebivolol	Quercetin
1	Water solubility	-3.123 mol/L	-2.925 mol/L
2	Caco2 permeability	1.15 cm/S	-0.229 cm/S
3	Intestinal absorption (human)	90.554 %	77.207 %
4	Skin Permeability	-2.879 log/Kp	-2.737 log Kp
5	P-glycoprotein substrate	Yes	No
6	P-glycoprotein I inhibitor	Yes	No
7	P-glycoprotein II inhibitor	Yes	No

4.14.1.3 Metabolic Properties Comparison

Metabolic properties are predicted on the basis of isoforms of cytochrome P450 which are CYP2D6, CYP3A4, CYP1A2, CYP2C19, and CYP2C9. Nebivolol shows itself as substrate of CYP2D6 & CYP3A4 isoforms whereas quercetin is not predicted as substrate of these isoforms. Nebivolol predicts itself as inhibitor of CYP3A4 which is a main isoform for drug metabolism while quercetin shows itself as inhibiting CYP1A2 isoform (Table 4.104).

Table 4.104: Metabolic Properties of Standard Drug -Lead Compound.

S.No	Ligand	Nebivolol	Quercetin
1	CYP2D6 substrate	Yes	No
2	CYP3A4 substrate	Yes	No
3	CYP1A2 inhibitor	No	Yes
4	CYP2C19 inhibitor	No	No
5	CYP2C9 inhibitor	No	No
6	CYP2D6 inhibitor	No	No
7	CYP3A4 inhibitor	Yes	No

4.14.1.4 Distribution Properties Comparison

First model of distribution properties VDss (human) predicts high value for nebivolol and low for quercetin. VDss low value considered safer because high value indicates that drug mostly distributed in tissue rather than plasma. Fu value of quercetin

is more than nebivolol which shows quercetin more effective than reference drug in case of unbounded friction present in plasma. BBB permeability <-1 means no harm to brain. CNS permeability <-3 considered as safe (Table 4.105).

Table 4.105: Distribution Properties of Standard Drug-Lead Compound.

S.No	Ligand	Nebivolol	Quercetin
1	VDss (human)	0.993 L/Kg	1.559 L/Kg
2	Fraction unbound (human)	0.283 Fu	0.206 Fu
3	BBB permeability	-0.888 log BB	-1.098 log BB
4	CNS permeability	-3.083 log PS	-3.065 log PS

4.14.1.5 Excretion Properties Comparison

Excretion properties consist on two models with predicted values are displayed in Table 4.106. Drug clearance is measured by total clearance which occurs as combination of hepatic clearance and renal clearance and expressed as log CL tot in ml/min/kg. Predicted value of drug clearance as total clearance of quercetin is high as compared to nebivolol.

Total clearance is related to bioavailability, and is important for determining dosing rates. Both compounds stand in 'No' category for Renal OCT2 substrate model, which means that they not interfere in the normal functioning of organic cation transporter 2 who plays role in renal clearance of drugs.

Table 4.106: Excretion Properties of Standard Drug-Lead Compound.

S.No	Ligand	Nebivolol	Quercetin
1	Total Clearance	0.89 ml/Kg	0.407 ml/Kg
2	Renal OCT2 substrate	No	No

4.14.2 Physiochemical Properties Comparison

Physiochemical properties describe the basic and fundamental properties of compounds which are also acts as primary screeners to sort out compounds with desirable properties. Nebivolol consists of 54 atoms of carbon, hydrogen, florin, and nitrogen whereas quercetin consists of 32 atoms of carbon, hydrogen, and oxygen which shows its simplicity as a bio-compound. Molecular weight, and log P value of nebivolol is also high than quercetin. Quercetin donates 2 more hydrogen than nebivolol which shows its oxidation power. Rotatable bonds if more than 10 shows decreased oral bioavailability and nebivolol has 6 rotatable bonds as compares to quercetin which has only 1 rotatable bond (Table 4.107).

Table 4.107: Physiochemical Properties of Standard Drug-Lead Compound.

S.No	**Drug**	**logP Value**	**Rotatable Bonds**	**H-bond Acceptor**	**H-bond Donor**	**Molecular Formula**	**Molecular Weight**
1	Nebivolol	2.44	6	7	3	$C_{22}H_{25}F_2NO_4$	405.4 g/mol
2	Quercetin	1.988	1	7	5	$C_{15}H_{10}O_7$	302.238 g/mol

4.14.3 Docking Score Comparison

Discovering protein-ligand binding sites and conformations are particularly important in drug discovery. Therefore, standard drug as ligand was docked against selected receptors by CB-dock which predicts the cavities of the protein and calculates the centers and sizes of the top 5 cavities for all the three proteins separately.

Final results of docking of standard drug and lead compound against selected three receptors namely catalase (CAT), superoxide dismutase 2 (SOD2), and glutathione peroxidase 1 (GPX1) are shown in table 4.108.

The highest binding score is -10 against CAT receptor shown by Quercetin which is higher than Nebivolol who shows -9.4 against same protein. Among top 5 cavities (n=5 by default), first one for both ligands are displayed in figure 4.46 & 4.47.

Minimized energy pose of Quercetin & CAT shows best and strong cavity interaction with the involvement of three chains of protein as compared to Nebivolol which shows weak interaction at top of protein with the involvement of two chains only. All the interaction visualization analysis studies are performed by PyMol molecular visualization tool and Ligplot^{+} (V.1.4.5).

Table 4.108: Docking Scores of Standard Drug and Lead Compound.

S.No	**Name of Ligands**	**Binding Score with CAT**	**Binding Score with SOD2**	**Binding Score with GPX1**
1	Nebivolol	-9.4	-8.2	-6.5
2	Quercetin	-10	-8.4	-6.5

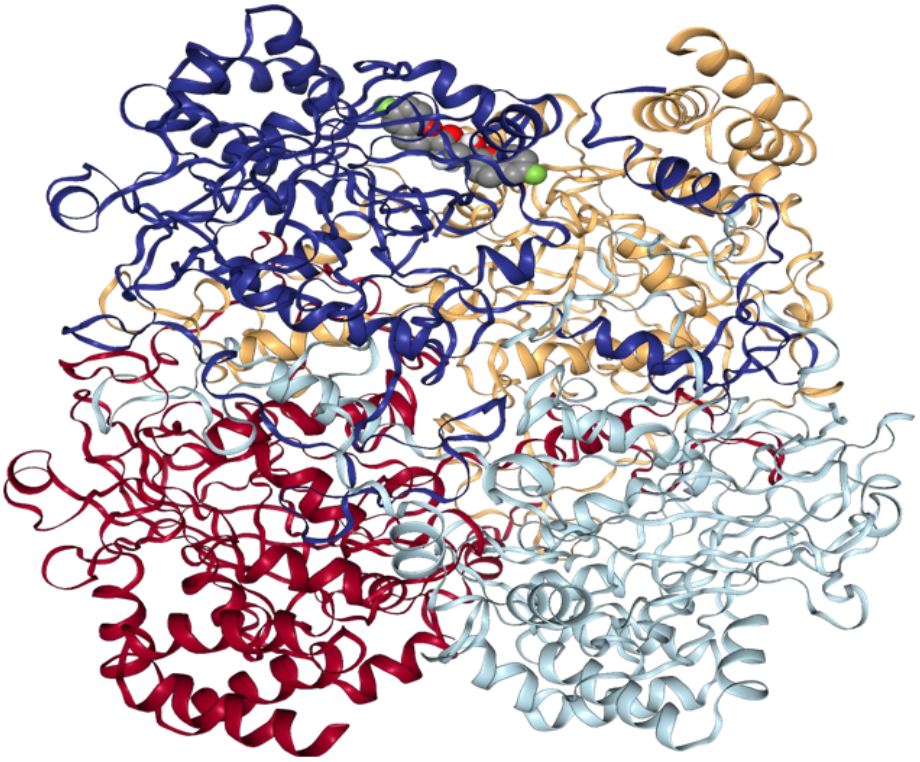

FIGURE 4.46: Best Pose Interaction of Nebivolol as Ligand With CAT Receptor.

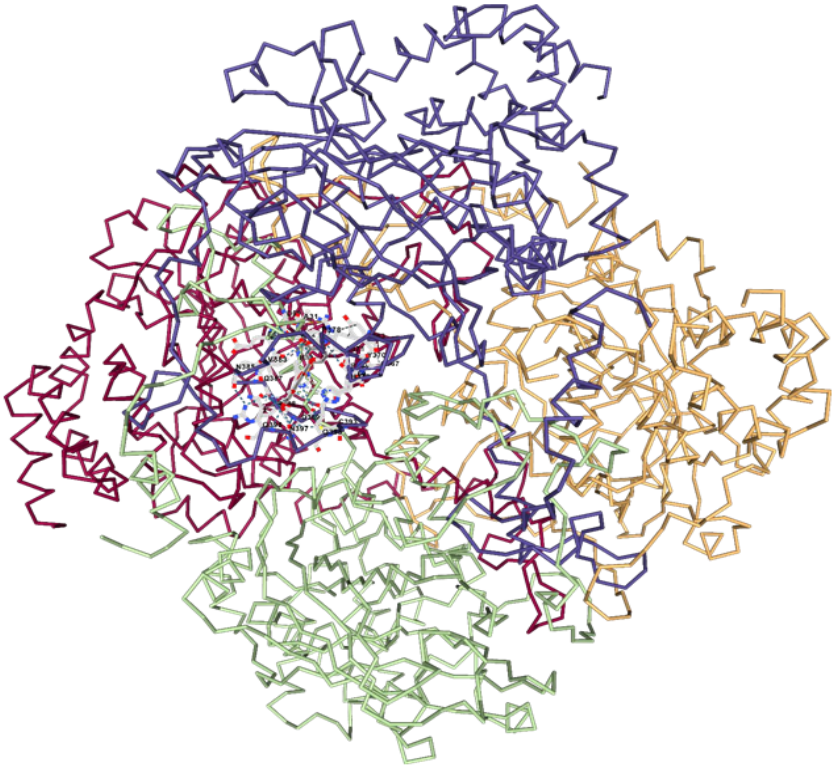

FIGURE 4.47: Best Pose Interaction of Quercetin as Ligand With CAT Receptor.

4.14.3.1 Docking Analysis Comparison

Best docking scores of reference drug and lead compound are analyzed by Ligplot^{+} (V.1.4.5), (figure 4.48 & 4.49). Docking results are analyzed on the basis of;

1. No. of hydrogen bonds.
2. No. of steric interactions.
3. No. of interacting amino acids.
4. Interaction with hydrophobic regions.

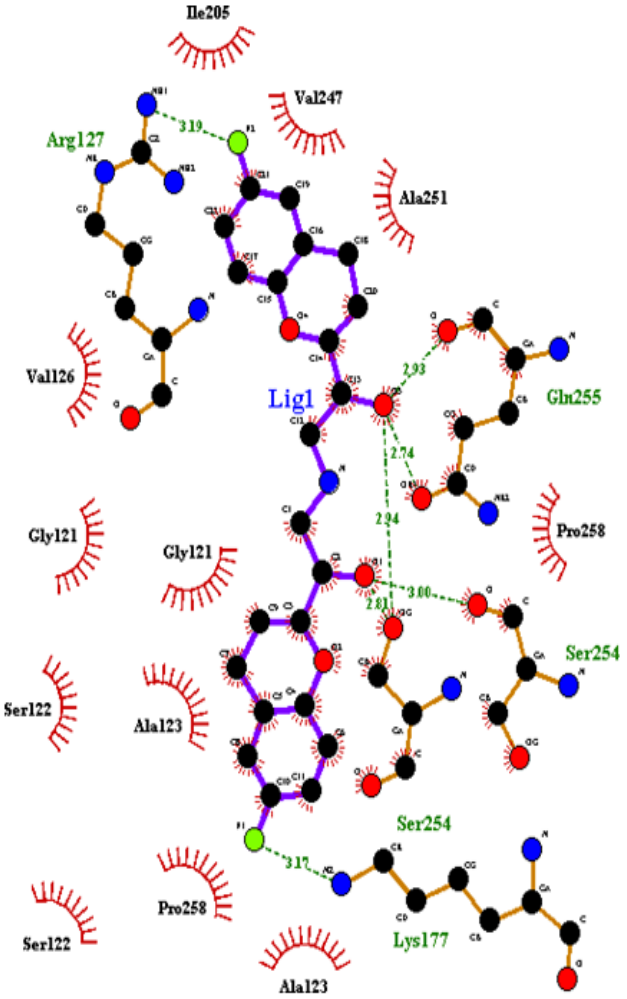

FIGURE 4.48: Hydrogen Bonds and Interactions of Nebivolol (ligand) With CAT (Receptor).

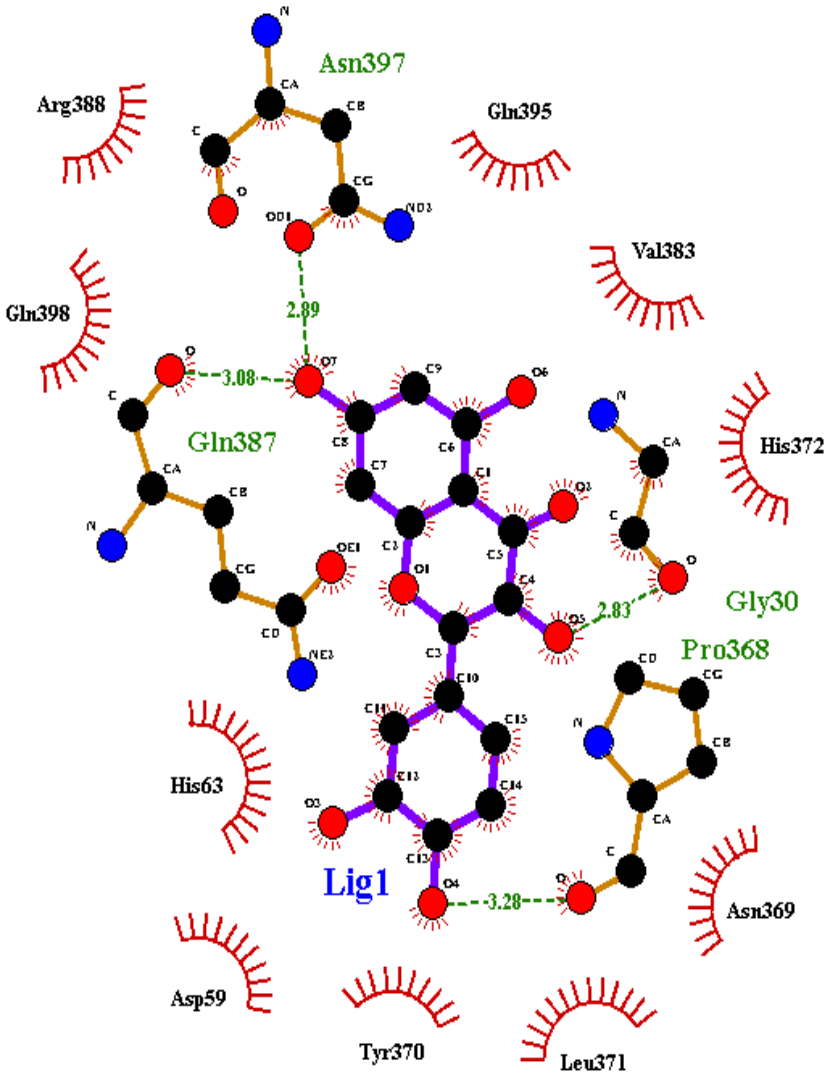

FIGURE 4.49: Hydrogen Bonds and Interactions of Standard Drug-Lead Compound Comparison.

The detail of hydrogen bonds and hydrophobic interactions are displayed in table 4.108. Oxygen atoms present in ligand play crucial role in H- bond formation with target proteins. Although nebivolol makes more hydrogen bonds due to having oxygen & fluorine electronegative atoms but the bond distances are shorter in case of quercetin. Interacting amino acids are 6 in case of reference drug and 4 in lead compound. Furthermore, hydrophobic interactions are strong and direct to ligand in case of quercetin, also more in number than nebivolol.

Table 4.109: Hydrogen Bonds and Interactions of Standard Drug-Lead Compound Comparison.

S.No	Ligand Name	No of H- Bonds	Hydrogen Bonding		Hydrophobic Bonding
			Amino Acids	Distance	
1	Nebivolol	6	N:Arg127:F1	3.19	Gly121
			O:Gln255:O5	2.93	Ala123
			O2:Gln255:O5	2.74	Val126
			O:Ser254:O1	3.00	Pro258
			O:Ser254:O5	2.94	Ala251
			N:Lys177:F2	3.17	Val247
					Arg388
2	Quercetin	4	OD1:Asn:O7	2.89	Gln398
			O:Gln:O7	3.08	Gln395
			O:Gly:O5	2.83	Val383
			O:Pro:O4	3.28	His372
					His63
					Asn369
					Asp59
					Tyr370
					Leu371

Chapter 5

Conclusions and Recommendations

The motive of the present research is to discover potential antioxidants from *Artemisia annua* and its derivatives. Thirtyseven phytocompounds (which represents almost all classes of natural antioxidant compounds) are selected from literature and databases. Drug targets are three endogenous antioxidant enzymes which serves as first line defense within human body, namely as catalase, superoxide dismutase 2, and glutathione peroxidase 1. Molecular docking is performed by CB-dock online tool and five best scoring phytocompounds namely as quercetin, luteolin, apigenin, kaempferol, and mearnsetin are identified as hit compounds. Drug likeliness of compounds are studied and reported by using primary and secondary filters (Lipinski rule of 5 as primary and Pharmacokinetics properties as secondary filter). Quercetin belongs to class polyphenol is predicted itself as lead compound and virtual screening results, physiochemical properties & Pharmacokinetics properties of this compound is compared with an FDA approved drug namely nebivolol. Quercetin is capable of binding protein targets (CAT, SOD2, & GPX1) more efficiently and shows less toxicity than standard drug.

5.1 Recommendations

- Lead compound "quercetin" as per this research results should be explored as a drug candidate for the treatment of oxidative stress and related chronic diseases.
- All hit and lead compound should also be tried as food preservatives and additives because natural antioxidants proves themselves best preservatives and additives with more efficiency and less or no toxicity than synthetic ones.
- These potential antioxidants of *Artemisia annua* should be tested as cosmetic ingredients as they can prevent skin from ultraviolet radiations.
- Natural antioxidants can also be used in petroleum industry as preservative so potential antioxidants of this research work should be tried for this purpose.

Bibliography

[1]. Aslam, M.S. and M.S. Ahmad, Worldwide importance of medicinal plants: current and historical perspectives. Recent Adv Biol Med, 2016. 2(2016): p. 909.

[2]. Adnan, M., et al., Ethnogynaecological assessment of medicinal plants in Pashtun's Tribal Society. BioMed research international, 2015. 2015.

[3]. Firenzuoli, F. and L. Gori, Herbal medicine today: clinical and research issues. Evidence-Based Complementary and Alternative Medicine, 2007. 4.

[4]. Petrovska, B.B., Historical review of medicinal plants' usage. Pharmacognosy reviews, 2012. 6(11): p. 1.

[5]. Eric, S., Artemisia annua: A Vital Partner in the Global Fight against Malaria. Science, 2012. 336: p. 80.

[6]. Willcox, M., Artemisia species: from traditional medicines to modern anti malarials and back again. The Journal of Alternative and Complementary Medicine, 2009. 15(2): p. 101-109.

[7]. Skowyra, M., et al., Antioxidant properties of Artemisia annua extracts in model food emulsions. Antioxidants, 2014. 3(1): p. 116-128.

[8]. Uttara, B., et al., Oxidative stress and neurodegenerative diseases: a review of upstream and downstream antioxidant therapeutic options. Current neuropharmacology, 2009. 7(1): p. 65-74.

[9]. Meng, X.-Y., et al., Molecular docking: a powerful approach for structure-based drug discovery. Current computer-aided drug design, 2011. 7(2): p. 146-157.

[10]. Liu, Y., et al., CB-Dock: a web server for cavity detection-guided protein–ligand blind docking. Acta Pharmacologica Sinica, 2020. 41(1): p. 138-144.

[11]. Pagadala, N.S., K. Syed, and J. Tuszynski, Software for molecular docking: a review. Biophysical reviews, 2017. 9(2): p. 91-102.

[12]. Adwas, A., et al., Oxidative stress and antioxidant mechanisms in human body. J. Appl. Biotechnol. Bioeng, 2019. 6(1): p. 43.

[13]. Valko, M., et al., Free radicals, metals and antioxidants in oxidative stress-induced cancer. Chemico- biological interactions, 2006. 160(1): p. 1-40.

[14]. Ridnour, L.A., et al., Nitric oxide regulates angiogenesis through a functional switch involving thrombospondin-1. Proceedings of the National Academy of Sciences, 2005. 102(37): p. 13147-13152.

[15]. Droge, W., Free radicals in the physiological control of cell function. Physiological reviews, 2002. 82(1): p. 47-95.

[16]. Halliwell, B., Biochemistry of oxidative stress. 2007, Portland Press Ltd.

[17]. Valko, M., et al., Free radicals and antioxidants in normal physiological functions and human disease. Int J Biochem Cell Biol, 2007. 39(1): p. 44-84.

[18]. Miller, D.M., G.R. Buettner, and S.D. Aust, Transition metals as catalysts of "autoxidation" reactions. Free Radical Biology and Medicine, 1990. 8(1): p. 95-108.

[19]. Valko, M., H. Morris, and M. Cronin, Metals, toxicity and oxidative stress. Current medicinal chemistry, 2005. 12(10): p. 1161-1208.

[20]. Cadenas, E. and H. Sies, The lag phase. Free Radic Res, 1998. 28(6): p. 601-9.

[21]. Muller, F.L., Y. Liu, and H. Van Remmen, Complex III releases superoxide to both sides of the inner mitochondrial membrane. Journal of Biological Chemistry, 2004. 279(47): p. 49064-49073.

[22]. Paravicini, T.M. and R.M. Touyz, NADPH oxidases, reactive oxygen species, and hypertension: clinical implications and therapeutic possibilities. Diabetes care, 2008. 31(Supplement 2): p. S170- S180.

[23]. Pastor, N., et al., A detailed interpretation of OH radical footprints in a TBP-DNA complex reveals the role of dynamics in the mechanism of sequence-specific binding. Journal of molecular biology, 2000. 304(1): p. 55-68.

[24]. Liochev, S.I. and I. Fridovich, The role of O2. in the production of HO.: in vitro and in vivo. Free Radical Biology and Medicine, 1994. 16(1): p. 29-33.

[25]. Leonard, S.S., G.K. Harris, and X. Shi, Metal-induced oxidative stress and signal transduction. Free Radical Biology and Medicine, 2004. 37(12): p. 1921-1942.

[26]. Liochev, S.I. and I. Fridovich, The Haber-Weiss cycle—70 years later: an alternative view. Redox report, 2002. 7(1): p. 55-57.

[27]. Aikens, J. and T. Dix, Perhydroxyl radical (HOO.) initiated lipid peroxidation. The role of fatty acid hydroperoxides. Journal of Biological Chemistry, 1991. 266(23): p. 15091-15098.

[28]. Valko, M., et al., Role of oxygen radicals in DNA damage and cancer incidence. Molecular and cellular biochemistry, 2004. 266(1-2): p. 37-56.

[29]. Decoursey, T. and E. Ligeti, Regulation and termination of NADPH oxidase activity. Cellular and Molecular Life Sciences CMLS, 2005. 62(19-20): p. 2173-2193.

[30]. Birben, E., et al., Oxidative stress and antioxidant defense. World Allergy Organization Journal, 2012. 5(1): p. 9-19.

[31]. Klatt, P. and S. Lamas, Regulation of protein function by S-glutathiolation in response to oxidative and nitrosative stress. European journal of biochemistry, 2000. 267(16): p. 4928-4944.

[32]. 32. Ridnour, L.A., et al., The chemistry of nitrosative stress induced by nitric oxide and reactive nitrogen oxide species. Putting perspective on stressful biological situations. Biological chemistry, 2004. 385(1): p. 1-10.

[33]. Ghafourifar, P. and E. Cadenas, Mitochondrial nitric oxide synthase. Trends in pharmacological sciences, 2005. 26(4): p. 190-195.

[34]. Beneš, L., Z. Ďuračková, and M. Ferenčik, Chemistry, physiology and pathology of free radicals. Life sciences, 1999. 65(18-19): p. 1865-1874.

[35]. Chiueh, C.C., Neuroprotective properties of nitric oxide. Annals of the New York Academy of Sciences, 1999. 890(1): p. 301-311.

[36]. Carr, A.C., M.R. McCall, and B. Frei, Oxidation of LDL by myeloperoxidase and reactive nitrogen species: reaction pathways and antioxidant protection. Arteriosclerosis, thrombosis, and vascular biology, 2000. 20(7): p. 1716-1723.

[37]. Flatt, T., A new definition of aging? Frontiers in genetics, 2012. 3: p. 148.

[38]. Beckman, K.B. and B.N. Ames, The free radical theory of aging matures. Physiological reviews, 1998.

[39]. Pole, A., M. Dimri, and G.P. Dimri, Oxidative stress, cellular senescence and ageing. 2016.

[40]. Chandrasekaran, A., M.d.P.S. Idelchik, and J.A. Melendez, Redox control of senescence and age- related disease. Redox biology, 2017. 11: p. 91-102.

[41]. Caramori, G. and A. Papi, Oxidants and asthma. Thorax, 2004. 59(2): p. 170-173.

[42]. Hoshino, Y. and M. Mishima, Redox-based therapeutics for lung diseases. Antioxidants & redox signaling, 2008. 10(4): p. 701-704.

[43]. Valko, M., et al., Free radicals and antioxidants in normal physiological functions and human disease. The international journal of biochemistry & cell biology, 2007. 39(1): p. 44-84.

[44]. Mahajan, A. and V.R. Tandon, Antioxidants and rheumatoid arthritis. J Indian Rheumatol Assoc, 2004. 12: p. 139-142.

[45]. Pizzino, G., et al., Oxidative Stress: Harms and Benefits for Human Health. Oxidative Medicine and Cellular Longevity, 2017. 2017.

[46]. Massicot, F., et al., Preventive effects of two PAF-antagonists, PMS 536 and PMS 549, on cyclosporin- induced LLC-PK 1 oxidative injury. Journal of lipid mediators and cell signalling, 1997. 15(2): p. 203- 214.

[47]. Interdonato, M., et al., Cadmium delays puberty onset and testis growth in adolescents. Clinical Endocrinology, 2015. 83(3): p. 357-362.

[48]. Imlay, J.A., Pathways of oxidative damage. Annual Reviews in Microbiology, 2003. 57(1): p. 395-418.

[49]. Duarte, T.L. and J. Lunec, When is an antioxidant not an antioxidant? A review of novel actions and reactions of vitamin C. Free radical research, 2005. 39(7): p. 671-686.

[50]. Cheung, C., et al., Relationships between tissue concentrations of polycyclic aromatic hydrocarbons and antioxidative responses of marine mussels, Perna viridis. Aquatic toxicology, 2001. 52(3-4): p. 189-203.

[51]. McCord, J.M. and I. Fridovich, Superoxide dismutase an enzymic function for erythrocuprein (hemocuprein). Journal of Biological chemistry, 1969. 244(22): p. 6049-6055.

[52]. Nozik-Grayck, E., H.B. Suliman, and C.A. Piantadosi, Extracellular superoxide dismutase. The international journal of biochemistry & cell biology, 2005. 37(12): p. 2466-2471.

[53]. Tappel, M.E., J. Chaudiere, and A.L. Tappel, Glutathione peroxidase activities of animal tissues. Comparative Biochemistry and Physiology Part B: Comparative Biochemistry, 1982. 73(4): p. 945- 949.

[54]. Hayes, J.D., J.U. Flanagan, and I.R. Jowsey, Glutathione transferases. Annu. Rev. Pharmacol. Toxicol., 2005. 45: p. 51-88.

[55]. Berg, J., et al., DNA replication, recombination and repair. Biochemistry. 5th edition. New York, WH Freeman & Co, pp1119-1120, 2002.

[56]. Ho, Y.-S., et al., Mice lacking catalase develop normally but show differential sensitivity to oxidant tissue injury. Journal of Biological Chemistry, 2004. 279(31): p. 32804-32812.

[57]. Linster, C.L. and E. Van Schaftingen, Vitamin c. The FEBS journal, 2007. 274(1): p. 1-22.

[58]. Sen, C.K., S. Khanna, and S. Roy, Tocotrienols: Vitamin E beyond tocopherols. Life sciences, 2006. 78(18): p. 2088-2098.

[59]. Frei, B. and J.V. Higdon, Antioxidant activity of tea polyphenols in vivo: evidence from animal studies. The Journal of nutrition, 2003. 133(10): p. 3275S-3284S.

[60]. Lakshmi, M., U. Reddy, and S. Rani, A review on medicinal plants for nephroprotective activity. Asian Journal of Pharmaceutical and Clinical Research, 2012. 5(4): p. 8-14.

[61]. Okada, K., et al., Curcumin and especially tetrahydrocurcumin ameliorate oxidative stress-induced renal injury in mice. The Journal of nutrition, 2001. 131(8): p. 2090-2095.

[62]. Arts, I.C., P.C. Hollman, and D. Kromhout, Chocolate as a source of tea flavonoids. The Lancet, 1999. 354(9177): p. 488.

[63]. Mosialou, E., et al., Evidence that rat liver microsomal glutathione transferase is responsible for glutathione-dependent protection against lipid peroxidation. Biochemical pharmacology, 1993. 45(8): p. 1645-1651.

[64]. Azab, A.E. and M.O. Albasha, Hepatoprotective effect of some medicinal plants and herbs against hepatic disorders induced by hepatotoxic agents. J Biotechnol Bioeng, 2018. 2(1): p. 8-23.

[65]. Azab, A.E., M.O. Albasha, and A.S.I. Elsayed, Prevention of nephropathy by some natural sources of antioxidants. Yangtze Medicine, 2017. 1(04): p. 235.

[66]. Sundararajan, R., A. Bharampuram, and R. Koduru, A review on phytoconstituents for nephroprotective activity. Pharmacophore, 2014. 5(1): p. 160-82.

[67]. Tan, B.L., et al., Antioxidant and Oxidative Stress: A Mutual Interplay in Age-Related Diseases. Front Pharmacol, 2018. 9: p. 1162.

[68]. Cheng, Y.-T., C.-C. Yang, and L.-F. Shyur, Phytomedicine-Modulating oxidative stress and the tumor microenvironment for cancer therapy. Pharmacological research, 2016. 114: p. 128-143.

[69]. Aggarwal, B.B., et al., Curcumin: the Indian solid gold, in The molecular targets and therapeutic uses of curcumin in health and disease. 2007, Springer. p. 1-75.

[70]. de Oliveira, M.R., et al., Resveratrol and the mitochondria: From triggering the intrinsic apoptotic pathway to inducing mitochondrial biogenesis, a mechanistic view. Biochimica et Biophysica Acta (BBA)-General Subjects, 2016. 1860(4): p. 727-745.

[71]. Stewart, J.R., M.C. Artime, and C.A. O'Brian, Resveratrol: a candidate nutritional substance for prostate cancer prevention. The Journal of nutrition, 2003. 133(7): p. 2440S-2443S.

[72]. Hurst, W.J., et al., Survey of the trans-resveratrol and trans-piceid content of cocoa-containing and chocolate products. Journal of agricultural and food chemistry, 2008. 56(18): p. 8374-8378.

[73]. Lee, W.-L. and L.-F. Shyur, Deoxyelephantopin impedes mammary adenocarcinoma cell motility by inhibiting calpain-mediated adhesion dynamics and inducing reactive oxygen species and aggresome formation. Free Radical Biology and Medicine, 2012. 52(8): p. 1423-1436.

[74]. Meeran, S.M., S. Katiyar, and S.K. Katiyar, Berberine-induced apoptosis in human prostate cancer cells is initiated by reactive oxygen species generation. Toxicology and applied pharmacology, 2008. 229(1): p. 33-43.

[75]. Zhu, C., et al., No evident dose-response relationship between cellular ROS level and its cytotoxicity–a paradoxical issue in ROS-based cancer therapy. Scientific reports, 2014. 4: p. 5029.

[76]. Quisbert-Valenzuela, E.O. and G.M. Calaf, Apoptotic effect of noscapine in breast cancer cell lines. International Journal of Oncology, 2016. 48(6): p. 2666-2674.

[77]. Kim, W.-H., et al., Critical role of reactive oxygen species and mitochondrial membrane potential in Korean mistletoe lectin-induced apoptosis in human hepatocarcinoma cells. Molecular pharmacology, 2004. 66(6): p. 1383-1396.

[78]. Fujiki, H., et al., Primary cancer prevention by green tea, and tertiary cancer prevention by the combination of green tea catechins and anticancer compounds. Journal of cancer prevention, 2015. 20(1): p. 1-4.

[79]. Kager, N., et al., Prevention of oxidative DNA damage in inner organs and lymphocytes of rats by green tea extract. Eur J Nutr, 2010. 49(4): p. 227-34.

[80]. Lu, Q.Y., et al., Green tea inhibits cycolooxygenase-2 in non-small cell lung cancer cells through the induction of Annexin-1. Biochem Biophys Res Commun, 2012. 427(4): p. 725-30.

[81]. Menon, S., et al., Effects of Antioxidants in Human Cancers: Differential Effects on Non-Coding Intronic RNA Expression. Antioxidants (Basel), 2016. 5(1).

[82]. Suzuki, K., et al., Effect of green tea extract on reactive oxygen species produced by neutrophils from cancer patients. Anticancer Res, 2012. 32(6): p. 2369-75.

[83]. Lin, C.H., et al., EGCG inhibits the growth and tumorigenicity of nasopharyngeal tumor-initiating cells through attenuation of STAT3 activation. Int J Clin Exp Pathol, 2014. 7(5): p. 2372-81.

[84]. Wang, Y., et al., Mechanism of the inhibition of the STAT3 signaling pathway by EGCG. Oncol Rep, 2013. 30(6): p. 2691-6.

[85]. Suganuma, M., et al., Synergistic effects of -epigallocatechin gallate with-epicatechin, sulindac, or tamoxifen on cancer-preventive activity in the human lung cancer cell line PC-9. Cancer Res, 1999. 59(1): p. 44-7.

[86]. Ahmed, R.S., et al., Biological and Mechanistic Characterization of Novel Prodrugs of Green Tea Polyphenol Epigallocatechin Gallate Analogs in Human Leiomyoma Cell Lines. J Cell Biochem, 2016. 117(10): p. 2357-69.

[87]. Murillo, G. and R.G. Mehta, Cruciferous vegetables and cancer prevention. Nutr Cancer, 2001. 41(1- 2): p. 17-28.

[88]. Augustin, Y., et al., The wisdom of crowds and the repurposing of artesunate as an anticancer drug. Ecancermedicalscience, 2015. 9: p. ed50.

[89]. Ansari, M.T., I. Iqbal, and V.B. Sunderland, Dihydroartemisinin-cyclodextrin complexation: Solubility and stability. Archives of Pharmacal Research, 2009. 32(1): p. 155-165.

[90]. Krishna, S., et al., Artemisinins: their growing importance in medicine. Trends Pharmacol Sci, 2008. 29(10): p. 520-7.

[91]. Schmidt, H.H., et al., Antioxidants in translational medicine. Antioxidants & redox signaling, 2015. 23(14): p. 1130-1143.

[92]. lker, S., P.P. McKeown, and . Bayraktutan, Vitamins reverse endothelial dysfunction through regulation of eNOS and NAD (P) H oxidase activities. Hypertension, 2003. 41(3): p. 534-539.

[93]. Malyszko, J., Mechanism of endothelial dysfunction in chronic kidney disease. Clinica chimica acta, 2010. 411(19-20): p. 1412-1420.

[94]. Ahmad, K.A., et al., Antioxidant therapy for management of oxidative stress induced hypertension. Free radical research, 2017. 51(4): p. 428-438.

[95]. De Ridder, S., F. Van der Kooy, and R. Verpoorte, Artemisia annua as a self-reliant treatment for malaria in developing countries. Journal of ethnopharmacology, 2008. 120(3): p. 302-314.

[96]. Bhakuni, D., et al., Screening of Indian plants for biological activity: Part XIV. Indian Journal of Experimental Biology, 1990. 28(7): p. 619-637.

[97]. Hayat, M.Q., et al., Ethnobotany of the genus Artemisia L.(Asteraceae) in Pakistan. 2009.

[98]. Morris, G.M. and M. Lim-Wilby, Molecular docking, in Molecular modeling of proteins. 2008, Springer. p. 365-382.

[99]. Chen, Y. and D. Zhi, Ligand–protein inverse docking and its potential use in the computer search of protein targets of a small molecule. Proteins: Structure, Function, and Bioinformatics, 2001. 43(2): p. 217-226.

[100]. Fan, J., A. Fu, and L. Zhang, Progress in molecular docking. Quantitative Biology, 2019: p. 1-7.

[101]. Baunthiyal, M., V. Singh, and S. Dwivedi, Insights of antioxidants as molecules for drug discovery. International Journal of Pharmacology, 2017. 13(7): p. 874-889.

[102]. Abdulfatai, U., A. Uzairu, and S. Uba, Quantitative structure-activity relationship and molecular docking studies of a series of quinazolinonyl analogues as inhibitors of gamma amino butyric acid aminotransferase. Journal of advanced research, 2017. 8(1): p. 33-43.

[103]. Montella, R., et al., On the virtualization of CUDA based GPU remoting on ARM and X86 machines in the GVirtuS framework. International Journal of Parallel Programming, 2017. 45(5): p. 1142-1163.

[104]. Gasteiger, E., et al., Protein identification and analysis tools on the ExPASy server, in The proteomics protocols handbook. 2005, Springer. p. 571-607.

[105]. Oany, A., et al., Computational structure analysis and function prediction of an uncharacterized protein (I6U7D0) of Pyrococcus furiosus Com1. Austin J Comput Biol Bioinform, 2014. 1(2): p. 5.

[106]. Punta, M., et al., The Pfam protein families database. Nucleic acids research, 2012. 40(D1): p. D290- D301.

[107]. Mitchell, A.L., et al., InterPro in 2019: improving coverage, classification and access to protein sequence annotations. Nucleic acids research, 2019. 47(D1): p. D351-D360.

[108]. Yuan, S., H.S. Chan, and Z. Hu, Using PyMOL as a platform for computational drug design. Wiley Interdisciplinary Reviews: Computational Molecular Science, 2017. 7(2): p. e1298.

[109]. Chaudhary, K.K. and N. Mishra, A review on molecular docking: novel tool for drug discovery. databases, 2016. 3(4).

[110]. Lipinski, C.A., Lead-and drug-like compounds: the rule-of-five revolution. Drug Discovery Today: Technologies, 2004. 1(4): p. 337-341.

[111]. Vardhan, S. and S.K. Sahoo, In silico ADMET and molecular docking study on searching potential inhibitors from limonoids and triterpenoids for COVID-19. Comput Biol Med, 2020. 124: p. 103936.

[112]. Liu, Y., et al., CB-Dock: a web server for cavity detection-guided protein-ligand blind docking. Acta Pharmacol Sin, 2020. 41(1): p. 138-144.

[113]. Wallace, A.C., R.A. Laskowski, and J.M. Thornton, LIGPLOT: a program to generate schematic diagrams of protein-ligand interactions. Protein Engineering, Design and Selection, 1995. 8(2): p. 127- 134.

[114]. Wallace, A.C., R.A. Laskowski, and J.M. Thornton, LIGPLOT: a program to generate schematic diagrams of protein-ligand interactions. Protein Eng, 1995. 8(2): p. 127-34.

[115]. Pires, D.E., T.L. Blundell, and D.B. Ascher, pkCSM: Predicting Small-Molecule Pharmacokinetic and Toxicity Properties Using Graph-Based Signatures. J Med Chem, 2015. 58(9): p. 4066-72.

[116]. Kanehisa, M. and S. Goto, KEGG: kyoto encyclopedia of genes and genomes. Nucleic Acids Res, 2000. 28(1): p. 27-30.

[117]. Iovoli, A.J., et al., Association of Nonsteroidal Anti-inflammatory Drug Use With Survival in Patients With Squamous Cell Carcinoma of the Head and Neck Treated With Chemoradiation Therapy. JAMA Netw Open, 2020. 3(6): p. e207199.

[118]. Augustyniak, A., et al., Natural and synthetic antioxidants: an updated overview. Free Radic Res, 2010. 44(10): p. 1216-62.

[119]. Morya, V.K., et al., In silico characterization of alkaline proteases from different species of Aspergillus. Applied biochemistry and biotechnology, 2012. 166(1): p. 243-257.

[120]. Yang, J. and Y. Zhang, I-TASSER server: new development for protein structure and function predictions. Nucleic acids research, 2015. 43(W1): p. W174-W181.

[121]. Mulder, N.J. and R. Apweiler, Tools and resources for identifying protein families, domains and motifs. Genome biology, 2001. 3(1): p. 1-8.

[122]. Kim, S., et al., PubChem Substance and Compound databases. Nucleic Acids Res, 2016. 44(D1): p. D1202-13.

[123]. Kumar, N., et al., Preclinical evaluation and molecular docking of 1, 3-benzodioxole propargyl ether derivatives as novel inhibitor for combating the histone deacetylase enzyme in cancer. Artificial cells,nanomedicine, and biotechnology, 2018. 46(6): p. 1288-1299.

[124]. Daina, A., O. Michielin, and V. Zoete, SwissADME: a free web tool to evaluate pharmacokinetics, drug-likeness and medicinal chemistry friendliness of small molecules. Scientific reports, 2017. 7: p. 42717-42717.

[125]. Pires, D.E., T.L. Blundell, and D.B. Ascher, pkCSM: predicting small-molecule pharmacokinetic and toxicity properties using graph-based signatures. Journal of medicinal chemistry, 2015. 58(9): p. 4066- 4072.

[126]. Morris, G.M., et al., AutoDock4 and AutoDockTools4: Automated docking with selective receptor flexibility. Journal of computational chemistry, 2009. 30(16): p. 2785-2791.

[127]. C, S., et al., Molecular docking, validation, dynamics simulations, and pharmacokinetic prediction of natural compounds against the SARS-CoV-2 main-protease. Journal of Biomolecular Structure and Dynamics, 2020: p. 1-27.

[128]. Laskowski, R.A. and M.B. Swindells, LigPlot+: multiple ligand-protein interaction diagrams for drug discovery. J Chem Inf Model, 2011. 51(10): p. 2778-86.

[129]. Umar, A.B., et al., Docking-based strategy to design novel flavone-based arylamides as potent V600E- BRAF inhibitors with prediction of their drug-likeness and ADMET properties. Bulletin of the National Research Centre, 2020. 44(1): p. 179.

[130]. Wang, P.H., Y.S. Tu, and Y.J. Tseng, PgpRules: a decision tree based prediction server for P- glycoprotein substrates and inhibitors. Bioinformatics, 2019. 35(20): p. 4193-4195.

[131]. Han, Y., et al., In silico ADME and Toxicity Prediction of Ceftazidime and Its Impurities. Front Pharmacol, 2019. 10: p. 434.

[132]. Ujan, R., et al., Drug-1,3,4-Thiadiazole Conjugates as Novel Mixed-Type Inhibitors of Acetylcholinesterase: Synthesis, Molecular Docking, Pharmacokinetics, and ADMET Evaluation. Molecules, 2019. 24(5).

[133]. Bauersachs, J., et al., Prevention of endothelial dysfunction in heart failure by vitamin E: attenuation of vascular superoxide anion formation and increase in soluble guanylyl cyclase expression. Cardiovasc Res, 2001. 51(2): p. 344-50.

[134]. Cinar, M.G., et al., Effect of dietary vitamin E supplementation on vascular reactivity of thoracic aorta in streptozotocin-diabetic rats. Pharmacology, 2001. 62(1): p. 56-64.

[135]. Kim, Y.-S., et al., Antihyperlipidemic and antioxidant effects of Insamsansaeum (Renshenshanzha-yin) in hypercholesterolemic rats. The Journal of Korean Medicine, 2006. 27(4): p. 96-104.

[136]. Ulker, S., P.P. McKeown, and U. Bayraktutan, Vitamins reverse endothelial dysfunction through regulation of eNOS and NAD(P)H oxidase activities. Hypertension, 2003. 41(3): p. 534-9.

[137]. Feig, D.I., B. Soletsky, and R.J. Johnson, Effect of allopurinol on blood pressure of adolescents with newly diagnosed essential hypertension: a randomized trial. Jama, 2008. 300(8): p. 924-32.

[138]. Pérez-Rodríguez, L., F. Mougeot, and C. Alonso-Alvarez, Carotenoid-based coloration predicts resistance to oxidative damage during immune challenge. Journal of Experimental Biology, 2010. 213(10): p. 1685-1690.

[139]. Rao, A.V. and L.G. Rao, Carotenoids and human health. Pharmacol Res, 2007. 55(3): p. 207-16.

[140]. Rains, T.M., S. Agarwal, and K.C. Maki, Antiobesity effects of green tea catechins: a mechanistic review. J Nutr Biochem, 2011. 22(1): p. 1-7.

[141]. Rena, G., D.G. Hardie, and E.R. Pearson, The mechanisms of action of metformin. Diabetologia, 2017. 60(9): p. 1577-1585.

[142]. Klein Geltink, R.I. and E.L. Pearce, The importance of methionine metabolism. Elife, 2019. 8.

[143]. Pechánová, O., et al., Effect of chronic N-acetylcysteine treatment on the development of spontaneous hypertension. Clin Sci (Lond), 2006. 110(2): p. 235-42.

[144]. Barrios, V., et al., N-acetylcysteine potentiates the antihypertensive effect of ACE inhibitors in hypertensive patients. Blood Press, 2002. 11(4): p. 235-9.

[145]. Mollnau, H., et al., Nebivolol prevents vascular NOS III uncoupling in experimental hyperlipidemia and inhibits NADPH oxidase activity in inflammatory cells. Arteriosclerosis, thrombosis, and vascular biology, 2003. 23(4): p. 615-621.

[146]. Münzel, T. and T. Gori, Nebivolol: the somewhat-different beta-adrenergic receptor blocker. J Am Coll Cardiol, 2009. 54(16): p. 1491-9.

[147]. Dong, W., Y. Zhou, and Z. Yang, Research progress of mechanism of action of resveratrol. Pharmacology & Pharmacy, 2016. 7(04): p. 170.

[148]. Costa, L.H.A., B.M. Santos, and L.G.S. Branco, Can selective serotonin reuptake inhibitors have a neuroprotective effect during COVID-19, Eur J Pharmacol, 2020. 889: p. 173629.

[149]. Wightman, E.L., et al., The effects of chronic trans-resveratrol supplementation on aspects of cognitive function, mood, sleep, health and cerebral blood

flow in healthy, young humans. British Journal of Nutrition, 2015. 114(9): p. 1427-1437.

[150]. Briciu, C., et al., A pharmacokinetic drug interaction study between nebivolol and paroxetine in healthy volunteers. J Clin Pharm Ther, 2014. 39(5): p. 535-40.

[151]. Shi, G., et al., A rare mutation of β 1-Adrenergic receptor affects sleep or wake behaviors. Neuron, 2019. 103(6): p. 1044-1055. e7.

[152]. Gupta, S. and H.M. Wright, Nebivolol: a highly selective beta1-adrenergic receptor blocker that causes vasodilation by increasing nitric oxide. Cardiovasc Ther, 2008. 26(3): p. 189-202.

[153]. Giles, T.D., et al., Rationale for nebivolol or valsartan combination for hypertension: review of preclinical and clinical data. J Hypertens, 2017. 35(9): p. 1758-1767.

[154]. Cheng, J.W., Nebivolol: a third-generation beta-blocker for hypertension. Clin Ther, 2009. 31(3): p. 447-62.

[155]. Wishart, D.S., et al., DrugBank 5.0: a major update to the DrugBank database for 2018. Nucleic Acids Res, 2018. 46(D1): p. D1074-d1082.